MECHANISMS OF HUMAN GENE EVOLUTION

by

Xiaoxia Wang

A dissertation submitted in partial fulfillment
of the requirements for the degree of
Doctor of Philosophy
(Ecology and Evolutionary Biology)
In The University of Michigan
2007

Doctoral Committee:

Associate Professor Jianzhi Zhang, Chair
Professor Jeffrey C. Long
Professor David P. Mindell
Professor Priscilla K. Tucker

To my father and mother

ACKNOWLEDGEMENTS

My sincerest thanks go to my advisor, Jianzhi Zhang, for his continuous support in my Ph.D. program. For the past five years, he has always been there to listen, give valuable advice and bring out the good ideas in me. His patience and generosity gave me a lot of courage and confidence. His wisdom and intelligence opened my mind, so I learned to enjoy the beauty of science and experience the world in an entirely new way.

I am also grateful to my dissertation committee for their patience, kindness, and constant guidance. Thanks also to my labmates and cohorts. Without their friendship and support, I cannot survive the competition in academic field. Particularly, Soochin Cho and Ondrej Podlaha offered me tremendous help on my study and work and kept me in good spirits. I am honored to work with so many intelligent people in Zhang lab, sharing my ideas with them and listening to their remarkable opinions.

I also owe many thanks to Prosanta Chakrabarty, LaDonna Walker, Julia Eussen for helping me at any time and solving any unsolvable problems for me.

Finally, I thank my parents for giving me my life in the first place, for supporting me to pursue my dream, and for listening to my complaints and frustrations. No matter how far I am away from them, I can feel their love surrounding me at any time.

TABLE OF CONTENTS

DEDICATION…………………………………………………………………... ii
ACNOWLEDGEMENTS………………………………………………….…..... iii
LIST OF FIGURES……….……………………………………………………. vi
LIST OF TABLES……………………………………………………………… viii
ABSTRACT…………………………………………………………………... ix
INTRODUCTION……………………………………………………….….... 1
CHAPTER 1: RAPID EVOLUTION OF MAMMALIAN X-LINKED TESTIS-EXPRESSED HOMEOBOX GENES………………………………….. 9
1.1 ABSTRACT..……………………………………………………….... 9
1.2 INTRODUCTION…………………………………………………… 10
1.3 RESULTS……………………………………………………………….. 11
1.4 DISCUSSION………………………………………………………... 19
1.5 MATERIALS AND METHODS……………………………………….. 22
1.6 ACKNOWLEDGMENTS…………………………………….......... 25
1.7 LITERACTURE CITED……………………………………………... 32
CHAPTER 2: RAPID EVOLUTION OF PRIMATE *ESX1*, AN X-LINKED PLACENTA- AND TESTIS-EXPRESSED HOMEOBOX GENE...................... 35
2.1 ABSTRACT..………………………………………………………... 35
2.2 INTRODUCTION…………………………………………………… 36
2.3 RESULTS……………………………………………………………….. 38
2.4 DISCUSSION………………………………………………………... 45
2.5 MATERIALS AND METHODS……………………………………….. 48
2.6 ACKNOWLEDGMENTS……………………………………………. 50
2.7 LITERACTURE CITED……………………………………………... 59
CHAPTER 3: RELAXATION OF SELECTIVE CONSTRAINT AND LOSS OF FUNCTION IN THE EVOLUTION OF HUMAN BITTER TASTE RECEPTOR GENES……………………………………………………………… 62
3.1 ABSTRACT..………………………………………………………... 62
3.2 INTRODUCTION…………………………………………………… 62
3.3 RESULTS……………………………………………………………. 64
3.4 DISCUSSION………………………………………………………... 72
3.5 MATERIALS AND METHODS……………………………………….. 76
3.6 ACKNOWLEDGMENTS……………………………………………. 78
3.7 LITERACTURE CITED……………………………………………... 85
CHAPTER 4: ADAPTIVE PSEUDOGENIZATION OF *CASPASE12* IN HUMAN EVOLUTION……………………………………………………… 89
4.1 ABSTRACT..………………………………………………………... 89

4.2 INTRODUCTION………………………………………………………… 89
4.3 RESULTS…………………………………………………………….. 92
4.4 DISCUSSION………………………………………………………... 98
4.5 MATERIALS AND METHODS……………………………………….. 101
4.6 ACKNOWLEDGMENTS………………………………………………. 105
4.7 LITERACTURE CITED…………………………………………………... 113

LIST OF FIGURES

Figure 1.1 Phylogenetic tree of *TGIFLX*, *TGIF2,* and *TGIF* genes………………… 26

Figure 1.2 Alignment of TGIFLX sequences of 16 primates………………………. 27

Figure 1.3 Pairwise comparisons of d_S and d_N among 16 primate *TGIFLX* sequences for (**A**) the entire sequence, (**B**) nonhomeodomain regions, and (**C**) the homeodomain………………………………………………………………………. 28

Figure 1.4 Numbers of synonymous (*s*) and nonsynonymous (*n*) substitutions in the evolution of primate *TGIFLX* genes……………………………………………… 29

Figure 1.5 Distribution of the evolutionary rate of 64 mammalian homeobox genes……………………………………………………………………………….... 30

Figure 2.1 Structures of the orthologous (**A**) human *ESX1* and (**B**) mouse *Esx1* genes, adapted from (Fohn and Behringer 2001) and (Li et al. 1997)………………... 51

Figure 2.2 Alignment of human and chimpanzee ESX1 protein sequences……...... 52

Figure 2.3 Protein sequence alignment for exon 4 of *ESX1* (*Esx1*) in (**A**) 12 primates and (**B**) 4 *Mus* species………………………………………………………. 53

Figure 2.4 Pairwise synonymous (d_S) and nonsynonymous (d_N) nucleotide distances for (**A**) the entire exon 4 of *ESX1* among 15 primates, (**B**) the C-terminal non-homeodomain region of *ESX1* among 15 primates, and (**C**) the exon 4 of *Esx1* among 4 *Mus* species………………………………………………………………. 54

Figure 2.5 Separate alignments of translated *ESX1* exon 4 of (**A**) hominoids, (**B**) Old World monkeys, and (**C**) New World monkeys………………………………….. 55

Figure 2.6 Numbers of synonymous (*s*) and nonsynonymous (*n*) substitutions in the evolution of primate *ESX1*……………………………………………………... 56

Figure 3.1 Evolutionary relationships of 113 putatively functional *TAS2R* genes from the human, chimpanzee, mouse, and rat………………………………………… 79

Figure 3.2 Comparison of d_N/d_S among different functional domains of TAS2Rs…. 80

Figure 3.3 Expected and observed distributions of d_N/d_S among 25 human *TAS2R* genes……………………………………………………………………………. 81

Figure 4.1 Intraspecific DNA sequence variation in noncoding regions linked with the human *CASPASE12* gene……………………………………………………………. 107

Figure 4.2 Genotypes of the 4 C/C homozygotes and 4 T/T homozygotes that were sequenced in all 9 noncoding regions………………………………………………… 108

Figure 4.3 Estimating the age of the null allele and the onset of the selective sweep 109

LIST OF TABLES

Table 1.1 Protein *p*-distances between orthologous human and mouse homeobox genes………………………………………………………………………………... 31

Table 2.1 *ESX1* exon 4 sequence variations among 32 men……………………… 57

Table 2.2 Primers used for amplifying different exons of *ESX1* in primates and *Esx1* in *Mus* species.…………………………………………………………... 58

Table 3.1 Intra- and inter- variations of human *TAS2R* genes.………...………….. 82

Table 3.2 Rates of synonymous and nonsynonymous nucleotide changes in human *TAS2R*s……………………………………………………………………… 83

Table 4.1 Intraspecific variations in 9 noncoding regions linked to human CASPASE12……………………………………………………………………… 110

Table 4.2 Results from coalescent simulations.…………………………………... 111

Table 4.3 SNPs identified in the noncoding regions linked with CASP12……….. 112

ABSTRACT

“What makes us humans?” is one of the most fascinating questions in evolution. The genetic basis of the phenotypic differences between humans and close evolutionary relatives has been a hot topic for molecular evolutionary studies. Investigating human genetic variations within the context of primates will provide valuable information about the development and function of important primate features and unique human features.

In Chapter 1 and 2, I conducted detailed evolutionary studies on two homeobox genes, *TGIFLX* and *ESX1*. Evolutionary analysis provided evidence for positive selection acting on the two genes during primate evolution. Given the key roles played by homeobox genes in various developmental processes, the identification of non-conserved homeobox genes is interesting, because such homeobox genes may regulate important developmental processes that vary among relatively closely related species. *TGIFLX* and *ESX1* are located on X chromosome and involved in male spermatogenesis process. The finding of positive selection in these genes suggests that even in the recent past of human and primate evolution, spermatogenesis has been subject to adaptive modifications.

Characterizing genetic variations within humans is also a powerful way to detect the genetic basis of human uniqueness. Gene loss is an important source of human-specific genetic change. Genes related to chemoreception and immunity account for a large proportion of lost genes in the human lineage. In Chapter 3, I reported the relaxation of selective constraint and loss of function in the evolution of human bitter taste receptor genes, probably due to the change in diet, use of fire, and reliance on other means of

toxin avoidance that emerged in human evolution. This finding provided further evidence for reduced sensory capabilities of humans in comparison to many other mammals.

Gene loss or pseudogenization has also been proposed to serve as an engine of evolutionary change, especially during human origins (the “less-is-more” hypothesis). In Chapter 4, I focused on *CASPASE12*, a cysteinyl aspartate proteinase participating in inflammatory and innate immune response to endotoxins. My results provided population genetic evidence that the nearly complete fixation of a null allele at *CASPASE12* has been driven by positive selection, probably because the null allele confers protection from severe sepsis. Furthermore, the identification and analysis of human-specific pseudogenes open the door for understanding the roles of gene losses in human origins, and the demonstration that gene loss itself can be adaptive supports and extends the ‘‘less-is-more’’ hypothesis.

INTRODUCTION

The finding of DNA double helix structure followed by dramatic achievements in biochemical techniques, such as PCR (Polymerase Chain Reaction), DNA sequencing, and genetic engineering opened a new era for evolutionary study. Characterizing genetic differences at the level of DNA molecules and its products (protein or RNA molecules) has moved the study of evolution into a brand new dimension. One of the most fascinating questions in evolution is what makes us humans. In addition to several well-known features, such as bipedalism, enlarged brains, language capability, and other high-order cognitive functions, numerous traits differentiate humans from other great apes (Varki and Altheide 2005). With rapid progress in human genetics, comparative genomes, and molecular evolution, the evolutioanry basis of these differences has begun to be unraveled.

Investigating our “humanness” in the context of primates will tell us what is common to primates and what is unique to humans. Phylogenetic analysis of primate genomic data can provide valuable clues about the development and function of important primate features and the genetic basis of human uniqueness. So far, finished or draft primate genome sequences are available only for human, common chimpanzee, and rhesus macaque. No New World monkey has been sequenced in genomic scale despite their evolutionary significance, one more step further the human-rhesus relationship. In order to learn the mechanism of molecular evolution in a phylogenetic framework encompassing the entire order Primates, I focused on candidate gene investigation in my dissertation work. A candidate gene approach takes advantage of *a priori* knowledge obtained from genetic, biochemical, or physiological assays about specific genes and can acquire striking outcomes (Varki and Altheide 2005). *FOXP2* evolution is a good example. The conserved transcriptional factor *FOXP2* is required for speech development in humans (Lai et al. 2001). Intriguingly, two adaptive amino acid replacements were found in hominin evolution, suggesting that these two substitutions were at least partially responsible for the emergence of human speech and language (Enard et al. 2002; Zhang et al. 2002).

In the first half of this thesis (Chapter 1 & 2), I provide evidence for positive selection acting on two homeobox genes, *TGIFLX* and *ESX1*, during primate evolution. Homeobox genes are characterized by the presence of a sequence motif known as the homeobox, which encodes the ~60-amino-acid homeodomain, a helix-turn-helix DNA binding domain (Gehring et al. 1994). In humans, there are about 230 homeobox genes (Nam and Nei 2005), encoding a large family of transcription factors that play key roles in various developmental processes such as body-plan specification, pattern formation, and cell-fate determination (Gehring et al. 1994). Due to their functional importance, most homeodomain proteins are evolutionarily highly conserved in sequence (McGinnis et al. 1984; Gehring et al. 1994; Zhang and Nei 1996). Hence, the identification of non-conserved homeobox genes would be particularly interesting, because such homeobox genes may regulate important developmental processes that vary among relatively closely related species.

Two such rapidly-evolving homeobox genes are well known, from fruit flies (*OdsH*) and rodents (*Rhox5*), respectively. *OdsH* is an X-linked gene involved in spermatogenesis and it is partly responsible for the hybrid male sterility between *Drosophila simulans* and *D. mauritiana* (Ting et al. 1998). Mouse *Rhox5* (also known as *Pem*) is expressed in both male and female reproductive tissues (Sutton and Wilkinson 1997). Targeted disruption of *Rhox5* increases male germ cell apoptosis and reduces sperm production, sperm motility, and fertility (Maclean et al. 2005). In fact, *Rhox5* is just one member of a recently expanded homeobox gene cluster known as the Rhox cluster on the mouse X chromosome (Maclean et al. 2005; MacLean et al. 2006; Morris et al. 2006; Wang and Zhang 2006). Several other members of the cluster are also expressed in reproductive tissues (Maclean et al. 2005) and evolve rapidly (Jackson et al. 2006; Wang and Zhang 2006). Interestingly, each of the two cases involves a homeobox gene that is X-linked and testis-expressed. In my work, I identified rapid evolution in another two X-linked testis-expressed homeobox genes from primates, *TGIFLX* (Chapter 1) and *ESX1* (Chapter 2). Positive selection has been acting on both genes during primate evolution. The evolutionary patterns in light of the structure and function of these two genes are discussed.

In the second half of this thesis (Chapter 3 & 4), I focus on human-specific gene evolution by characterizing genetic variations within humans. In addition to amino acid replacements (like the cases presented in Chapter 1 & 2), gene expression modification, generation of new genes and loss of existing genes are also genetic mechanisms underlying human uniqueness. In particular, gene loss, or pseudogenization, leads to immediate loss of gene function, which probably affects organisms to a greater extent than most amino acid replacements do. A number of genes are known to have been lost in the human lineage since its divergence from the chimpanzee lineage (Chou et al. 1998; Szabo et al. 1999; Winter et al. 2001; Gilad et al. 2003; Hamann et al. 2003; Meyer-Olson et al. 2003; Stedman et al. 2004; Wang et al. 2004; Fischer et al. 2005; Go et al. 2005; Perry et al. 2005). Many of these genes are involved in chemoreception and immunity, such as the olfactory receptor (OR) genes (Gilad et al. 2003) and vomeronasal pheromone receptor genes (Zhang and Webb 2003; Grus et al. 2005). These cases of gene loss may reflect significant changes in the way humans interact with each other or with the environment, human diet, and human behavior during the past few million years. In Chapter 3, I present my finding of relaxation of selective constraint and loss of function in the evolution of human bitter taste receptor genes, which provide further evidence for reduced sensory capabilities of humans in comparison to many other mammals.

Recently, Olson (1999) and Olson and Varki (2003) proposed the “less-is-more” hypothesis, suggesting that gene loss may serve as an engine of evolutionary change. This hypothesis is particularly intriguing for human evolution, as several human gene losses have been proposed to provide opportunities for adaptations and be responsible for human-specific phenotypes. For example, the pseudogenization of the sarcomeric myosin gene *MYH16* at the time of the emergence of the genus *Homo* is thought to be responsible for the marked size reduction in hominin masticatory muscles, which may have allowed the brain-size expansion (Stedman et al. 2004) (but also see Perry et al. 2005). In another example, the human-specific inactivation of the gene encoding the enzyme CMP-N-acetylneuraminic acid hydroxylase (CMAH) led to the deficiency of the mammalian common sialic acid Neu5Gc (N-glycolylneuraminic acid) on the human cell surface (Chou et al. 1998). This inactivation was due to an Alu-mediated sequence replacement (Hayakawa et al. 2001) that occurred ~2.7 million years ago (Chou et al. 2002) and may have had several important consequences for human biology and evolution (Varki 2001). In Chapter 4, I present a case of adaptive gene loss in humans. I provide evidence that the nearly complete fixation of a null allele at *CASPASE12* (*CASP12*) has been driven by positive selection, probably because the allele confers lowered susceptibility to severe sepsis. This finding opens the door for understanding the roles of gene losses in human origins, and the demonstration that gene loss itself can be adaptive supports and extends the “less-is-more” hypothesis.

LITERATURE CITED

Chou HH, Hayakawa T, Diaz S, Krings M, Indriati E, Leakey M, Paabo S, Satta Y, Takahata N, Varki A (2002) Inactivation of CMP-N-acetylneuraminic acid hydroxylase occurred prior to brain expansion during human evolution. Proc Natl Acad Sci U S A 99:11736-11741

Chou HH, Takematsu H, Diaz S, Iber J, Nickerson E, Wright KL, Muchmore EA, Nelson DL, Warren ST, Varki A (1998) A mutation in human CMP-sialic acid hydroxylase occurred after the Homo-Pan divergence. Proc Natl Acad Sci U S A 95:11751-11756

Enard W, Przeworski M, Fisher SE, Lai CSL, Wiebe V, Kitano T, Monaco AP, Paabo S (2002) Molecular evolution of FOXP2, a gene involved in speech and language. Nature 418:869-872

Fischer A, Gilad Y, Man O, Paabo S (2005) Evolution of bitter taste receptors in humans and apes. Mol Biol Evol 22:432-436

Gehring WJ, Affolter M, Burglin T (1994) Homeodomain proteins. Annual review of biochemistry 63:487-526

Gilad Y, Man O, Paabo S, Lancet D (2003) Human specific loss of olfactory receptor genes. Proc Natl Acad Sci U S A 100:3324-3327

Go Y, Satta Y, Takenaka O, Takahata N (2005) Lineage-specific loss of function of bitter taste receptor genes in humans and nonhuman primates. Genetics 170:313-326

Grus WE, Shi P, Zhang YP, Zhang JZ (2005) Dramatic variation of the vomeronasal pheromone receptor gene repertoire among five orders of placental and marsupial mammals. Proceedings of the National Academy of Sciences of the United States of America 102:5767-5772

Hamann J, Kwakkenbos MJ, de Jong EC, Heus H, Olsen AS, van Lier RA (2003) Inactivation of the EGF-TM7 receptor EMR4 after the Pan-Homo divergence. Eur J Immunol 33:1365-1371

Hayakawa T, Satta Y, Gagneux P, Varki A, Takahata N (2001) Alu-mediated inactivation of the human CMP- N-acetylneuraminic acid hydroxylase gene. Proc Natl Acad Sci U S A 98:11399-11404

Jackson M, Watt AJ, Gautier P, Gilchrist D, Driehaus J, Graham GJ, Keebler J, Prugnolle F, Awadalla P, Forrester LM (2006) A murine specific expansion of the Rhox cluster involved in embryonic stem cell biology is under natural selection. BMC genomics 7:212

Lai CSL, Fisher SE, Hurst JA, Vargha-Khadem F, Monaco AP (2001) A forkhead-domain gene is mutated in a severe speech and language disorder. Nature 413:519-523

Maclean JA, 2nd, Chen MA, Wayne CM, Bruce SR, Rao M, Meistrich ML, Macleod C, Wilkinson MF (2005) Rhox: a new homeobox gene cluster. Cell 120:369-382

MacLean JA, 2nd, Lorenzetti D, Hu Z, Salerno WJ, Miller J, Wilkinson MF (2006) Rhox homeobox gene cluster: recent duplication of three family members. Genesis

44:122-129

McGinnis W, Hart CP, Gehring WJ, Ruddle FH (1984) Molecular cloning and chromosome mapping of a mouse DNA sequence homologous to homeotic genes of Drosophila. Cell 38:675-680

Meyer-Olson D, Brady KW, Blackard JT, Allen TM, Islam S, Shoukry NH, Hartman K, Walker CM, Kalams SA (2003) Analysis of the TCR beta variable gene repertoire in chimpanzees: identification of functional homologs to human pseudogenes. J Immunol 170:4161-4169

Morris L, Gordon J, Blackburn CC (2006) Identification of a tandem duplicated array in the Rhox alpha locus on mouse chromosome X. Mamm Genome 17:178-187

Nam J, Nei M (2005) Evolutionary change of the numbers of homeobox genes in bilateral animals. Molecular biology and evolution 22:2386-2394

Olson MV (1999) When less is more: gene loss as an engine of evolutionary change. Am J Hum Genet 64:18-23

Olson MV, Varki A (2003) Sequencing the chimpanzee genome: insights into human evolution and disease. Nat Rev Genet 4:20-28

Perry GH, Verrelli BC, Stone AC (2005) Comparative analyses reveal a complex history of molecular evolution for human MYH16. Mol Biol Evol 22:379-382

Stedman HH, Kozyak BW, Nelson A, Thesier DM, Su LT, Low DW, Bridges CR, Shrager JB, Minugh-Purvis N, Mitchell MA (2004) Myosin gene mutation correlates with anatomical changes in the human lineage. Nature 428:415-418

Sutton KA, Wilkinson MF (1997) Rapid evolution of a homeodomain: evidence for positive selection. J Mol Evol 45:579-588

Szabo Z, Levi-Minzi SA, Christiano AM, Struminger C, Stoneking M, Batzer MA, Boyd CD (1999) Sequential loss of two neighboring exons of the tropoelastin gene during primate evolution. J Mol Evol 49:664-671

Ting CT, Tsaur SC, Wu ML, Wu CI (1998) A rapidly evolving homeobox at the site of a hybrid sterility gene. Science 282:1501-1504

Varki A (2001) Loss of N-glycolylneuraminic acid in humans: Mechanisms, consequences, and implications for hominid evolution. Am J Phys Anthropol Suppl 33:54-69

Varki A, Altheide TK (2005) Comparing the human and chimpanzee genomes: Searching for needles in a haystack. Genome Research 15:1746-1758

Wang X, Thomas SD, Zhang J (2004) Relaxation of selective constraint and loss of function in the evolution of human bitter taste receptor genes. Hum Mol Genet 13:2671-2678

Wang X, Zhang J (2006) Remarkable expansions of an X-linked reproductive homeobox gene cluster in rodent evolution. Genomics 88:34-43

Winter H, Langbein L, Krawczak M, Cooper DN, Jave-Suarez LF, Rogers MA, Praetzel S, Heidt PJ, Schweizer J (2001) Human type I hair keratin pseudogene phihHaA has functional orthologs in the chimpanzee and gorilla: evidence for recent inactivation of the human gene after the Pan-Homo divergence. Hum Genet 108:37-42

Zhang J, Nei M (1996) Evolution of Antennapedia-class homeobox genes. Genetics 142:295-303

Zhang JZ, Webb DM (2003) Evolutionary deterioration of the vomeronasal pheromone transduction pathway in catarrhine primates. Proceedings of the National Academy of Sciences of the United States of America 100:8337-8341

Zhang JZ, Webb DM, Podlaha O (2002) Accelerated protein evolution and origins of human-specific features: FOXP2 as an example. Genetics 162:1825-1835

CHAPTER 1

RAPID EVOLUTION OF MAMMALIAN X-LINKED TESTIS-EXPRESSED HOMEOBOX GENES

1.1 ABSTRACT

Homeobox genes encode transcription factors that function in various developmental processes and are usually evolutionarily conserved in their sequences. However, two X-chromosome-linked testis-expressed homeobox genes, one from rodents and the other from fruit flies, are known to evolve rapidly under positive Darwinian selection. Here we report yet another case, from primates. *TGIFLX* is an X-linked homeobox gene that originated by retroposition of the autosomal gene *TGIF2*, most likely in a common ancestor of rodents and primates. While *TGIF2* is ubiquitously expressed, *TGIFLX* is exclusively expressed in adult testis. A comparison of the *TGIFLX* sequences among 16 anthropoid primates revealed a significantly higher rate of nonsynonymous nucleotide substitution (d_N) than synonymous substitution (d_S), strongly suggesting the action of positive selection. Although the high d_N/d_S ratio is most evident outside the homeobox, the homeobox has a d_N/d_S of ~0.89 and includes two codons that are likely under selection. Furthermore, the rate of radical amino acid substitutions that alter amino acid charge is significantly greater than that of conservative substitutions, suggesting that the selection promotes diversity of the protein charge profile. More interestingly, an analysis of 64 orthologous homeobox genes from humans and mice shows substantially higher rates of amino acid substitution in X-linked testis-expressed genes than in other

genes. These results suggest a general pattern of rapid evolution of mammalian X-linked testis-expressed homeobox genes. Although the physiological function of and the exact selective agent on *TGIFLX* and other rapidly evolving homeobox genes are unclear, the common expression pattern of these transcription factor genes led us to conjecture that the selection is related to one or more aspects of male reproduction and may contribute to speciation.

1.2 INTRODUCTION

Homeobox genes are characterized by the presence of an ~60-codon sequence motif known as the homeobox, which encodes a helix-turn-helix DNA-binding domain named the homeodomain (Gehring et al. 1994a). Initially identified from fruit flies (Mcginnis et al. 1984; Scott and Weiner 1984), homeobox-containing genes have now been found in fungi, plants, and animals and form a large gene superfamily (Kappen et al. 1993; Bharathan et al. 1997; Kappen 2000; Banerjee-Basu and Baxevanis 2001). Homeobox genes function as transcription factors that regulate the expressions of their target genes in various developmental processes such as body-plan specification, pattern formation, and cell fate determination (Gehring et al. 1994a). Because of their fundamental importance in development, homeobox genes are of substantial interest to evolutionary biologists as they may provide key information on the evolution of development (Shepherd et al. 1984; Garciafernandez and Holland 1994; Zhang and Nei 1996; Carroll et al. 2001). Earlier studies showed that homeobox genes, particularly the homeobox region, are conserved in evolution (Mcginnis et al. 1984; Gehring et al. 1994a), although two notable exceptions, *Pem* in rodents and *OdsH* in Drosophila, have been reported (Sutton and Wilkinson 1997; Ting et al. 1998). In both cases, high rates of amino acid substitution were found in the homeodomain and the action of positive selection was suggested. Interestingly, both genes are located on X chromosomes and are expressed in testis, although *Pem* is also expressed in female reproductive tissues. *OdsH* is in part responsible for the hybrid male sterility between *Drosophila simulans* and *D. mauritiana* (Ting et al. 1998). These intriguing findings suggest that homeobox genes may also be involved in developmental processes that vary among closely related species. Because such developmental variations may lead to reproductive isolation and speciation (Ting et al. 1998), it is of interest to identify new cases of rapidly evolving homeobox genes. Here we describe the identification of such a rapidly evolving homeobox gene, *TGIFLX* [TG-interacting factor (TGIF)-like X], from primates. TGIFLX is a member of TGIFs, a group of transcription factors of the three amino-acid loop extension (TALE) superclass of the homeodomain protein family (Bertolino et al. 1995; Blanco-Arias et al. 2002). Earlier evolutionary analyses suggested that the X-chromosome-linked *TGIFLX* gene originated by retroposition of the autosomal *TGIF2* gene, a member of TGIFs (Blanco-Arias et al. 2002). In contrast to *TGIF2*, which is ubiquitously expressed, *TGIFLX* is specifically expressed in the germ cells of adult testis (Blanco-Arias et al. 2002; Lai et al. 2002). In this report, we show that (1) the retroposition event predated the divergence of primates and rodents, (2) *TGIFLX* evolved rapidly in primates under positive selection, and (3) mammalian X-linked testis-expressed homeobox genes evolve rapidly in general.

1.3 RESULTS

1.3.1 Retroposition predated the human-mouse separation

To determine when the retroposition that generated *TGIFLX* occurred in evolution, we conducted a BLAST search in the GenBank for homologous sequences to *TGIFLX* and its mother gene *TGIF2*. We identified a homeobox gene *Tex1* (also known as *Tgifx1-pending*) in the mouse that is mapped to a region of the X chromosome that is syntenic with human Xq21.3, where *TGIFLX* is located. *Tex1* is also specifically expressed in the germ cells of mouse testis (Lai et al. 2002). These facts suggest that mouse *Tex1* is orthologous to human *TGIFLX*. Furthermore, we obtained the gene sequences of human and mouse *TGIF2* from GenBank and conducted a phylogenetic analysis of these sequences. The human and mouse *TGIF* sequences are used as outgroups. The gene tree shows high bootstrap support for the retroposition that gave birth to *TGIFLX* occurring in a common ancestor of primates and rodents (Figure 1.1).

Although retroposition usually generates pseudogenes, a number of retroposition-mediated functional genes have been identified (Long 2001). *TGIFLX* is apparently a functional gene as its open reading frame has been maintained throughout mammalian evolution. Retroposition is a mutation-prone process due to a high error rate in retrotranscription. Also, newly duplicated genes often have elevated rates of evolution due to relaxation of functional constraints and/or positive selection (Zhang 2003). Thus, one may expect to see a burst of substitutions in the *TGIFLX* branch immediately following the retroposition. Interestingly, the phylogenetic tree (Figure 1.1) shows that *TGIFLX* evolves more rapidly than *TGIF2* not only in this branch, but also throughout its evolutionary history. We found that the number of amino acid substitutions per site (Poisson distance) between the orthologous human and mouse *TGIFLX* genes is 0.814 ±

0.080, and the corresponding number for *TGIF2* is 0.031 ± 0.013, their difference being statistically significant (*P* < 0.001). Of 1880 orthologous human and rodent genes analyzed by Makalowski and Boguski (1998), only 6 have substitution rates greater than that of *TGIFLX*, suggesting that it is evolving at an exceptionally high rate. To further characterize the substitution rate of *TGIFLX*, we conducted a detailed evolutionary study of this gene in primates.

1.3.2 Positive selection on primate *TGIFLX*

The *TGIFLX* coding sequences from five hominoids and four OW monkeys were reported by Blanco-Arias *et al.* (2002). We here determined the orthologous sequences in two additional OW monkeys and five NW monkeys. Thus, a total of 16 primate sequences are analyzed here. The alignment of these 16 protein sequences shows that they are highly variable (Figure 1.2). The nonhomeodomain regions show the highest variability, although 25 of the 63 amino acid positions in the homeodomain are also variable among the 16 primates. Hydrophobic amino acids are usually conserved in homeodomains; in the present case 22 of the 29 hydrophobic sites are completely conserved among the primate sequences, and the remaining 7 also involve only hydrophobic amino acid changes. In the third helix of the homeodomain, four amino acids (W51, F52, N54, and R56; positions in the homeodomain) are known to be conserved (Banerjee-Basu and Baxevanis 2001), which is also the case here. Position 53 is usually occupied by a polar amino acid in homeodomains, but was found to have a small, nonpolar amino acid in a previous analysis of TALE homeodomains (Burglin 1997). In our sequences, position 53 is variable with either polar or nonpolar amino acids.

To examine whether the high sequence variability is a result of positive selection, we computed the synonymous (d_S) and nonsynonymous (d_N) distances between each pair of the sequences. For the entire coding region, higher d_N than d_S is observed in 93 of 120 pairwise comparisons (Figure 1.3A), suggesting the possible action of positive selection. This pattern is more apparent when only the nonhomeodomain regions are analyzed, as 98 of the comparisons show $d_N > d_S$ (Figure 1.3B). For the homeodomain, however, only 39 of the comparisons show $d_N > d_S$ (Figure 1.3C). These results indicate that the substitution rate and pattern may be different between amino acid positions inside and outside the homeodomain.

To test the hypothesis of positive selection more rigorously, we used a phylogeny-based approach (Zhang and Nei 1997). The phylogentic relationships of the 16 primates are assumed to follow the tree in Figure 1.4 . This phylogeny is relatively well established, especially for the major divisions (Goodman et al. 1998; Page and Goodman 2001; Singer et al. 2003; Steiper and Ruvolo 2003), and use of alternative trees does not affect our main conclusion. On the basis of this tree, we inferred the ancestral *TGIFLX* gene sequences at all interior nodes of the tree and counted the numbers of synonymous (s) and nonsynonymous (n) substitutions on each tree branch (Figure 1.4). We found that the sums of n and s for all branches are 195.5 and 58.5, respectively, for the nonhomeodomain regions. The potential numbers of nonsynonymous (N) and synonymous (S) sites are 322 and 128, respectively. Thus $n/s = 3.34$ is significantly greater than $N/S = 2.51$ ($P = 0.031$, binomial test). The binomial test used here is more conservative than Fisher's exact test used in Zhang *et al.* (1997) and is more appropriate here because of multiple substitutions that may have occurred at individual sites (Zhang and Rosenberg 2002). Fisher's exact test would have given a *P* value of 0.002 here. We also analyzed *n*/*s* in hominoids, OW monkeys, and NW monkeys separately, but did not find significant differences (Figure 1.4). The average number of synonymous substitutions per site is 0.155 between hominoids and New World monkeys and 0.0819 between hominoids and Old World monkeys. These values are virtually identical to the corresponding numbers obtained from multiple intron and noncoding sequences of primate genomes (0.149 and 0.079, respectively; Li 1997, pp. 221–224), suggesting that the synonymous substitution rate in *TGIFLX* is normal. Thus, our results strongly suggest that positive selection is responsible for the rapid evolution at nonsynonymous sites of the nonhomeodomain regions.

For the homeodomain, we found that *n*/*s* (2.42) is slightly lower than *N*/*S* (2.73) and that the null hypothesis of *n*/*s* = *N*/*S* cannot be rejected. This may suggest that the homeodomain is under no functional constraints. It may also suggest that some sites in the homeodomain are under positive selection while other sites are under purifying selection, giving an overall pattern of similar average substitution rates at synonymous and nonsynonymous sites (see below). When we examine the substitution patterns of hominoids, OW monkeys, and NW monkeys separately, we find that the *n*/*s* ratio is higher among hominoids and OW monkeys (23.5/4.5 = 5.22) than among NW monkeys (25/12 = 2.08; Figure 1.4). However, this difference is not significant (*P* = 0.132). The *n*/*s* ratio is not significantly different from *N*/*S* for hominoids and OW monkeys (*P* = 0.150).

Statistical methods for identifying individual codons that are under positive selection have been developed in recent years (Suzuki and Gojobori 1999; Yang et al. 2000). We first applied the likelihood method (Yang et al. 2000) to the *TGIFLX* data and compared the likelihoods under models 7 and 8. Here model 7 assumes that the d_N/d_S ratio for individual sites follows a ß-distribution between 0 and 1, while model 8 adds an extra class of sites to model 7. We found that model 8 fits the data significantly better than model 7 (χ^2 = 15.2, d.f. = 2, P < 0.001), with an additional class of sites of d_N/d_S = 2.42. Four codons were identified to be under positive selection with posterior probabilities >90%, and they are marked on the sequences shown in Figure 1.2. Similar results were obtained when models 1 and 2 were compared (see Yang et al. 2000) for details of the model description). Because the likelihood method has been shown to generate false-positive results occasionally (Suzuki and Nei 2002), we examined the evidence for selection at the four codons by a more conservative parsimony-based method (Suzuki and Gojobori 1999). None of the four codons show significant results of positive selection when they are tested individually (P = 0.19–0.59). When they are tested together, however, significant evidence for positive selection is found (average d_N/d_S = 5.10, P = 0.021), suggesting that one or more of the four codons are under positive selection. It is interesting to note that two of the four codons are located within the homeodomain while the other two are adjacent to the 3' end of the homeodomain, suggesting that the homeodomain may indeed be under positive selection (Figure 1.2). The two residues within the homeodomain are not among the completely conserved residues of all homeodomains, indicating that substitutions at these sites are unlikely to disrupt the basic structure and function of homeodomains. Furthermore, crystal structures of homeodomains show that the first of the two residues is involved in DNA-protein binding and that it contributes significantly to the functional specificity of homeodomains (Gehring et al. 1994b). The second of the two residues belongs to helix I of the homeodomain, and it may also be involved in DNA-protein binding, although a more specific molecular function has yet to be defined.

1.3.3 Selection promotes the diversity of charge profile

To investigate what types of nonsynonymous substitutions are favored by selection, we counted the numbers of conservative and radical nonsynonymous substitutions on each branch of the tree in Figure 1.4. Conservative nonsynonymous substitutions are those that do not alter the charge of the encoded amino acids and radical substitutions are those that alter the charge of the amino acids. We found a total number of r = 91.5 radical substitutions and c = 104 conservative substitutions in the tree for the nonhomeodomain regions. The potential numbers of radical and conservative sites are R = 128 and C = 195, respectively. The radical substitution rate (r/R = 0.715) is significantly greater than the conservative substitution rate (c/C = 0.533) at P = 0.027 (binomial test). This is in sharp contrast to the situation in most mammalian genes where the radical substitution rate is below the conservative rate (Zhang 2000). This result suggests that selection may favor alterations of amino acid charge in TGIFLX evolution. We also tested the hypothesis that selection may favor an alternation of amino acid polarity, but obtained no supporting evidence. For the homeodomain, there is no evidence for selection promoting the diversity of either amino acid polarity or charge.

In the above, we compared the number of radical substitutions per radical site (r/R) with the number of conservative substitutions per conservative site (c/C). This comparison provides information on differential selections at radical *vs.* conservative sites, as long as the four parameters (r, c, R, and C) are correctly estimated (Smith 2003). In contrast, comparisons between r and c can be misleading, because the potential numbers of radical (*R*) and conservative (*C*) sites in a gene sequence are usually different and they are affected by many factors unrelated to selection (Dagan et al. 2002).

1.3.4 Rapid evolution of mammalian X-linked testis-expressed homeobox genes

As mentioned, two other homeobox genes, *Pem* and *OdsH*, were reported to evolve rapidly (Sutton and Wilkinson 1997; Ting et al. 1998). The d_N/d_S ratio of *Pem* ranges from 0.65 to 1.56 for the homeodomain between *Mus musculus* and several related rodents (Sutton and Wilkinson 1997). We reanalyzed the *OdsH* homeodomain sequences from *D. simulans* and *D. mauritiana* (Ting et al. 1998) and obtained a d_N/d_S ratio of 1.55. Interestingly, *TGIFLX*, *Pem*, and *OdsH* are all located in X chromosomes and are all testis expressed. This observation prompted us to wonder whether it is a general pattern for X-linked testis-expressed homeobox genes to evolve rapidly. To test this hypothesis, we searched for orthologous homeobox genes from the human and mouse genome sequences. Our search was not exhaustive, but random. Of the 64 genes found, 4 are X-linked and testis expressed, 3 are X-linked and non-testis expressed, 13 are autosomal and testis expressed, and 44 are autosomal and non-testis expressed. Note that there appear to be only 7 X-linked homeobox genes, as a further exhaustive search did not find additional genes. Here "testis expression" simply means that the gene is expressed in testis, regardless of its expression in other tissues. We aligned the sequences and computed the amino acid *p*-distance for each orthologous pair. As shown in Table 1.1 and Figure 1.5A , when the entire protein is considered, autosomal homeobox genes (regardless of the expression pattern) and X-chromosomal non-testis-expressed homeobox genes have similar amino acid *p*-distances on average, which are an order of magnitude lower than those of X-linked testis-expressed homeobox genes, and their difference is statistically significant ($P < 0.0001$, permutation test). The same pattern is observed when only the homeodomain or nonhomeodomain regions are considered (Table 1.1; Figure 1.5, B and C). These results suggest that it is a general pattern for mammalian X-linked testis-expressed homeobox genes to evolve rapidly. In addition to *TGIFLX*, the other X-linked testis-expressed homeobox genes are *ESX1L*, *OTEX*, and *PEPP-2*. While the mouse ortholog of human *ESX1L* is clearly defined by a phylogenetic analysis (data not shown) and chromosomal locations, the orthologs of human *OTEX* and *PEPP-2* are not uniquely defined, probably because of independent gene duplications in rodents and primates after their separation (Wayne et al. 2002). From the mouse genome sequence, we identified a total of 15 homologs of the human *OTEX* and *PEPP-2* genes and conducted a phylogenetic analysis of these genes. The phylogeny is not well resolved and has low bootstrap supports (not shown). To be conservative, we computed protein *p*-distances for the human *OTEX* with each of the 15 mouse genes and presented the smallest distance in Table 1.1. We also did the same for the human *PEPP-2* gene. Considering possible nonindependent comparisons involved, we also repeated all the statistical tests when only one of the *OTEX* and *PEPP-2* genes was used. We found that the statistical results remain unchanged.

1.4 DISCUSSION

In this report, we provide evidence that *TGIFLX* evolves rapidly under positive selection in primates and that the selection favors diversity in charge profile. Although positive selection acts mainly in the nonhomeodomain regions of the protein, it may also operate at a few sites in the homeodomain. The homeodomain is used in binding DNA sequences in transcription regulation, while the nonhomeodomain regions in TGIFLX might be used in protein-protein interaction as in the case of TGIF and TGIF2 (Bertolino et al. 1995; Melhuish and Wotton 2000; Melhuish et al. 2001). Rapid evolution at these sites thus may alter the DNA- and protein-binding properties of TGIFLX. In mouse, the *TGIFLX* ortholog *Tex1* is exclusively expressed in the germ cells at the spermatid stage (Lai et al. 2002) and apparently escapes the inactivation that most X-linked genes are supposed to experience in spermatogenesis (Lifschyt and Lindsley 1972). Although the physiological function of *TGIFLX* is unknown, the restricted temporal and spatial expression pattern suggests a role of this gene in spermatogenesis and the detected positive selection on *TGIFLX* may be related to spermatogenesis as well.

Our analysis of homeobox genes of humans and mice revealed a general pattern of rapid evolution of X-linked, testis-expressed homeobox genes, although the number of such genes is relatively small. It is interesting to note that among autosomal homeobox genes, testis-expressed genes and non-testis-expressed genes show similar rates of amino acid substitution (Figure 1.5). Thus, testis expression alone does not explain high rates of protein evolution. Among non-testis-expressed homeobox genes, there is also no significant difference in substitution rate between autosomal genes and X-linked genes, suggesting that chromosomal location alone also does not explain the difference in amino acid substitution rate. We noted in collecting the expression pattern data that 3 of the 4 X-linked testis-expressed genes (*TGIFLX*, *OTEX*, and *PEPP*-2), but only 1 (*NKX3.1*) of the 13 autosomal testis-expressed genes, have exclusive or highly selective expressions in testis. This difference suggests that the majority of the autosomal testis-expressed genes may be under greater functional constraints due to their multifaceted roles in many tissues and developmental processes and thus evolve more slowly. Indeed, *NKX3.1*, which is expressed only in testis, has the highest substitution rate among the 13 autosomal testis-expressed genes (Table 1.1). On the contrary, most of the X-linked testis-expressed homeobox genes are expressed exclusively or highly in testis and may thus be specifically involved in male reproduction. Many authors showed that genes involved in male reproduction evolve rapidly under positive selection (*e.g.* Lee et al. 1995; Swanson and Vacquier 1995; Metz and Palumbi 1996; Tsaur and Wu 1997; Rooney and Zhang 1999; Wyckoff et al. 2000; Swanson and Vacquier 2002; Podlaha and Zhang 2003). In particular, Torgerson and Singh (2003) recently showed that mammalian X-linked sperm proteins evolve faster than autosomal ones. Our finding of rapid evolution of mammalian X-linked testis-expressed homeobox genes is thus consistent with these previous observations.

Wang *et al.* (2001) reported that the mammalian X chromosome harbors disproportionately more spermatogonia-expressed genes than autosomes. Spermatogonia are the mitotic germ cells of the testis from which sperm arise by spermatogenesis. Spermatogonia-expressed genes are probably involved in male reproduction. In our random sample of 64 homeobox genes, 57% of the 7 X-linked genes and 23% of the 57 autosomal genes are testis expressed. Thus, even for homeobox genes, the X chromosome appears to harbor a higher proportion of testis-expressed genes than autosomes (P = 0.074). If only those genes that are exclusively (or highly selectively) expressed in testis are considered, the X chromosome harbors an even higher percentage of such genes (3/7 = 43%) than autosomes (1/57 = 2%), and their difference is significant (P = 0.003). Sex-chromosome meiotic drive and/or sexual antagonism have been invoked as possible explanations for a higher proportion of X-linked genes to function in male reproduction, and these hypotheses have been discussed extensively in Wang *et al.* (2001).

It has also been proposed that X-linked genes evolve more rapidly than autosomal genes (Charlesworth et al. 1987). This is particularly so when the X-linked genes are expressed only in males, because all newly arising advantageous alleles, dominant or recessive, are exposed to positive Darwinian selection. In contrast, recessive advantageous alleles at autosomal loci are effectively neutral when the allele frequencies are very low. This might explain the effectiveness of positive selection on X-linked testis-expressed genes.

The X chromosome has been shown to be of special importance in hybrid sterility between closely related species (reviewed in Coyne 1992). The importance of homeobox genes in hybrid sterility, however, is not well recognized, probably because most homeobox genes are evolutionarily conserved. It was thus a surprise to identify the rapidly evolving *OdsH*, an X-linked testis-expressed homeobox gene that is in part responsible for the hybrid male sterility between *D. simulans* and *D. mauritiana* (Ting et al. 1998). This study showed that it is a general pattern for mammalian X-linked testis-expressed homeobox genes to evolve rapidly. This suggests the intriguing possibility that it is a rule rather than an exception that homeobox genes such as *OdsH* play important roles in reproductive isolation. In the future, it will be of great interest to work out the developmental pathways in which these homeobox genes function and the biological significance of their rapid pace of evolution.

1.5 MATERIALS AND METHODS

1.5.1 DNA amplification and sequencing

The *TGIFLX* coding region does not contain introns. The coding region was amplified from genomic DNAs of two Old World (OW) monkeys (green monkey *Cercopithecus aethiops* and douc langur *Pygathrix nemaeus*) and five New World (NW) monkeys (marmoset *Callithrix jacchus*, tamarin *Saguinus oedipus*, owl monkey *Aotus trivirgatus*, squirrel monkey *Saimiri sciureus*, and woolly monkey *Lagothrix lagotricha*), using polymerase chain reaction (PCR). For green monkey and douc langur, primers 2XL (5'-TTTGAATATGGAGGCCGCTG) and 2XR (5'-CATCATCAATCATGGATTAG) were used; for tamarin, woolly monkey, and marmoset, primers 2XL and XIA1 (5'-GGATTAGACTCTTGCTTCTTCT) were used; for owl monkey and squirrel monkey, primers X2 (5'-ATATGGAGGCCGCTGCAgAAGAC) and X3 (5'-GGCTCTTGCTTCTTCTCTAGC) were used. PCRs were performed with MasterTaq under conditions recommended by the manufacturer (Eppendorf, Hamburg, Germany). The products were then purified and sequenced from both directions, using the dideoxy chain termination method with an automated sequencer.

1.5.2 Analysis of TGIFLX gene sequences

The DNA sequences of the *TGIFLX* coding region from five hominoids (humans and apes) and four OW monkeys (Blanco-Arias et al. 2002) were obtained from GenBank. The accession numbers are: human (*Homo sapiens*), AJ427749; chimpanzee (*Pan troglodytes*), AJ345073; gorilla (*Gorilla gorilla*), AJ345074; orangutan (*Pongo pygmaeus*), AJ345075; gibbon (*Hylobates lar*), AJ345076; talapoin (*Miopithecus talapoin*), AJ345077; rhesus monkey (*Macaca mulatta*), AJ345078; crab-eating macaque

(*M. fascicularis*), AJ345079; and baboon (*Papio hamadryas*), AJ345080. These publicly available sequences are analyzed together with those determined in this study. Seven amino acids at the N terminus and 10 amino acids at the C terminus of the sequences are encoded by the primer sequences and were not included in data analysis. A total of 16 TGIFLX protein sequences were aligned using the software DAMBE (Xia and Xie 2001) followed by manual adjustments. The DNA sequence alignment was then made following the protein alignment. The MEGA2 program (Kumar et al. 2001) was used for phylogenetic analysis. The number of synonymous nucleotide substitutions per synonymous site (d_S) and that of nonsynonymous substitutions per nonsynonymous site (d_N) were computed using the modified Nei-Gojobori method (Nei and Gojobori 1986; Zhang et al. 1998), with an estimated transition/transversion ratio of 1.6. On the basis of the phylogeny of the 16 primates, we inferred ancestral *TGIFLX* sequences at all interior nodes of this tree, using the distance-based Bayesian method (Zhang and Nei 1997). The numbers of synonymous (*s*) and nonsynonymous (*n*) substitutions on each branch of the tree were then counted. Radical and conservative nonsynonymous substitutions with regard to amino acid charge and polarity were computed following Zhang (2000). Positive selection at individual codons was tested using the likelihood-based (Yang et al. 2000) and parsimony-based (Suzuki and Gojobori 1999) methods.

1.5.3 Analysis of other homeobox genes of human and mouse

We searched for homeobox genes from the human genome resources (http://www.ncbi.nlm.nih.gov/genome/guide/human/) and then found their mouse orthologs using the UniGene tool (http://www.ncbi.nlm.nih.gov/entrez/query.fcgi?db=unigene). We downloaded the human and mouse protein sequences, aligned them using DAMBE, and computed protein *p*-distances (proportional differences; Nei and Kumar 2000) between human and mouse orthologs. The information on gene location and expression pattern was found using human genome resources and the LocusLink tool (http://www.ncbi.nlm.nih.gov/LocusLink/).

1.6 ACKNOWLEDGMENTS

We thank Lizhi Gao, Ondrej Podlaha, David Webb, and two anonymous reviewers for valuable comments. This work was supported by a startup fund from the University of Michigan and a National Institutes of Health grant (GM67030) to J.Z.

Figure 1.1 Phylogenetic tree of *TGIFLX*, *TGIF2*, and *TGIF* genes. The tree is reconstructed with the neighbor-joining method with the protein Poisson distances. Bootstrap percentages from 1000 replications are shown on tree branches. Branch lengths show the numbers of amino acid substitutions per site. *TGIF* genes are used as outgroups.

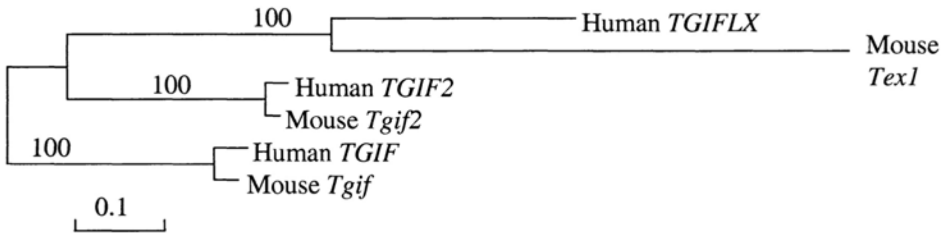

Figure 1.2 Alignment of TGIFLX sequences of 16 primates. A dot indicates identity to the human sequence and a dash indicates a gap. The first 7 and last 10 amino acid positions are primer encoded in various sequences and are not used in subsequent sequence analysis. The four positively selected sites with posterior probabilities >90% (see text) are in boldface type.

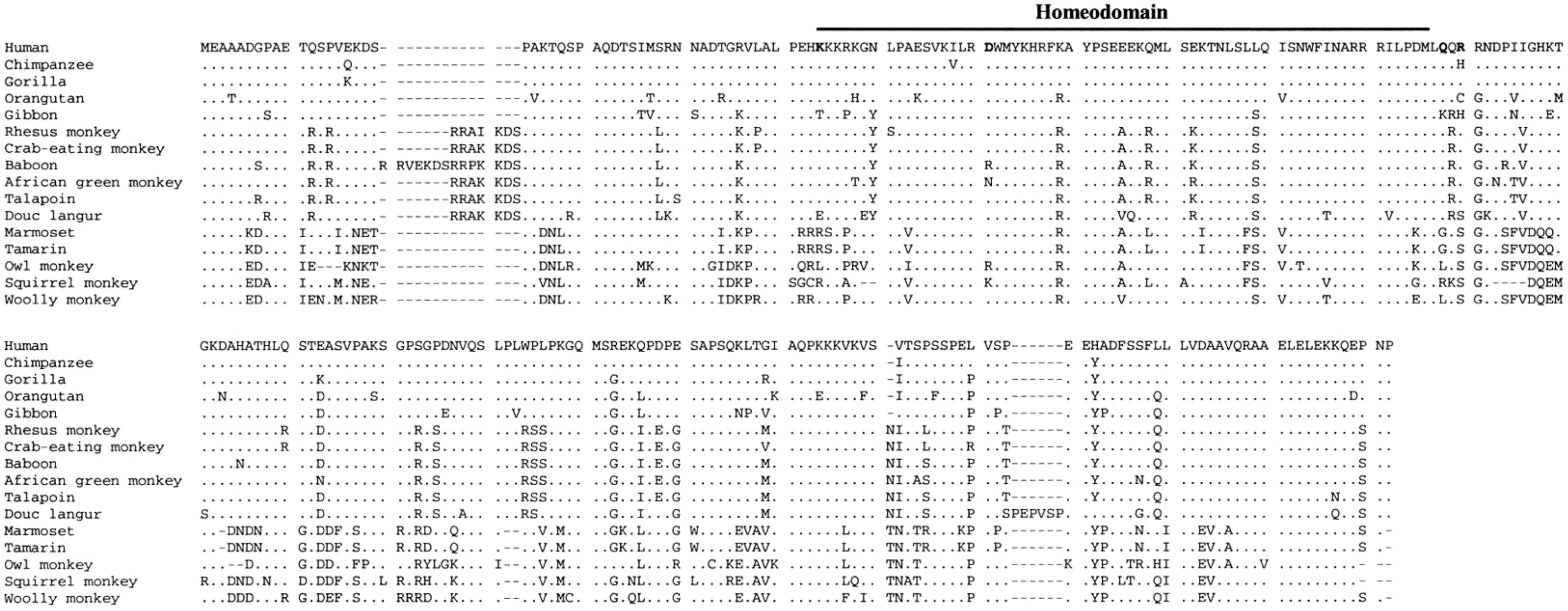
Homeodomain

```
Human                MEAAADGPAE TQSPVEKDS- ---------- ---PAKTQSP AQDTSIMSRN NADTGRVLAL PEHKKKRKGN LPAESVKILR DWMYKHRFKA YPSEEEKQML SEKTNLSLLQ ISNWFINARR RILPDMLQQR RNDPIIGHKT
Chimpanzee           .......... .....Q...- ---------- ---....... .......... .......... .......... .......V.. .......... .......... .......... .......... .........H ..........
Gorilla              .......... .....K...- ---------- ---....... .......... .......... .......... .......... .......... .......... .......... .......... .......... ..........
Orangutan            ...T...... .........- ---------- ---.V..... ......T... ...R...... .......H.. ...K...... ........R. .......... .......... V......... .........C G...V....M
Gibbon               .......S.. .........- ---------- ---....... .....TV... S....K.... ...T..P..Y .......... .......... .......... ........S. .......... .......KRH G...N...E.
Rhesus monkey        .......... .R.R.....- ------RRAI KDS....... .......L.. .....K.P.. .........Y S......... ........R. ....A..R.. .K......S. .......... .........R. G....V....
Crab-eating monkey   .......... .R.R.....- ------RRAK KDS....... .......L.. .....K.P.. .........Y .......... ........R. ....A..R.. .K......S. .......... .........R. G....V....
Baboon               ......S... .R.R.....R RVEKDSRRPK KDS....... .......L.. .....K.... .........Y .......... R.......R. ....A..R.. .K......S. .......... .........R. G..R.V....
African green monkey .......... .R.R.....- ------RRAK KDS....... .......L.. .....K.... .......T.Y .......... N.......R. ....A..R.. .R......S. .......... .........R. G.N.TV....
Talapoin             ......R... .R.R.....- ------RRAK KDS....... .......L.S .....K.... .........Y .......... ........R. ....A..R.. .K......S. .......... .........R. G...TV....
Douc langur          .......R.. .R.......- ------RRAK KDS.....R. .......LK. .....K.... ...E....EY .......... ........R. ....VQ.... .R......S. .....T.... .V......RS GK...V....
Marmoset             .....KD... I...I.NET- ---------- ---..DNL.. .......... ...I.KP... .RRRS.P... ..V....... ........R. ....A..L.. ..I....FS. V......... ....K..G.S G..SFVDQQ.
Tamarin              .....KD... I...I.NET- ---------- ---..DNL.. .......... ...I.KP... .RRRS.P... ..V....... ........R. ....A..L.. ..I....FS. V......... ....K..G.S G..SFVDQQ.
Owl monkey           .....ED... IE---KNKT- ---------- ---..DNLR. .....MK... ..GIDKP... .QRL..PRV. ..I....... R.......R. ....A..... .......FS. V.T....... ....K..L.S G..SFVDQEM
Squirrel monkey      .....EDA.. I...M.NE.- ---------- ---..VNL.. .....M.... ...IDKP... SGCR..A.-- ..V....... K.......R. ....A..L.. A......FS. .....V.... ....G..RKS G.----DQEM
Woolly monkey        .....ED... IEN.M.NER- ---------- ---..DNL.. ........K. ...IDKPR.. .RR...P... ..V....... ........R. ....V..... ........S. V....T.... ....E..L.S G..SFVDQEM

Human                GKDAHATHLQ STEASVPAKS GPSGPDNVQS LPLWPLPKGQ MSREKQPDPE SAPSQKLTGI AQPKKKVKVS -VTSPSSPEL VSP------E EHADFSSFLL LVDAAVQRAA ELELEKKQEP NP
Chimpanzee           .......... .......... .......... .......... .......... .......... .......... -I........ ...------. .Y........ .......... .......... ..
Gorilla              .......... ..K....... .......... .......... ..G....... ........R. .......... -I.......P ...------. .Y........ .......... .......... ..
Orangutan            ..N....... ..D.....S. .......... .......... ..G..L.... .........K ...E....F. -I...F...P ...------. .Y......Q. .......... ........D. ..
Gibbon               .......... ..D....... .....E.... ..V....... ..G..L.... .....NP.V. .......... -........P .P.------. .YP.....Q. .......... .......... ..
Rhesus monkey        .........R ..D....... ..R.S..... ...RSS.... ..G..I.E.G ........M. .......... NI..L....P ..T------. .Y......Q. .......... .........S ..
Crab-eating monkey   .........R ..D....... ..R.S..... ...RSS.... ..G..I.E.G ........V. .......... NI..L....R ..T------. .Y......Q. .......... .........S ..
Baboon               ....N..... ..D....... ..R.S..... ...RSS.... ..G..I.E.G ........M. .......... NI..S....P ..T------. .Y......Q. .......... .........S ..
African green monkey .......... ..N....... ..R.S..... ...RSS.... ..G..I.E.G ........M. .......... NI.AS....P ..T------. .Y....N.Q. .......... .........S ..
Talapoin             .......... ..D....... ..R.S..... ...RSS.... ..G..I.E.G ........M. .......... NI..S....P ..T------. .Y......Q. .......... ......N..S ..
Douc langur          S......... ..D....... ..R.S..A.. ...RS..... ..G..I...G ........M. .......... NI..S....P ..SPEPVSP. ......G.Q. .......... ......Q..S ..
Marmoset             ..-DNDN... G.DDF.S... R.RD..Q... .--..V.M.. ..GK.L...G W....EVAV. ......L... TN.TR...KP .P.------. .YP...N..I ..EV.A.... .........S .-
Tamarin              ..-DNDN... G.DDF.S... R.RD..Q... .--..V.M.. ..GK.L...G W....EVAV. ......L... TN.TR...KP .P.------. .YP...N..I ..EV.A.... .........S .-
Owl monkey           ...--D.... G.DD..FP.. ..RYLGK... I--..V.M.. .....L...R ..C.KE.AVK ......L... TN.T.....P ...------K .YP..TR.HI ..EV.A...V .........- --
Squirrel monkey      R..DND.N.. D.DDF.S..L R.RH..K... .--..V.M.. ..G.NL...G L...RE.AV. ......LQ.. TNAT.....P ...------. .YP.LT..QI ..EV...... .........- --
Woolly monkey        ...DDD...R G.DEF.S... RRRD..K... .--..V.MC. ..G.QL...G .....E.AV. ......F.I. TN.T.....P ...------. .YP.....QI ..EV...... .........S .-
```

Figure 1.3 Pairwise comparisons of d_S and d_N among 16 primate *TGIFLX* sequences for (**A**) the entire sequence, (**B**) nonhomeodomain regions, and (**C**) the homeodomain.

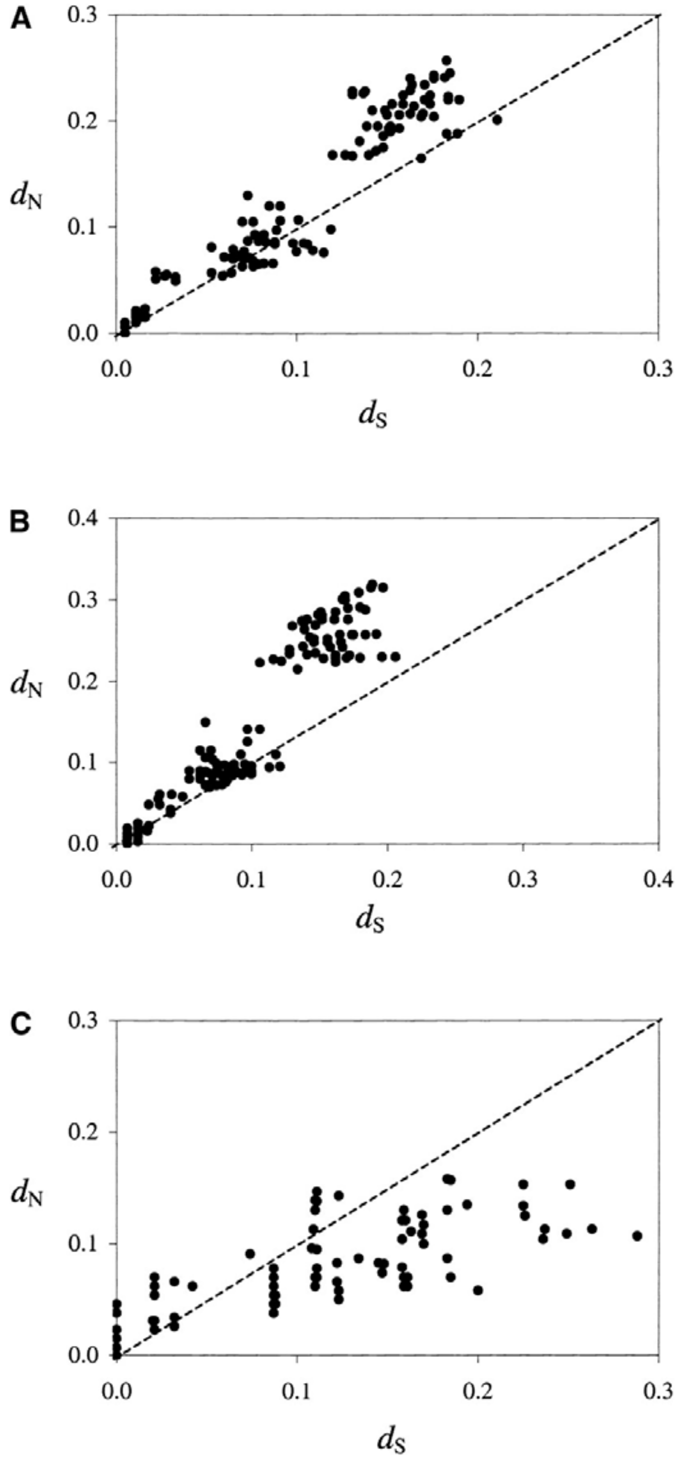

Figure 1.4 Numbers of synonymous (*s*) and nonsynonymous (*n*) substitutions in the evolution of primate *TGIFLX* genes. Shown above each branch is *n*/*s* for the nonhomeodomain regions and below each branch is *n*/*s* for the homeodomain. *N* and *S* are the potential numbers of nonsynonymous and synonymous sites, respectively (see text).

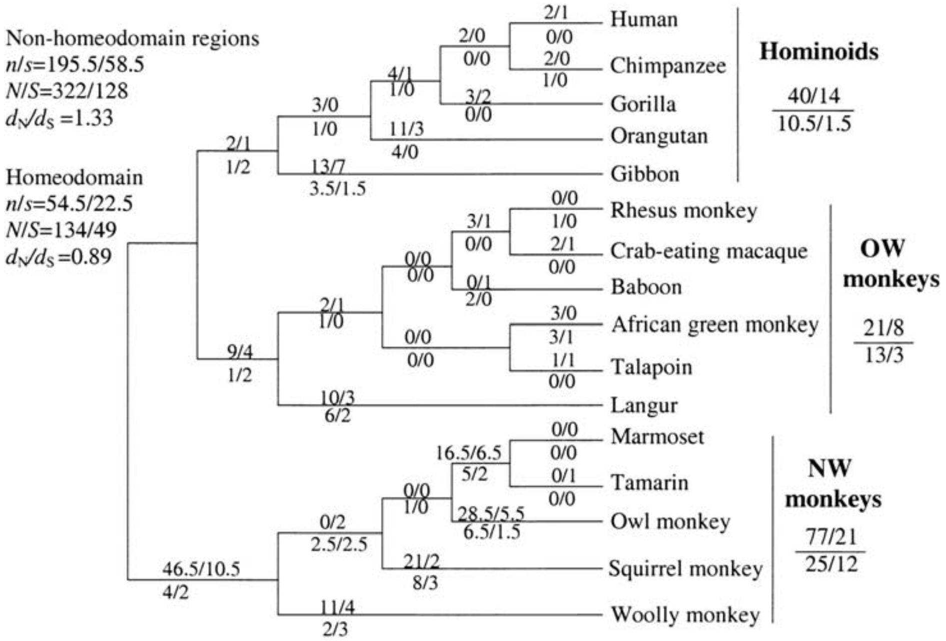

Figure 1.5 Distribution of the evolutionary rate of 64 mammalian homeobox genes. The evolutionary rate is measured by protein *p*-distance between the human and mouse orthologous genes for (**A**) the entire sequence, (**B**) the homeodomain, and (**C**) nonhomeodomain regions. Solid bars, X-linked testis-expressed genes; shaded bars, X-linked non-testis expressed; hatched bars, autosomal testis expressed; open bars, autosomal non-testis expressed.

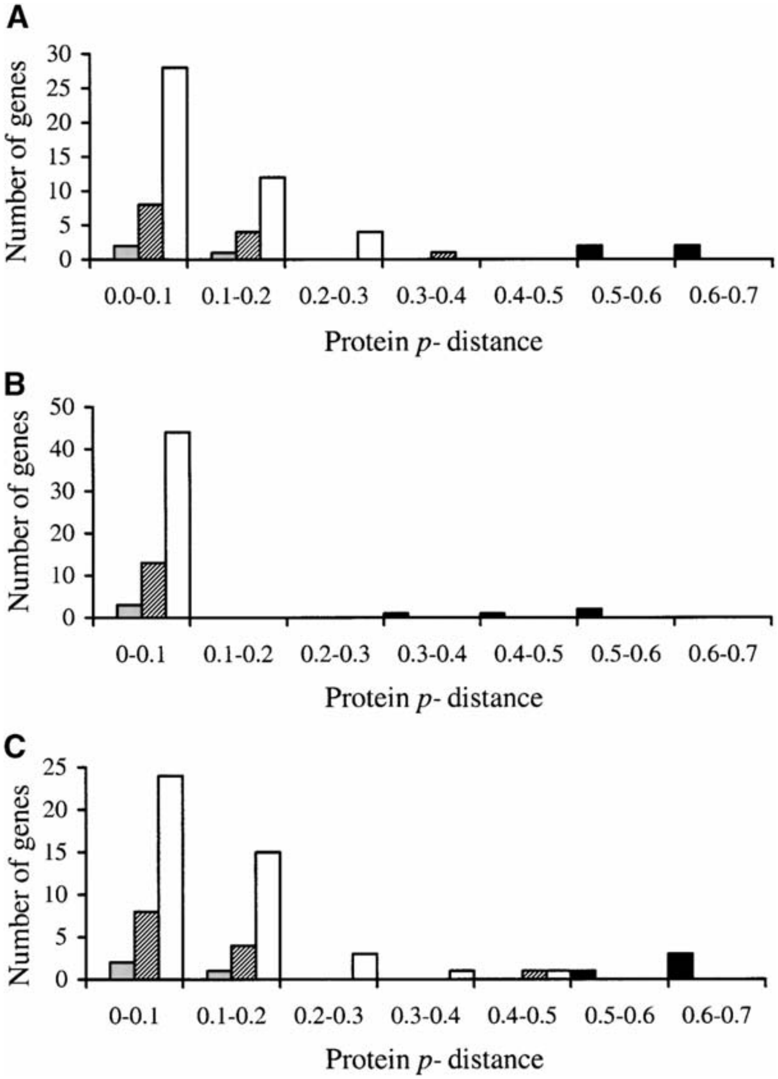

Table 1.1 Protein *p*-distances between orthologous human and mouse homeobox genes.

		Protein *p*-distance		
Gene name	Protein length (amino acids)	Entire protein	homeodomain	Non-homeodomain region
X-linked, testis expressed				
TGIFLX	222	0.550	0.456	0.582
ESX1L	310	0.565	0.333	0.620
OTEX	176	0.625	0.544	0.664
PEPP-2	208	0.606	0.526	0.636
Mean±s.e.m		0.587±0.018	0.465±0.048	0.626±0.017
X-linked, non-testis expressed				
ARX	560	0.036	0.000	0.040
CDX4	282	0.167	0.017	0.207
POU3F4	361	0.011	0.000	0.013
Mean±s.e.m		0.071±0.048	0.006±0.006	0.087±0.061
Autosomal, testis expressed				
IRX2	471	0.104	0.000	0.119
LHX2	389	0.010	0.000	0.012
LHX9	321	0.006	0.000	0.007
NKX3.1	230	0.322	0.000	0.435
NKX6-2	277	0.029	0.000	0.036
PBX2	430	0.021	0.000	0.024
PKNOX2	305	0.011	0.000	0.012
TIX1 [a]	949	0.144	0.037	0.175
ZHX3 [a]	522	0.123	0.030	0.154
SIX1	273	0.015	0.000	0.019
TGIF	272	0.103	0.000	0.134
TGIF2	237	0.063	0.000	0.084
ZFHX1B	1214	0.034	0.017	0.035
Mean±s.e.m		0.076±0.024	0.006±0.004	0.096±0.033
Autosomal, non-testis expressed				
ALX3	343	0.085	0.000	0.102
ALX4	397	0.111	0.000	0.129
BAPX1	333	0.153	0.000	0.187
BARX2	254	0.130	0.000	0.162
CRX	299	0.033	0.000	0.042
DLX4	168	0.274	0.017	0.417
GHS-2	303	0.092	0.000	0.114
HHEX	303	0.070	0.018	0.085
IPF1	283	0.120	0.000	0.150
IRX3	501	0.102	0.000	0.116
IRX4	512	0.158	0.000	0.180
IRX5	417	0.113	0.000	0.132
IRX6	438	0.233	0.048	0.263
LHX1	406	0.005	0.000	0.006
LHX3	398	0.101	0.000	0.117
LHX4	367	0.008	0.000	0.010
LHX5	402	0.012	0.000	0.014
LHX6	340	0.168	0.000	0.201
LMX1A	382	0.029	0.000	0.034
LMX1B	372	0.003	0.000	0.003
OTX1	354	0.025	0.000	0.030
PHOX2A	280	0.021	0.000	0.027
PHOX2B	314	0.000	0.000	0.000
PITX1	314	0.035	0.000	0.043
PITX2	317	0.013	0.000	0.015
PITX3	302	0.017	0.000	0.020
PKNOX1	314	0.039	0.000	0.045
PROP1	223	0.265	0.070	0.331
PROX1	736	0.023	0.000	0.025
PRX2	246	0.077	0.000	0.102
RAX	342	0.140	0.000	0.170
SHOX2	330	0.015	0.000	0.019
SIX2	436	0.014	0.023	0.012
SIX3	332	0.024	0.000	0.029
SIX4	753	0.089	0.000	0.103
SIX5	657	0.139	0.000	0.150
SIX6	246	0.024	0.017	0.027
TLX1	330	0.027	0.000	0.033
TLX2	284	0.070	0.000	0.088
TLX3	291	0.010	0.000	0.013
VAX1	279	0.029	0.000	0.036
VAX2	290	0.121	0.000	0.150
VSX1	354	0.229	0.040	0.260
ZFH4	3525	0.082	0.009	0.087
Mean±s.e.m		0.080±0.011	0.006±0.002	0.097±0.014

[a] The mouse sequence is not available. Instead, the rat sequence is analyzed here.

1.7 LITERATURE CITED

Banerjee-Basu S, Baxevanis AD (2001) Molecular evolution of the homeodomain family of transcription factors. Nucleic Acids Research 29:3258-3269

Bertolino E, Reimund B, WildtPerinic D, Clerc RG (1995) A novel homeobox protein which recognizes a TGT core and functionally interferes with a retinoid-responsive motif. Journal of Biological Chemistry 270:31178-31188

Bharathan G, Janssen BJ, Kellogg EA, Sinha N (1997) Did homeodomain proteins duplicate before the origin of angiosperms, fungi, and metazoa? Proceedings of the National Academy of Sciences of the United States of America 94:13749-13753

Blanco-Arias P, Sargent CA, Affara NA (2002) The human-specific Yp11.2/Xq21.3 homology block encodes a potentially functional testis-specific TGIF-like retroposon. Mammalian Genome 13:463-468

Burglin TR (1997) Analysis of TALE superclass homeobox genes (MEIS, PBC, KNOX, Iroquois, TGIF) reveals a novel domain conserved between plants and animals. Nucleic Acids Research 25:4173-4180

Charlesworth B, Coyne JA, Barton NH (1987) The Relative Rates of Evolution of Sex-Chromosomes and Autosomes. American Naturalist 130:113-146

Coyne JA (1992) Genetics and Speciation. Nature 355:511-515

Dagan T, Talmor Y, Graur D (2002) Ratios of radical to conservative amino acid replacement are affected by mutational and compositional factors and may not be indicative of positive Darwinian selection. Molecular Biology and Evolution 19:1022-1025

Garciafernandez J, Holland PWH (1994) Archetypal Organization of the Amphioxus Hox Gene-Cluster. Nature 370:563-566

Gehring WJ, Affolter M, Burglin T (1994a) Homeodomain Proteins. Annual Review of Biochemistry 63:487-526

Gehring WJ, Qian YQ, Billeter M, Furukubotokunaga K, Schier AF, Resendezperez D, Affolter M, Otting G, Wuthrich K (1994b) Homeodomain-DNA Recognition. Cell 78:211-223

Goodman M, Porter CA, Czelusniak J, Page SL, Schneider H, Shoshani J, Gunnell G, Groves CP (1998) Toward a phylogenetic classification of primates based on DNA evidence complemented by fossil evidence. Molecular Phylogenetics and Evolution 9:585-598

Kappen C (2000) The homeodomain: an ancient evolutionary motif in animals and plants. Computers & Chemistry 24:95-103

Kappen C, Schughart K, Ruddle FH (1993) Early Evolutionary Origin of Major Homeodomain Sequence Classes. Genomics 18:54-70

Kumar S, Tamura K, Jakobsen IB, Nei M (2001) MEGA2: molecular evolutionary genetics analysis software. Bioinformatics 17:1244-1245

Lai YL, Li H, Chiang HS, Hsieh-Li HM (2002) Expression of a novel TGIF subclass homeobox gene, Tex1, in the spermatids of mouse testis during spermatogenesis. Mechanisms of Development 113:185-187

Lee YH, Ota T, Vacquier VD (1995) Positive Selection Is a General Phenomenon in the Evolution of Abalone Sperm Lysin. Molecular Biology and Evolution 12:231-238

Lifschyt E, Lindsley DL (1972) Role of X-Chromosome Inactivation during Spermatogenesis. Proceedings of the National Academy of Sciences of the United States of America 69:182-&

Long M (2001) Evolution of novel genes. Current Opinion in Genetics & Development 11:673-680

Mcginnis W, Garber RL, Wirz J, Kuroiwa A, Gehring WJ (1984) A Homologous Protein-Coding Sequence in Drosophila Homeotic Genes and Its Conservation in Other Metazoans. Cell 37:403-408

Melhuish TA, Gallo CM, Wotton D (2001) TGIF2 interacts with histone deacetylase I and represses transcription. Journal of Biological Chemistry 276:32109-32114

Melhuish TA, Wotton D (2000) The interaction of the carboxyl terminus-binding protein with the Smad corepressor TGIF is disrupted by a holoprosencephaly mutation in TGIF. Journal of Biological Chemistry 275:39762-39766

Metz EC, Palumbi SR (1996) Positive selection and sequence rearrangements generate extensive polymorphism in the gamete recognition protein bindin. Molecular Biology and Evolution 13:397-406

Nei M, Gojobori T (1986) Simple Methods for Estimating the Numbers of Synonymous and Nonsynonymous Nucleotide Substitutions. Molecular Biology and Evolution 3:418-426

Page SL, Goodman M (2001) Catarrhine phylogeny: Noncoding DNA evidence for a diphyletic origin of the mangabeys and for a human-chimpanzee clade. Molecular Phylogenetics and Evolution 18:14-25

Podlaha O, Zhang JZ (2003) Positive selection on protein-length in the evolution of a primate sperm ion channel. Proceedings of the National Academy of Sciences of the United States of America 100:12241-12246

Rooney AP, Zhang JZ (1999) Rapid evolution of a primate sperm protein: Relaxation of functional constraint or positive Darwinian selection? Molecular Biology and Evolution 16:706-710

Scott MP, Weiner AJ (1984) Structural Relationships among Genes That Control Development - Sequence Homology between the Antennapedia, Ultrabithorax, and Fushi Tarazu Loci of Drosophila. Proceedings of the National Academy of Sciences of the United States of America-Biological Sciences 81:4115-4119

Singer SS, Schmitz J, Schwiegk C, Zischler H (2003) Molecular cladistic markers in New World monkey phylogeny (Platyrrhini, Primates). Molecular Phylogenetics and Evolution 26:490-501

Smith NGC (2003) Are radical and conservative substitution rates useful statistics in molecular evolution? Journal of Molecular Evolution 57:467-478

Steiper ME, Ruvolo M (2003) New World monkey phylogeny based on X-linked G6PD DNA sequences. Molecular Phylogenetics and Evolution 27:121-130

Sutton KA, Wilkinson MF (1997) Rapid evolution of a homeodomain: Evidence for positive selection. Journal of Molecular Evolution 45:579-588

Suzuki Y, Gojobori T (1999) A method for detecting positive selection at single amino acid sites. Molecular Biology and Evolution 16:1315-1328

Suzuki Y, Nei M (2002) Simulation study of the reliability and robustness of the statistical methods for detecting positive selection at single amino acid sites. Molecular Biology and Evolution 19:1865-1869

Swanson WJ, Vacquier VD (1995) Extraordinary Divergence and Positive Darwinian Selection in a Fusagenic Protein Coating the Acrosomal Process of Abalone Spermatozoa. Proceedings of the National Academy of Sciences of the United States of America 92:4957-4961

Swanson WJ, Vacquier VD (2002) The rapid evolution of reproductive proteins. Nature Reviews Genetics 3:137-144

Ting CT, Tsaur SC, Wu ML, Wu CI (1998) A rapidly evolving homeobox at the site of a hybrid sterility gene. Science 282:1501-1504

Tsaur SC, Wu CI (1997) Positive selection and the molecular evolution of a gene of male reproduction, Acp26Aa of Drosophila. Molecular Biology and Evolution 14:544-549

Wayne CM, MacLean JA, Cornwall G, Wilkinson MF (2002) Two novel human X-linked homeobox genes, hPEPP1 and hPEPP2, selectively expressed in the testis. Gene 301:1-11

Wyckoff GJ, Wang W, Wu CI (2000) Rapid evolution of male reproductive genes in the descent of man. Nature 403:304-309

Xia X, Xie Z (2001) DAMBE: Software package for data analysis in molecular biology and evolution. Journal of Heredity 92:371-373

Yang ZH, Nielsen R, Goldman N, Pedersen AMK (2000) Codon-substitution models for heterogeneous selection pressure at amino acid sites. Genetics 155:431-449

Zhang JZ (2000) Rates of conservative and radical nonsynonymous nucleotide substitutions in mammalian nuclear genes. Journal of Molecular Evolution 50:56-68

Zhang JZ (2003) Evolution by gene duplication: an update. Trends in Ecology & Evolution 18:292-298

Zhang JZ, Nei M (1996) Evolution of antennapedia-class homeobox genes. Genetics 142:295-303

Zhang JZ, Nei M (1997) Accuracies of ancestral amino acid sequences inferred by the parsimony, likelihood, and distance methods. Journal of Molecular Evolution 44:S139-S146

Zhang JZ, Rosenberg HF (2002) Diversifying selection of the tumor-growth promoter angiogenin in primate evolution. Molecular Biology and Evolution 19:438-445

Zhang JZ, Rosenberg HF, Nei M (1998) Positive Darwinian selection after gene duplication in primate ribonuclease genes. Proceedings of the National Academy of Sciences of the United States of America 95:3708-3713

CHAPTER 2

RAPID EVOLUTION OF PRIMATE *ESX1*, AN X-LINEKD PLACENTA- AND TESTIS-EXPRESSED HOMEOBOX GENE

2.1 ABSTRACT

Homeobox genes encode transcription factors that play important roles in various developmental processes and are usually evolutionarily conserved. Here we report a case of rapid evolution of a homeobox gene in humans and non-human primates. *ESX1* is an X-linked homeobox gene primarily expressed in the placenta and testis, with physiological functions in placenta/fetus development and spermatogenesis. *ESX1* is paternally imprinted in mice, but is not imprinted in humans. We provide evidence for a significantly higher nonsynonymous substitution rate than synonymous rate in *ESX1* between humans and chimps as well as among a total of 15 primate species. Population genetic data also show signals of recent selective sweeps within humans. Positive selection appears to be concentrated in the C-terminal non-homeodomain region, which has been implicated in regulating human male germ cell division by prohibiting the degradation of cyclins. By contrast, mouse *Esx1* has a substantively different C-terminal region subject to strong purifying selection. These and other results suggest that even the fundamental process of spermatogenesis has been targeted by positive selection in primate and human evolution and that mouse may not be a suitable model for studying human reproduction.

2.2 INTRODUCTION

Homeobox genes are characterized by the presence of a sequence motif known as the homeobox, which encodes the ~60-amino-acid homeodomain, a helix-turn-helix DNA binding domain (Gehring et al. 1994). In humans, there are about 230 homeobox genes (Nam and Nei 2005), encoding a large family of transcription factors that play key roles in various developmental processes such as body-plan specification, pattern formation, and cell-fate determination (Gehring et al. 1994). Due to their functional importance, most homeodomain proteins are evolutionarily highly conserved in sequence (McGinnis et al. 1984; Gehring et al. 1994; Zhang and Nei 1996). Hence, the identification of non-conserved homeobox genes would be particularly interesting, because such homeobox genes may regulate important developmental processes that vary among relatively closely related species. Three such rapidly-evolving homeobox genes are known, from fruit flies (*OdsH*), rodents (*Rhox5*), and primates (*TGIFLX*), respectively. *OdsH* is an X-linked gene involved in spermatogenesis and it is partly responsible for the hybrid male sterility between *Drosophila simulans* and *D. mauritiana* (Ting et al. 1998). Mouse *Rhox5* (also known as *Pem*) is expressed in both male and female reproductive tissues (Sutton and Wilkinson 1997). Targeted disruption of *Rhox5* increases male germ cell apoptosis and reduces sperm production, sperm motility, and fertility (Maclean et al. 2005). In fact, *Rhox5* is just one member of a recently expanded homeobox gene cluster known as the Rhox cluster on the mouse X chromosome (Maclean et al. 2005; MacLean et al. 2006; Morris et al. 2006; Wang and Zhang 2006). Several other members of the cluster are also expressed in reproductive tissues (Maclean et al. 2005) and evolve rapidly (Jackson et al. 2006; Wang and Zhang 2006). *TGIFLX* is a retroduplicate formed in the common ancestor of primates and rodents by retroposition of the autosomal gene *TGIF2* to the X chromosome, and is specifically expressed in the germ cells of adult testis (Wang and Zhang 2004). Interestingly, each of the three cases involves a homeobox gene that is X-linked and testis-expressed. Here we report yet another case of rapid evolution of an X-linked testis-expressed homeobox gene, *ESX1*.

Human *ESX1*, also known as *ESX1L* and *ESXR1*, is a paired-like homeobox gene located on Xq22.1 (Fohn and Behringer 2001). ESX1 protein contains two functional domains, the homeodomain and the proline-rich domain (Figure 2.1A) (Fohn and Behringer 2001). Esx1, the mouse ortholog, has an extra domain known as the PN/PF motif, located at the C-terminus (Figure 2.1B) (Yan et al. 2000). In humans, *ESX1* is specifically expressed in placenta from 5 weeks of gestation until term (Figueiredo et al. 2004) and in adult testis (Fohn and Behringer 2001). A recent study shows decreased *ESX1* expression in human pre-term idiopathic fetal growth restriction, a clinically significant pregnancy disorder in which the fetus fails to achieve its full growth potential in utero (Murthi et al. 2006). In mice, *Esx1* is also expressed in placenta and testis (Branford et al. 1997; Li et al. 1997). More specifically, during embryogenesis, it is expressed in the extraembryonic tissues, including the endoderm of the visceral yolk sac, the ectoderm of the chorion, and subsequently the labyrinthine trophoblast of the chorioallantoic placenta (Li et al. 1997). In adults, *Esx1* is expressed in male germ cells only, particularly the spermatogonia/preleptotene spermatocytes and round spermatids of spermatogenic stages IV-VII (Branford et al. 1997; Li et al. 1997). These restricted temporal and spatial expression patterns suggest that ESX1/Esx1 is involved in placental development and spermatogenesis. Mouse *Esx1* is paternally imprinted in the placenta, with only the maternally derived allele expressed (Li and Behringer 1998). Heterozygous female mice inheriting a null *Esx1* allele from their mother are born 20% smaller than normal, suggesting that *Esx1* is required for placental development and fetal growth in mice (Li and Behringer 1998). By contrast, biparental expression of *ESX1* is found in human placenta (Grati et al. 2004).

Our preliminary comparison between human ESX1 and mouse Esx1 proteins showed an unexpectedly high level of sequence divergence (34%), suggesting that the gene might be evolving rapidly in primates and/or rodents as a result of positive Darwinian selection (Wang and Zhang 2004). Below we first describe the evolutionary pattern of *ESX1* in primates and then compare it to the evolutionary pattern in rodents. We show that positive selection has acted on *ESX1* within humans, between humans and chimpanzees, and among a large array of primate species, whereas purifying selection has dominated *Esx1* evolution in rodents. We discuss these evolutionary patterns in light of the structure and function of the gene.

2.3 RESULTS

2.3.1 Comparison of *ESX1* sequences between humans and chimps and within humans

We obtained the *ESX1* gene sequence from the chimpanzee genome sequence (http://genome.wustl.edu/) and compared it with the human *ESX1* sequence available in GenBank (AY114148). The alignment shows a high level of sequence divergence. Of the aligned 406 amino acid sites, there are 25 amino acid replacements, in addition to two gaps totaling 12 amino acids (Figure 2.2). A comparison of synonymous (d_S) and nonsynonymous (d_N) nucleotide distances between gene sequences can inform us about the nature and strength of selection acting on a gene. A higher d_N than d_S indicates positive selection, whereas a lower d_N than d_S indicates negative or purifying selection. The vast majority of genes in the human genome are under negative selection, with a genomic average d_N/d_S ratio of 0.26 (Bakewell et al. 2007). In *ESX1*, however, d_N (0.031) is significantly greater than d_S (0.009) ($P = 0.028$; Fisher's exact test (Zhang et al. 1997)). Because the d_S value of *ESX1* is not significantly different from the genomic average d_S of 0.012 (Consortium 2005), the above observation strongly suggests that positive selection has promoted nonsynonymous substitutions in *ESX1* during the divergence between humans and chimps.

To identify the regions where positive selection has been operating, we divided the ESX1 protein sequence into three segments, the N-terminus, homeodomain, and C-terminus (Figure 2.2). The homeodomain is completely identical in amino acid sequence between human and chimp and thus has not been targeted by positive selection ($d_N = 0$, $d_S = 0.019$, $P = 0.29$; Fisher's exact test). In the N-terminus, d_N (0.024) and d_S (0) are not significantly different ($P = 0.1$) and hence neutrality cannot be rejected. In the C-terminus, however, d_N (0.047) is significantly greater than d_S (0.012) ($P = 0.035$). Thus, positive selection has been concentrated in the C-terminus. As aforementioned, the C-terminus is mainly composed of proline-rich repeats. The two alignment gaps between human and chimp also occur in the C-terminus (Figure 2.2). Compared to the human sequence, the chimp sequence lost a complete nine-amino-acid repeat and part of another repeat.

To further examine whether the positive selection might have happened in the recent history of human evolution, we sequenced exon 4 of *ESX1* in 32 unrelated male humans of diverse geographic origins (4 Pygmy Africans, 6 African Americans, 12 Caucasians, 3 Southeast Asians, 2 Chinese, 2 Pacific Islanders, and 3 Andes Indians). Exon 4 encodes 14 amino acids of the homeodomain, corresponding roughly to the third helix of the homeodomain, and the complete C-terminus of ESX1, the likely target of positive selection (Figures 2.1 and 2.2). From the 32 alleles, we observed 4 insertion/deletion (indel) polymorphisms and 9 single nucleotide polymorphisms (SNPs). All of these polymorphisms occur in the C-terminus (non-homeodomain) region and none of them disrupt the open reading frame (Figure 2.2). Table 2.1 lists the polymorphisms and their associated allele frequencies. The polymorphic data allow us to compute the level of DNA polymorphism in exon 4. Nucleotide diversity per sequence (π) is 0.897 and Watterson's polymorphism per sequence (θ) is 1.27. A comparison between expected and observed distributions of allelic frequencies can tell us whether a genomic region is likely to have been subject to recent selective sweeps, which render π lower than θ and high-frequency alleles enriched, generating negative values of Tajima's *D* (Tajima 1989) and Fay and Wu's *H* (Fay and Wu 2000). Combining the information from *D* and *H*, Zeng and colleagues recently invented a new test known as the *DH* test of positive selection (Zeng et al. 2006). This test is superior to the individual *D* and *H* tests because it is more powerful and is insensitive to common confounding factors such as background selection, population growth, and population subdivision (Zeng et al. 2006). We found that the *DH* test rejects the neutral hypothesis for the exon 4 sequences of 32 humans (P<0.039). For samples with African, Caucasian, and Asian origins, the tail probability of the *DH* test is 0.067, 0.31, and 0.26, respectively. Thus, selective sweeps might have occurred among Africans. Consistent with this result, the *H* test also yields a significant result for the African samples (*P*=0.044), and this *P* value is lower than 128 of the 132 genes that were recently surveyed in Africans (Akey et al. 2004). In other words, *ESX1* is among the bottom 3% of human genes for *H* value in Africans. These results support the hypothesis of recent selective sweeps at human *ESX1* or linked genomic regions. We also sequenced exons 1, 2, and 3 of *ESX1* in 8 male humans with diverse geographic origins (1 Pygmy African, 3 African Americans, 1 Caucasian, 2 Chinese, and 1 Pacific Islander), but observed no polymorphisms.

2.3.2 Positive selection at the C-terminus of ESX1 in many primates

To examine whether *ESX1* has also been under positive selection in other primates, we obtained the rhesus monkey *ESX1* gene sequence by searching its recently completed draft genome sequence (http://www.ncbi.nlm.nih.gov/). We then sequenced exon 4 of *ESX1* in 12 additional primate species, including three hominoids, four Old World monkeys, and five New World monkeys (see Materials and Methods). Together with the three known sequences from human, chimp, and rhesus, a total of 15 primate sequences of exon 4 were conceptually translated and aligned by Clustal W with manual adjustment. DNA sequences were subsequently aligned by following the protein alignment (Figure 2.3A). A gene tree of the 15 sequences was reconstructed using the neighbor-joining method (Saitou and Nei 1987). The tree topology is consistent with the known species tree, suggesting that the sequences analyzed are orthologous to each other. We found that the length of exon 4 is highly variable among species. The shortest proline-rich repeat region is found in marmoset and tamarin, while the longest is observed in orangutan. The nine-amino-acid repeat unit has variable sequences among the primate species, although proline is always the most frequent amino acid.

To examine the potential action of positive selection in exon 4 of primate *ESX1*, we computed pairwise d_N and d_S among the 15 sequences. Excluding alignment gaps, we analyzed a total of 312 nucleotide sites. Higher d_N than d_S is observed in 79 (75.2%) of 105 pairwise comparisons (Figure 2.4A). There is no apparent difference in this pattern among hominoids, Old World monkeys, and New World monkeys. When only the (non-homeodomain) C-terminus is analyzed, 86 (81.9%) comparisons showed $d_N > d_S$ (Figure 2.4B). In our dataset, the average d_S is 0.12 between hominoids and Old World monkeys, 0.18 between hominoids and New World monkeys, and 0.16 between Old World monkeys and New World monkeys. All three numbers are greater than the corresponding values (0.08, 0.12 and 0.15, respectively) previously estimated from multiple different intron and noncoding sequences of the same species pairs (Li 1997). Thus, the synonymous substitution rate of *ESX1* is not reduced and the overall higher d_N over d_S suggests positive selection.

Due to the occurrence of many indels in the proline-rich region of primate ESX1, the sequence alignment may not be reliable. Because closely related species are more likely to share the same repeat sequence, which facilitates alignment, we made separate alignments for hominoids, Old World monkeys, and New World monkeys, respectively (Figure 2.5). The d_N and d_S values were then computed for species pairs within each of the three groups. It happened that each of the three groups has 5 species. Of the 30 pairwise comparisons, 23 (76.7%) show $d_N > d_S$. This finding is similar to the above result when all 15 sequences are aligned and analyzed together.

To test positive selection in primate *ESX1* more rigorously, we conducted a phylogeny-based analysis (22). We inferred the ancestral sequences for the C-terminus at all interior nodes of the primate tree (Figure 2.6) using PAML (Yang 1997) and then counted the numbers of nonsynonymous and synonymous substitutions on each tree branch. We found that the ratio of the total number of nonsynonymous substitutions and that of synonymous substitutions over all branches of the tree equals $n/s = 139/38 = 3.66$, significantly greater than the expected value of N/S=177/93=1.90 (P=0.002, Fisher's exact test). Here N and S are the numbers of nonsynonymous and synonymous sites, respectively, in the C-terminus.

We also conducted a likelihood-based analysis to detect positive selection on individual codons within the C-terminus using PAML. We compared the null model M8a with the alternative model M8. M8a, introduced by Swanson *et al.* (Swanson et al. 2003), assumes that the d_N/d_S ratio of individual codons follows a beta distribution between 0 and 1, with an extra class of codons with fixed d_N/d_S of 1. M8 is identical to M8a except for the presence of an additional class of codons with any d_N/d_S. M8 is found to fit the data significantly better than M8a ($\chi^2 = 49.63$, df = 2, $P < 10^{-10}$). M8 suggests that ~66% of codons in the C-terminus have been subject to positive selection with $d_N/d_S = 4.04$. Analysis using another pair of models, M1a and M2a, also supports a large proportion of codons under positive selection ($\chi^2 = 49.77$, df = 2, $P < 10^{-10}$). Taken together, various analyses provide strong evidence that positive selection has acted in the C-terminus of primate ESX1 to promote amino acid substitutions. We note that although sequence alignment is not easy for ESX1, alignment errors cannot render d_N significantly greater than d_S, because even when the alignment is completely random, d_N is expected to be equal to d_S.

2.3.3 Purifying selection on rodent *Esx1*

To test whether positive selection on ESX1 extends to non-primate mammals, we turn to rodents. We first obtained the *Esx1* gene sequence of *Mus musculus* from GenBank and determined the sequence of exons 2 and 4 of *Esx1* from *M. spretus*. Coding for only two and 15 amino acids, respectively, exons 1 and 3 are not studied here. Esx1 possesses a unique PF/PN motif at its C-terminus, consisting of PF (proline-phenylalanine) tandem repeats followed by PN (proline-asparagine) tandem repeats (Figure 2.1B). An earlier study found that the PF/PN motif can inhibit both nuclear localization and DNA binding activity of the Esx1 protein (Yan et al. 2000). A comparison of exons 2 and 4 sequences of *M. musculus* and *M. spretus* shows strong purifying selection on *Esx1*, as d_N (0.006) is significantly lower than d_S (0.032) ($P = 0.01$, Fisher's exact test). Exon 4 was also sequenced in *M. cervicolor* and *M. cookii* (Figure 2.3B). Significantly lower d_N than d_S is observed in all pairwise comparisons among the four *Mus* species with the exception of the comparison between *M. cervicolor* and *M. cookii*, probably owing to the small number of substitutions involved (Figure 2.4C). Sequence length variation is observed in the PN/PF motif but not in the proline-rich region. Overall, our results suggest that *Esx1* has been subject to purifying selection in the *Mus* genus of rodents.

2.4 DISCUSSION

In this work, we provide evidence for positive selection acting in the C-terminus region of the homeodomain-containing protein ESX1 during primate evolution as well as in human populations. In adult humans, ESX1 is primarily expressed in testis. A previous study showed that ESX1 is proteolytically processed into a 45-kDa N-terminal fragment (including the homeodomain) and a 20-kDa C-terminal fragment. The C-terminal fragment is found in cytoplasm and can inhibit the degradation of cyclin A and B1, causing cell-cycle arrest in human cells (Ozawa et al. 2004). Cyclins are a family of proteins controlling transitions through different phases of the cell cycle. Thus, it has been proposed that the C-terminal fragment of ESX1 plays a role in spermatogenesis, functioning as a checkpoint in male germ cell division (Ozawa et al. 2004). In contrast, the N-terminal fragment, including the homeodomain, functions as a transcriptional repressor in nucleus (Ozawa et al. 2004; Yanagihara et al. 2005). Our observations of conserved sequences in the N-terminal fragment but rapid sequence changes in the C-terminal fragment are explainable by the distinct functions of the two regions. The finding of positive selection in the C-terminus of primate ESX1 suggests that even in the recent past of human and primate evolution, spermatogenesis has been subject to adaptive modifications (Wyckoff et al. 2000). Because different species reach sexual maturity at different ages, the optimal time of germ cell division may also vary among species. The observed positive selection on *ESX1* may reflect such adaptations in individual species. In general, our finding is consistent with many reports of rapid evolution of proteins involved in animal male reproduction (Swanson and Vacquier 2002). Furthermore, mammalian sperm proteins on the X chromosome have been found to evolve faster than those on autosomes (Torgerson and Singh 2003). Thus, the rapid evolution of ESX1 is likely related to its role in spermatogenesis as well as its location in the X chromosome.

Interestingly, male mice with null *Esx1* are fertile, indicating that *Esx1* is not essential for spermatogenesis in mice (Li and Behringer 1998). The observation of purifying selection acting on the C-terminal region of Esx1 in mice may be explained by the fact that the gene function has changed between primates and rodents. It is likely that *Esx1* is more important for placenta development rather than spermatogenesis in mice (Li and Behringer 1998). Biochemical studies also showed that the nuclear localization of mouse Esx1 is regulated by the presence of the PF/PN motif (Yan et al. 2000), which is lacking in primate ESX1, further suggesting functional differences between primate ESX1 and rodent Esx1. To examine the C-terminal sequence of ESX1 in other mammals, we TBLASTN-searched the GenBank with human *ESX1* and mouse *Esx1* as queries. We found putative orthologous *Esx1* genes in rat, dog, and cow. In horse, only a partial sequence was identified by WISE2 (http://www.ebi.ac.uk/Wise2/). We did not find Esx1 orthologs in opossum and chicken genome sequences. The estimated d_N/d_S ratio between mouse and rat in the C-terminal region of Esx1 is significantly lower than 1 (P<0.01), consistent with our findings in the *Mus* genus. Rat Esx1 has a similar domain structure as mouse Esx1, with the exception that all of the PF repeats are replaced by PN repeats in the PF/PN motif. By contrast, the C-terminus of cow and horse Esx1 proteins is similar to that of primates, with the proline-rich region but not the PF/PN motif. The putative Esx1 in dog has neither the proline-rich region nor the PF/PN motif at its C-terminus. It seems likely that the PF/PN motif was acquired by Esx1 in rodent evolution.

The different evolutionary patterns of primate ESX1 and rodent Esx1 suggest that the utility of the mouse model for studying human reproduction may be limited. Previous studies also reported several other reproduction-related genes that show substantive human-mouse differences. For example, SED1, a protein involved in sperm-egg binding in mice, has lost an important protein-protein binding domain in ancestral primates, which was accompanied by rapid sequence changes in another domain by positive selection (Podlaha et al. 2006). In another example, three human X-linked homeobox genes, *PEPP1*, *PEPP2*, and *PEPP3*, correspond to a cluster to 30 *Rhox* genes in mouse, due to dramatic expansions of the gene cluster in rodent evolution (Wang and Zhang 2006). The mouse *Rhox* genes are expressed in male and female reproductive tissues and at least one of them (*Rhox5*) is involved in male reproduction, evident from reduced fertilities of *Rhox5*-knockout mice (Maclean et al. 2005).

Esx1 is paternally imprinted in mouse placenta and is functionally important to placenta morphogenesis and fetal growth (Li et al. 1997; Li and Behringer 1998). In contrast, *ESX1* is not imprinted in human placenta (Grati et al. 2004). Imprinting is an important regulatory pathway involved in the development and function of the placenta in eutherian mammals. The imprinting of *Esx1* is consistent with the general phenomenon in mice that the paternally derived X chromosome is preferentially inactivated in placental tissues of female embryos (West et al. 1977; Wagschal and Feil 2006). Recently, Monk and colleagues reported that several human orthologs of mouse placenta-imprinted genes are un-imprinted (Monk et al. 2006). In addition, an earlier investigation revealed a widespread reduction in the maintenance of imprinting in humans (Morison et al. 2005). If imprinted genes tend to be involved in intra-genomic conflict and hence evolve rapidly by arms race (Haig 1993), our observation of rapid evolution of the un-imprinted primate *ESX1* but slow evolution of imprinted rodent *Esx1* is unexpected. While a change in spermatogenesis function might explain the unexpected evolutionary pattern for *ESX1*/*Esx1*, in the future, it would be interesting to test the genomic conflict hypothesis by comparing the evolutionary rates of all mouse imprinted genes with those of their un-imprinted human orthologs.

2.5 MATERIALS AND METHODS

2.5.1 DNA samples

One individual from each of 12 primate species, 32 male humans, one *Mus spretus*, one *Mus cookie*, and one *Mus cervicolor* were surveyed. The 12 primate species include three hominoids (gorilla *Gorilla gorilla*, orangutan *Pongo pygmaeus*, and gibbon *Hylobates lar*), four Old World monkeys (green monkey *Cercopithecus aethiops*, langur *Pygathrix nemaeus,* talapoin *Miopithecus talapoin*, and baboon *Papio hamadryas*), and five New World monkeys (marmoset *Callithrix jacchus*, tamarin *Saguinus oedipus*, owl monkey *Aotus trivirgatus*, squirrel monkey *Saimiri sciureus*, and woolly monkey *Lagothrix lagotricha*). The animal DNA samples were from (Wang and Zhang 2004) and (Podlaha et al. 2005), whereas the human DNA samples were purchased from Coriell (http://ccr.coriell.org/),

2.5.2 Gene amplification and DNA sequencing

The amplified *ESX1* regions in different species and the primers used for amplification are described in Table 2.2. Primers were designed according to the published human (NT_011651) and mouse (NM_007957) sequences. Polymerase chain reactions (PCRs) were performed with MasterTaq or TripleMasterTaq under conditions recommended by the manufacturer (Eppendorf, Hamburg, Germany). DMSO (Dimethyl sulfoxide) was used in PCR amplification and DNA sequencing of exon 4. Amplified exon 4 sequences from 12 primates were cloned into PCR4TOPO vector (Invitrogen) and then sequenced from both directions. Other PCR products were purified and directly sequenced from both directions. The dideoxy chain termination method was used in DNA sequencing by an automated sequencer. Sequencher (GeneCodes) was used to assemble the sequences and identify DNA polymorphisms in humans.

2.5.3 Human population genetic analysis

The *DH* test was conducted by program DH.jar (Zeng et al. 2006). The population recombination rate used in the test was estimated to be $R=3Nr$ $=3\times10{,}000\times(0.18\times10^{-6}\times723) = 4$ per sequence per generation. Here $N=10{,}000$ is the effective population size of humans, 0.18×10^{-6} is the pedigree-based recombination rate per generation per nucleotide at the *ESX1* locus (Kong et al. 2002), and 723 is the number of nucleotides of the human *ESX1* exon 4 sequence. For samples of African, Caucasian, and Asian origins, we used $N=10{,}000$, 4,000, and 4,000, respectively, as their effective population sizes (Tenesa et al. 2007). The chimpanzee *ESX1* sequence was used as the outgroup in computing *DH* except for one site where the gorilla sequence was used as the outgroup because the chimpanzee sequence is different from both human alleles. *P* values in the *DH* test and *H* test were estimated using 100,000 replications of coalescent simulation.

2.5.4 Evolutionary analysis

The coding sequences of human *ESX1* and mouse *Esx1* were obtained from GenBank with accession numbers AY114148 and NM_007957, respectively. Clustal W (Thompson et al. 1994) was used to conduct sequence alignment for the primates and the *Mus* species, respectively. MEGA3 (Kumar et al. 2004) was used for phylogenetic analysis. Pairwise synonymous (d_S) and nonsynonymous (d_N) distances were calculated using the modified Nei-Gojobori method (Zhang et al. 1998), with estimated transition/transversion ratios. Based on the phylogeny of 15 primates, we inferred ancestral *ESX1* sequences at all interior nodes of the tree by using the likelihood method under the M8 model in PAML3.15 (Yang 1997). The number of synonymous (*s*) and nonsynonymous (*n*) substitutions on each branch of the tree were then counted. The numbers of synonymous (*S*) and nonsynonymous (*N*) sites were also estimated by PAML.

2.6 ACKNOWLEDGEMENTS

We thank Kai Zeng for assistance with the *DH* test and Meg Bakewell, Soochin Cho, and Ondrej Podlaha for valuable comments. This work was supported by research grants from the University of Michigan and National Institutes of Health to J.Z.

Figure 2.1 Structures of the orthologous (**A**) human *ESX1* and (**B**) mouse *Esx1* genes, adapted from (Fohn and Behringer 2001) and (Li et al. 1997). Exons are boxed, with coding regions shown in grey and homeobox shown by hatches. The approximate length of each intron is given in parentheses. Pro-rich and PN/PF motifs are indicated underneath the gene structure.

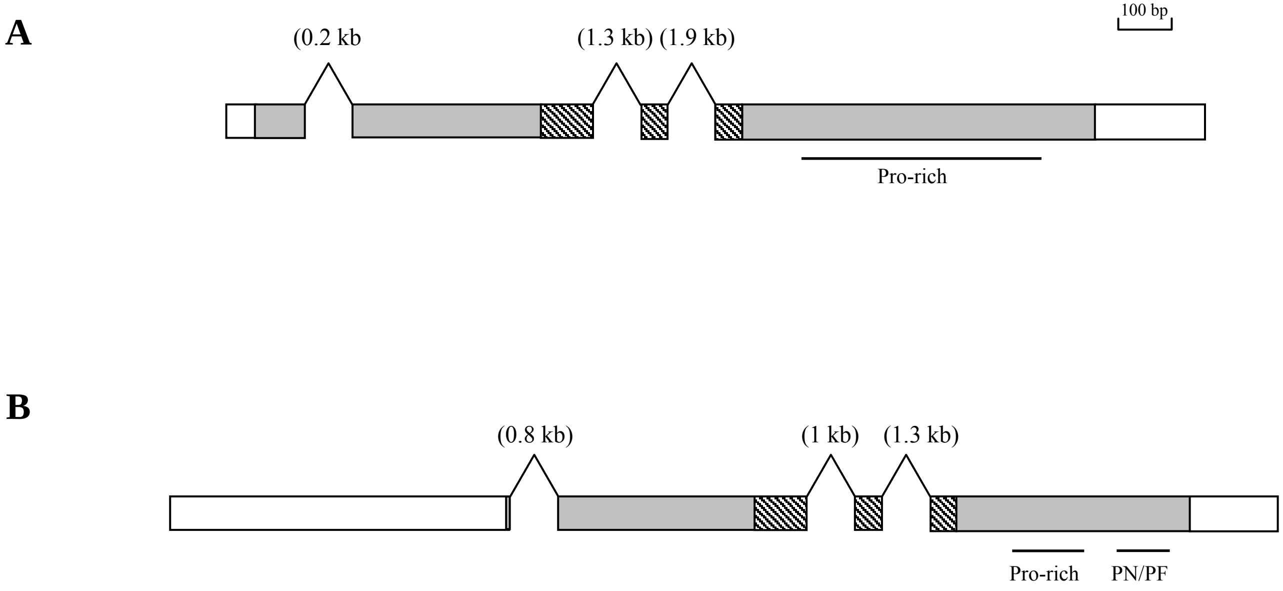

Figure 2.2 Alignment of human and chimpanzee ESX1 protein sequences. The human sequence is from GenBank (accession number AY114148). The homeodomain is boxed. Single nucleotide polymorphisms (SNPs) detected in humans are shaded. For each nonsynonymous SNP, the alternative amino acid is shown above the human sequence. For each synonymous SNP, no alternative amino acid is shown. Triangles indicate indel polymorphisms observed in humans, with deletions shown by triangles pointing upwards and insertions shown by triangles pointing downwards. The width of the triangle shows the size of the indel. "." indicates identity to the human sequence and "-" indicates a gap.

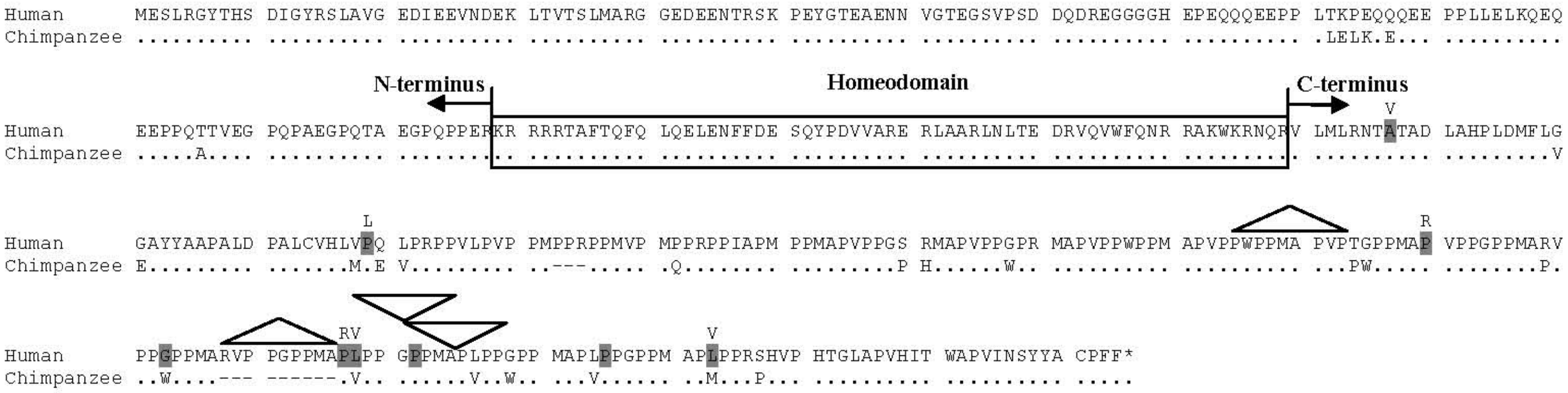

```
Human       MESLRGYTHS DIGYRSLAVG EDIEEVNDEK LTVTSLMARG GEDEENTRSK PEYGTEAENN VGTEGSVPSD DQDREGGGGH EPEQQQEEPP LTKPEQQQEE PPLLELKQEQ
Chimpanzee  .......... .......... .......... .......... .......... .......... .......... .......... .......... .LELK.E... ..........

                                                                                                              V
Human       EEPPQTTVEG PQPAEGPQTA EGPQPPERKR RRRTAFTQFQ LQELENFFDE SQYPDVVARE RLAARLNLTE DRVQVWFQNR RAKWKRNQRV LMLRNTATAD LAHPLDMFLG
Chimpanzee  .....A.... .......... .......... .......... .......... .......... .......... .......... .......... .......... .........V

                               L                                                                             R
Human       GAYYAAPALD PALCVHLVPQ LPRPPVLPVP PMPPRPPMVP MPPRPPIAPM PPMAPVPPGS RMAPVPPGPR MAPVPPWPPM APVPPWPPMA PVPTGPPMAP VPPGPPMARV
Chimpanzee  E......... .......M.E V......... ..---..... .Q........ .........P H......W.. .......... .......... ...PW..... ........P.

                             RV                             V
Human       PPGPPMARVP PGPPMAPLPP GPPMAPLPPGPP MAPLPPGPPM APLPPRSHVP HTGLAPVHIT WAPVINSYYA CPFF*
Chimpanzee  ..W....--- ------.V.. ......V..W.. ...V...... ..M...P... .......... .......... .....
```

Figure 2.3 Protein sequence alignment for exon 4 of *ESX1* (*Esx1*) in (**A**) 12 primates and (**B**) 4 *Mus* species. "." indicates identity to the first sequence in each alignment. "-" indicates an alignment gap, and "*" indicates a stop codon. The partial homeodomain region is indicated. "OW", Old World; "NW", New World.

A

```
                                Homeodomain
Hominoids   Human           VWFQNRRAKW KRNQRVLMLR NTATADLAHP LDMFLGGAYY AAPALDPALC VHLVPQLPRP PVLPVPPMPP RPPMVPMPPR PPIAPMPP-- -MAPVPPGSR MAPVPPGPRM APVPPWPPMA
            Chimpanzee      .......... .......... .......... .....VE... .......... ...M.EV... .......... ---....Q.. ........-- -.......PH ......W... ..........
            Gorilla         .......... .......... .....A.... S........N .......... .......... .A........ .......Q.. ........-- -.......P. ........C. .....G....
            Orangutan       .......... .......... .I.A.T..R. S........N .......... .......... .........L .......Q.. ..M.....GP R.......P. .......... .....G.R.V
            Gibbon          .......... .......... .I.A.A.... E.T....P.D ........F. ...M.EI... ......S... G......Q.G ..M.....GP P.......PC ...M...... .....G...V
OW monkeys  Rhesus monkey   .......... .......... .I.A.A..R. AEV....P.N .T.S...... .......... ---....... .......Q.. ..M.....GP P...---.PP RP..V.MQP- ----------
            Baboon          .......... .......... .I.A.A..R. TEV....P.N .T.S...... .......... ---....... .......Q.. ..M..----- -------VPP RP.MV.MQP- ----------
            Green monkey    .......... .......... .I.A.A..R. TEV....P.N .T.S...... .......... ---....... .......Q.. ..M.....GP PRP.MA.VPP RP.MV.MQP- ----------
            Talapoin        .......... .......... .I.A.A..R. AEV....P.N .T.S...... ........T. ---...---- -----..Q.. ..M.....R- --P.MA.VPP RP..V.MQP- ----------
            Langur          ....Y..... .......... .I.A.AV.P. AEV....P.N .T.S...... ...M....T. ---....... .........G ..M.....G- --PSMV.MPP RP..V.MQP- --------RP
NW monkeys  Marmoset        .......... R....M..-. .V.ALA..PA VE.I..AP.D .V.V....W. ...A.RP--- ---.R..VA. V.HTA...AG ..M....VG- --P.MA.MPP GP..V----- ----------
            Tamarin         .......... R....M..-. .V.ALA..PA VE.I..APHD .V.V....W. ...A.RP--- ---.R..VA. V.H.A...AG ..M....VG- --P.MA.MPP GP..V----- ----------
            Owl monkey      .......T.. R....M.... .M.DDA.PPA VEVI.DMP.D .V.V....W. ...A..PLG. ---.G..VV. M...A.AQA. ..M.G..AGP PVV.M...AP ...M..M--- ----------
            Squirrel monkey .......... R....M.... .M.A.P.VP. VEVI..AP.D .V.V....W. .N.A..P--- ---.R..V.. MQ..A..QA. ..M.G..ARP P.P.M..EQP ...M....-- ----------
            Woolly monkey   .......... R....M.... .L.A.A..PA VEVI..AP.D .V.V....W. ...A..---- -----..RQ. VL..A..QAG ....G..AGP P...M...PP ...M....PA .---------

            Human           PVPPWPPMAP VPTGPPMAPV PPGPPMARVP PGPPMARVPP GPPMAPLPPG PPMAPLPP-- -GPPMAPLPP GPPMAPLPPR SHVP-HTGLA PVHITWAPVI NSYYACPFF*
            Chimpanzee      .......... ..PW...... .......P.. .W....P... ......V..W .....----- -------V.. ......M... P...-..... .......... ..........
            Gorilla         ....G..... ..P.....RM .......P.. .......... ......V... .....----- -------V.. ......VA.G P...-..... ..P..T.... .....R....
            Orangutan       ....G....R M.P....... ........M. ......L... ......G... .....G..MA L......V.. ......M... PR..-.P... ..R....... .....G....
            Gibbon          HM..G...VH M.P....VHM ......TPM. ......P... ......M... ....------ ------.V.. ..LV..M... P...-..... ..R....... .....G....
            Rhesus monkey   ---------- ---R...VRM ..R....P.. .....VPM.. R.....V..R ....------ ---------- -----.M... PP..-RI... ..R....... .....G....
            Baboon          ---------- ---R...VRM ..R....P.. T....VPM.. R.....V..R ....------ ---------- -----.M... PP..-RI... ..R....... .....G....
            Green monkey    ---------- ---R...VRM ..R....P.. .....VPM.. ---...V..R ....------ ---------- --------.M PP..-RI... ..R....... .....G....
            Talapoin        ---------- ---R...VRM ..R....P.. .....VPM.. R.....V..R ....------ ---------- -----.M... PP..-RI... ..R....... .....G....
            Langur          .MVHM..... ..P..S...M ..R..VVPMQ .R...VHM.. R.....V..R ....------ ---------- -----.M... PP..-RI... ..R....... ....TG....
            Marmoset        ---------- ---------- ---------- ---------- ---------- ---------- ---------- -----.M..G APM.-.F... ..G.A...FN ....VG....
            Tamarin         ---------- ---------- ---------- ---------- ---------- ---------- ---------- -----.M..G APM.-.F... ..G.A...FN ....VG....
            Owl monkey      --------.R TQAR....RM QAR....GM. A...VVPM.. .A....M... ..VV------ ---------- -----.M... APM.-DI.Q. .LG.A..... .G.HVG....
            Squirrel monkey ---------- ---------- ---------- ---------- ---------- ---------- ---------- -----.M... APM.-YI... ..G....... .G..VG..Y.
            Woolly monkey   ---------- ---------- ---------- ---------- ---------- ---------- ---------- -----.M... APM.H.I... ..G.A..... .G..VR....
```

B

```
                      Homeodomain
*Mus musculus*    VWFQNRRAKW RRLRRAQAFR NMVPVAMSPP VGVYLDDHYG PIPIVEVIWK CYPMVPRPMH PQMMPLPPRP PPGFRMPPPF RPPPLPPFPW PPVPPDAHIP NAAREYNPFP FPFPFPFPFP
*Nus cookie*      .......... .......... .......... .......... .......... .......... .......... .......L.. .......... ....H.V... .......--. L.......--
*Mus cervicolor*  .......... .......... .......... .......... .......... .......... .......... .......L.. .......... .......... ........L. ........--
*Mus spretus*     .......... .......... .......... .......... .......... .......... .......... .......... .......... .......... .......... ........N.

*Mus musculus*    NPFPNPNPNP NPNPNPNPNP NQNFAGPK*- --
*Nus cookii*      --.....--- ---------- -......RYR Y*
*Mus cervicolor*  --.....--- ---------- -......RYR Y*
*Mus spretus*     --........ .......... .......RYR Y*
```

Figure 2.4 Pairwise synonymous (d_S) and nonsynonymous (d_N) nucleotide distances for (**A**) the entire exon 4 of *ESX1* among 15 primates, (**B**) the C-terminal non-homeodomain region of *ESX1* among 15 primates, and (**C**) the exon 4 of *Esx1* among 4 *Mus* species.

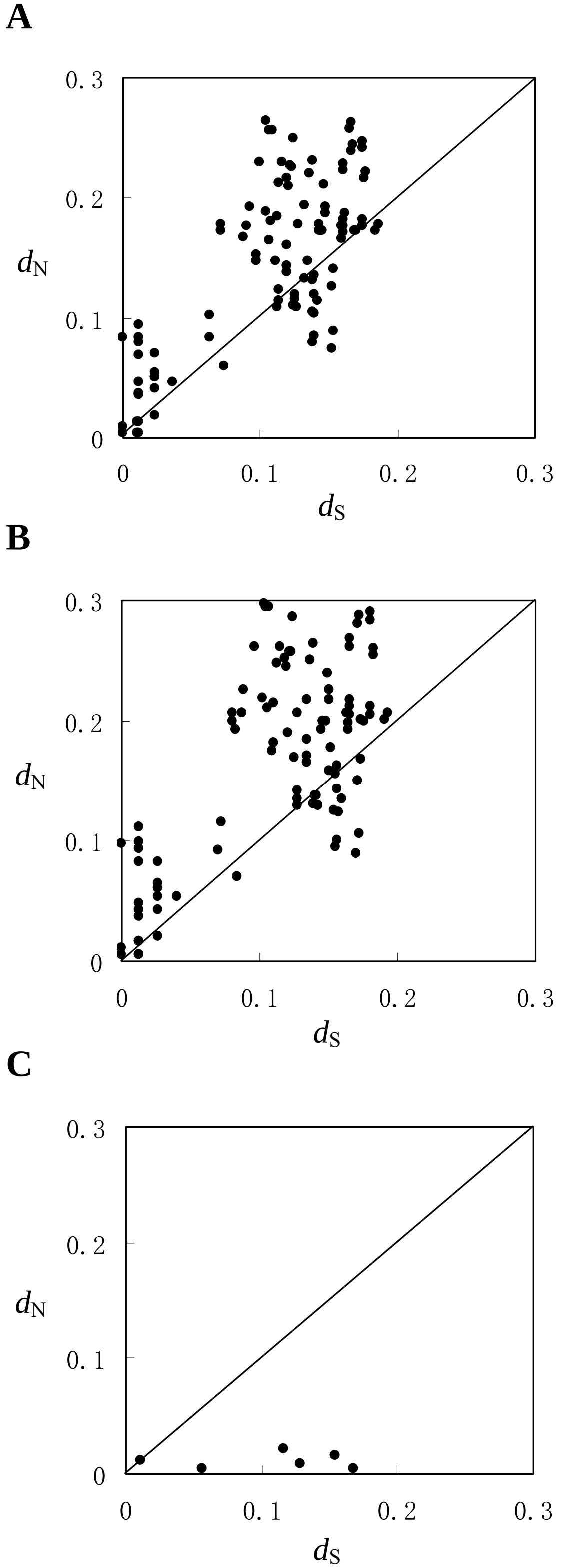

Figure 2.5 Separate alignments of translated *ESX1* exon 4 of (**A**) hominoids, (**B**) Old World monkeys, and (**C**) New World monkeys. "." indicates identity to the top sequence, "-" indicates a gap, and "*" indicates a stop codon.

A

```
Human          VWFQNRRAKW KRNQRVLMLR NTATADLAHP LDMFLGGAYY AAPALDPALC VHLVPQLPRP PVLPVPPMPP
Chimpanzee     ---------- .......... .......... .....VE... .......... ...M.EV... ..........
Gorilla        .......... .......... .....A.... S........N .......... .......... .A........
Orangutan      .......... .......... .I.A.T..R. S........N .......... .......... .........L
Gibbon         .......... .......... .I.A.A.... E.T....P.D ........F. ...M.EI... ......S...

Human          RPPMVPMPPR PPIAPMPP-- -MAPVPPGSR MAPVPPGPRM APVPPWPPMA PVPPWPPMAP VPTGPPMAPV
Chimpanzee     ---....Q.. ........-- -.......PH ......W... .......... .......... ..PW......
Gorilla        .......Q.. ........-- -.......P. ........C. .....G.... ....G..... ..P.....RM
Orangutan      .......Q.. ..M.....GP R.......P. .......... .....G.R.V ....G....R M.P.......
Gibbon         G......Q.G ..M.....GP P.......PC ...M...... .....G...V HM..G...VH M.P....VHM

Human          P--------- PGPPMARVPP GPPMARVPPG PPMAPLPPGP PMAPLPP--- GPPMAPLPPG PPMAPLPPRS
Chimpanzee     .--------- ---------. .....P...W .....V.... ....V..--- W.....V... .....M...P
Gorilla        .--------- ---------. .....P.... ....RV.... ....V..--- ......V... .....VA.GP
Orangutan      .--------- .......M.. .....L.... .....G.... ....G..MAL ......V... .....M...P
Gibbon         .--------- ---------. ....TPM... .....V.... ....M..--- ......V... .LV..M...P

Human          HVPHTGLAPV HITWAPVINS YYACPFF*
Chimpanzee     ......---- ---------- --------
Gorilla        .......... P...T..... ...R....
Orangutan      R...P..... R......... ...G....
Gibbon         .......... R......... ...G....
```

B

```
Baboon          VWFQNRRAKW KRNQRVLMLR NIAAAALARP TEVFLGGPYN ATPSLDPALC VHLVPQLPRP PVPPMPPRPP
Green monkey    .......... .......... .......... .......... .......... .......... ..........
Rhesus monkey   .......... .......... .......... A......... .......... .......... ..........
Langur          ....Y..... .......... ......V.P. A......... .......... ...M....T. ..........
Talapoin        .......... .......... .......... A......... .......... ........T. .....Q....

Baboon          MVPMQPRP-- ---------- PMAPVPPRPP MVPMQPRPPM VRMP------ ---------P RPPMAPVPTG
Green monkey    ........PM APMPPGPPRP .......... .......... ....------ ---------. ........P.
Rhesus monkey   ........PM APMPPGP--- ....G..... V......... ....------ ---------. ........P.
Langur          ....P.G.PM APMPPGP--- S.V.M..... V......... .H..PMAPVP PGPSMAPMP. ...VV.MQPR
Talapoin        .A..P...-- ---------- .......... V......... ....------ ---------. ........P.

Baboon          PPMVPMPPRP PMAPVPPRPP MAPMPPRPPV PRIGLAPVRI TWAPVINSYY AGPFF*
Green monkey    .......--- .......... .....---.. .......... .......... ......
Rhesus monkey   .......... .......... .......... .......... .......... ......
Langur          ....H..... .......... .......... .......... .......... T.....
Talapoin        .......... .......... .......... .......... .......... ......
```

C

```
Marmoset        VWFQNRRAKW RRNQRMLM-R NVAALALAPA VEMILGAPYD AVPVLDPAWC VHLAPR---P PRPPVAPVPH
Tamarin         .......... ........-. .......... ........H. .......... ......---. ..........
Owl monkey      .......T.. ........L. .M.DD..P.. ..V..DM... .......... .....QPLG. .G...V.M.P
Squirrel monkey .......... ........L. .M..AP.V.P ..V....... .......... .N...Q---. .....P.MQP
Woolly monkey   .......... ........L. .L..A..... ..V....... .......... .....Q---. ..Q..L.MAP

Marmoset        TAP------- --MPAGP--- PMAP------ ---------- ---------- ---------- ---MPVGPPM
Tamarin         M..------- --.....--- ....------ ---------- ---------- ---------- ---.......
Owl monkey      M..AQARPPM AG.....PVV ..P.GAPMAP MPPMARTQAR PPMARMQARP PMAGMPAGPP VVP..P.A..
Squirrel monkey M..MQARPPM AG...R.--- ..P.------ ---------- ---------- ---------- ---..PEQ..
Woolly monkey   MQAGPP---I AG.....--- ....------ ---------- ---------- ---------- ---..P....

Marmoset        APMPPGPPVV PMPPGAPMP- HFGLAPVGIA WAPFNNSYYV GPFF*
Tamarin         .......... .........- .......... .......... .....
Owl monkey      .......... ....R....- DI.Q..L... ...VI.G.H. .....
Squirrel monkey .......--- ....R....- YI.......T ...VI.G... ...Y.
Woolly monkey   ........AA ....R....H .I........ ...VI.G... R....
```

Figure 2.6 Numbers of synonymous (*s*) and nonsynonymous (*n*) substitutions in the evolution of primate *ESX1*. Shown on each branch are the *n* and *s* values for the C-terminal non-homeodomain region. The numbers of nonsynonymous (*N*) and synonymous (*S*) sites for the same region are also given.

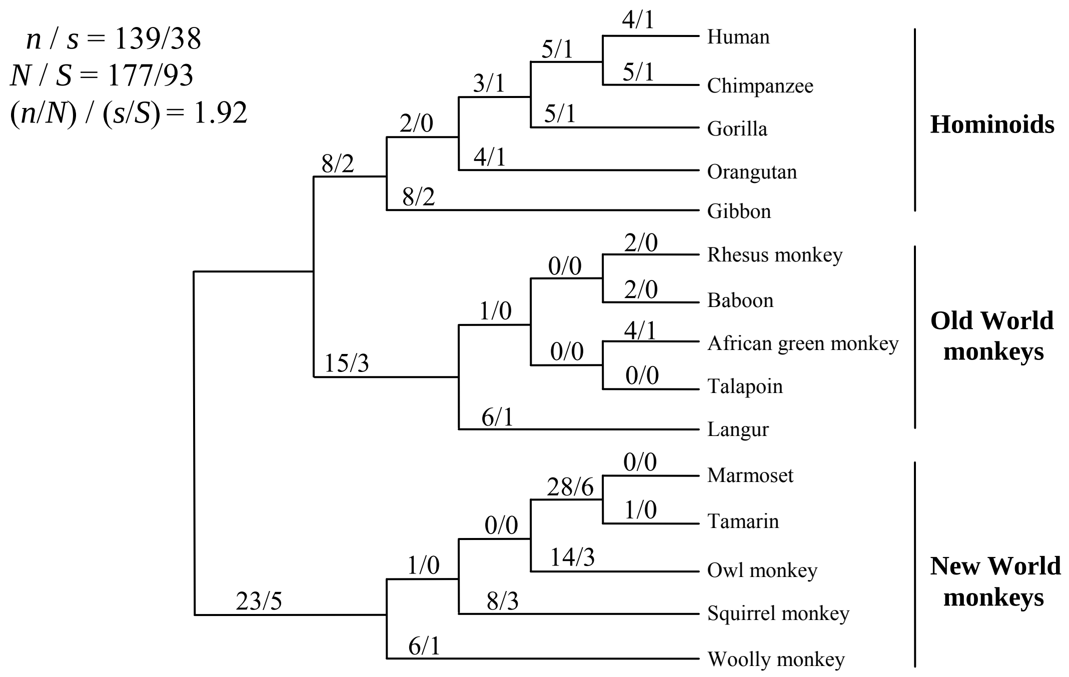

Table 2.1 *ESX1* exon 4 sequence variations among 32 men. The position of each polymorphism follows the GenBank sequence AY114148, starting from the first nucleotide of exon 4. The polymorphisms and their corresponding allele frequencies are given. For each polymorphism, we present the allele from the GenBank sequence, followed by the deviating allele. Polymorphisms are classified into synonymous (s), nonsynonymous (n), insertion (i), and deletion (d) types. The indel length in nucleotides is shown for each indel polymorphism.

Nucleotide position	Polymorphism	Type	Frequency
68	C(Ala)/T(Val)	n	0.97/0.03
164	C (Pro)/T (Leu)	n	0.97/0.03
361-387	27/-	d	0.97/0.03
407	C(Pro)/G(Arg)	n	0.94/0.06
447	G(Gly)/C(Gly)	s	0.97/0.03
460-486	27/-	d	0.94/0.06
488	C(Pro)/G(Arg)	n	0.59/0.41
490	C(Leu)/G(Val)	n	0.59/0.41
504	G(Pro)/A(Pro)	s	0.97/0.03
After 513	-/27	i	0.97/0.03
before 514	-/27	i	0.37/0.63
549	A(Pro)/G(Pro)	s	0.97/0.03
571	C(Leu)/G(Val)	n	0.94/0.06

Table 2.2 Primers used for amplifying different exons of *ESX1* in primates and *Esx1* in *Mus* species.

Species	Primers	Exons amplified	Length (bp)
Human	L: 5'-tgcctcactcgctttaccctagt-3' R: 5'-tgcacagctttatcgacagcgc-3'	Exons 1 and 2	424
	L: 5'-tggagagaaagacagatacag-3' R: 5'-atccacaactccaaatactg-3'	Exon 3	46
	L: 5'-cacaatttctatctggcagg-3' R: 5'-atagcttcacctgttgcagt-3'	Exon 4	642,669,696,723
Gorilla	L: 5'-agcatctaacgaattacttg-3' R: 5'-aaagtctcagtggcatatag-3'		642
Orangutan	L: 5'-ccaacgtactattaagtcac-3' R: 5'-ctcctctaagatatttcagc-3'		687
Gibbon			651
Rhesus monkey	L: 5'-cacaatttctatctggcagg-3' R: 5'-aaagtctcagtggcatatag-3'		534
Baboon			507
African green monkey			525
Talapoin			507
Tamarin			387
Marmoset			387
Squirrel monkey			408
Woolly monkey			411
Owl monkey			552
Langur	L: 5'-ccaacgtactattaagtcac-3' R: 5'-atagcttcacctgttgcagt-3'		579
Mus spretus	L: 5'-caccaacgagctggtcttg-3' R: 5'-agtctgcctgccacatggt-3'	Exon 2	436
Mus spretus	L: 5'-gacattcatggtccaatatcc-3' R: 5'-gcgtgatagtgtttacaaacg-3'	Exon 4	450
Mus cervicolor			402
Mus cookii			396

2.7 LITERATURE CITED

Akey JM, Eberle MA, Rieder MJ, Carlson CS, Shriver MD, Nickerson DA, Kruglyak L (2004) Population history and natural selection shape patterns of genetic variation in 132 genes. PLoS Biol 2:e286

Bakewell MA, Shi P, Zhang J (2007) More genes underwent positive selection in chimpanzee evolution than in human evolution. Proc Natl Acad Sci USA 104:in press

Branford WW, Zhao GQ, Valerius MT, Weinstein M, Birkenmeier EH, Rowe LB, Potter SS (1997) Spx1, a novel X-linked homeobox gene expressed during spermatogenesis. Mechanisms of development 65:87-98

Consortium CSaA (2005) Initial sequence of the chimpanzee genome and comparison with the human genome. Nature 437:69-87

Fay JC, Wu CI (2000) Hitchhiking under positive Darwinian selection. Genetics 155:1405-1413

Figueiredo AL, Salles MG, Albano RM, Porto LC (2004) Molecular and morphologic analyses of expression of ESX1L in different stages of human placental development. J Cell Mol Med 8:545-550

Fohn LE, Behringer RR (2001) ESX1L, a novel X chromosome-linked human homeobox gene expressed in the placenta and testis. Genomics 74:105-108

Gehring WJ, Affolter M, Burglin T (1994) Homeodomain proteins. Annual review of biochemistry 63:487-526

Grati FR, Sirchia SM, Gentilin B, Rossella F, Ramoscelli L, Antonazzo P, Cavallari U, Bulfamante G, Cetin I, Simoni G, Miozzo M (2004) Biparental expression of ESX1L gene in placentas from normal and intrauterine growth-restricted pregnancies. Eur J Hum Genet 12:272-278

Haig D (1993) Genetic conflicts in human pregnancy. The Quarterly review of biology 68:495-532

Jackson M, Watt AJ, Gautier P, Gilchrist D, Driehaus J, Graham GJ, Keebler J, Prugnolle F, Awadalla P, Forrester LM (2006) A murine specific expansion of the Rhox cluster involved in embryonic stem cell biology is under natural selection. BMC genomics 7:212

Kong A, Gudbjartsson DF, Sainz J, Jonsdottir GM, Gudjonsson SA, Richardsson B, Sigurdardottir S, Barnard J, Hallbeck B, Masson G, Shlien A, Palsson ST, Frigge ML, Thorgeirsson TE, Gulcher JR, Stefansson K (2002) A high-resolution recombination map of the human genome. Nature genetics 31:241-247

Kumar S, Tamura K, Nei M (2004) MEGA3: Integrated software for Molecular Evolutionary Genetics Analysis and sequence alignment. Brief Bioinform 5:150-163

Li W (1997) Molecular Evolution. Sinauer, Sunderland, Mass.

Li Y, Behringer RR (1998) Esx1 is an X-chromosome-imprinted regulator of placental development and fetal growth. Nat Genet 20:309-311

Li Y, Lemaire P, Behringer RR (1997) Esx1, a novel X chromosome-linked homeobox gene expressed in mouse extraembryonic tissues and male germ cells. Dev Biol 188:85-95

Maclean JA, 2nd, Chen MA, Wayne CM, Bruce SR, Rao M, Meistrich ML, Macleod C, Wilkinson MF (2005) Rhox: a new homeobox gene cluster. Cell 120:369-382

MacLean JA, 2nd, Lorenzetti D, Hu Z, Salerno WJ, Miller J, Wilkinson MF (2006) Rhox homeobox gene cluster: recent duplication of three family members. Genesis 44:122-129

McGinnis W, Hart CP, Gehring WJ, Ruddle FH (1984) Molecular cloning and chromosome mapping of a mouse DNA sequence homologous to homeotic genes of Drosophila. Cell 38:675-680

Monk D, Arnaud P, Apostolidou S, Hills FA, Kelsey G, Stanier P, Feil R, Moore GE (2006) Limited evolutionary conservation of imprinting in the human placenta. Proc Natl Acad Sci U S A 103:6623-6628

Morison IM, Ramsay JP, Spencer HG (2005) A census of mammalian imprinting. Trends Genet 21:457-465

Morris L, Gordon J, Blackburn CC (2006) Identification of a tandem duplicated array in the Rhox alpha locus on mouse chromosome X. Mamm Genome 17:178-187

Murthi P, Doherty VL, Said JM, Donath S, Brennecke SP, Kalionis B (2006) Homeobox gene ESX1L expression is decreased in human pre-term idiopathic fetal growth restriction. Mol Hum Reprod 12:335-340

Nam J, Nei M (2005) Evolutionary change of the numbers of homeobox genes in bilateral animals. Molecular biology and evolution 22:2386-2394

Ozawa H, Ashizawa S, Naito M, Yanagihara M, Ohnishi N, Maeda T, Matsuda Y, Jo Y, Higashi H, Kakita A, Hatakeyama M (2004) Paired-like homeodomain protein ESXR1 possesses a cleavable C-terminal region that inhibits cyclin degradation. Oncogene 23:6590-6602

Podlaha O, Webb DM, Tucker PK, Zhang J (2005) Positive Selection for Indel Substitutions in the Rodent Sperm Protein Catsper1. Molecular biology and evolution 22:1845-1852

Podlaha O, Webb DM, Zhang J (2006) Accelerated evolution and loss of a domain of the sperm-egg-binding protein SED1 in ancestral primates. Molecular biology and evolution 23:1828-1831

Saitou N, Nei M (1987) The neighbor-joining method: a new method for reconstructing phylogenetic trees. Molecular biology and evolution 4:406-425

Sutton KA, Wilkinson MF (1997) Rapid evolution of a homeodomain: evidence for positive selection. J Mol Evol 45:579-588

Swanson WJ, Nielsen R, Yang Q (2003) Pervasive adaptive evolution in mammalian fertilization proteins. Mol Biol Evol 20:18-20

Swanson WJ, Vacquier VD (2002) The rapid evolution of reproductive proteins. Nat Rev Genet 3:137-144

Tajima F (1989) Statistical method for testing the neutral mutation hypothesis by DNA polymorphism. Genetics 123:585-595

Tenesa A, Navarro P, Hayes BJ, Duffy DL, Clarke GM, Goddard ME, Visscher PM (2007) Recent human effective population size estimated from linkage disequilibrium. Genome Research 17:520-526

Thompson JD, Higgins DG, Gibson TJ (1994) CLUSTAL W: improving the sensitivity of progressive multiple sequence alignment through sequence weighting, position-specific gap penalties and weight matrix choice. Nucleic acids research 22:4673-4680

Ting CT, Tsaur SC, Wu ML, Wu CI (1998) A rapidly evolving homeobox at the site of a hybrid sterility gene. Science 282:1501-1504

Torgerson DG, Singh RS (2003) Sex-linked mammalian sperm proteins evolve faster than autosomal ones. Mol Biol Evol 20:1705-1709

Wagschal A, Feil R (2006) Genomic imprinting in the placenta. Cytogenet Genome Res 113:90-98

Wang X, Zhang J (2004) Rapid evolution of mammalian X-linked testis-expressed homeobox genes. Genetics 167:879-888

Wang X, Zhang J (2006) Remarkable expansions of an X-linked reproductive homeobox gene cluster in rodent evolution. Genomics 88:34-43

West JD, Frels WI, Chapman VM, Papaioannou VE (1977) Preferential expression of the maternally derived X chromosome in the mouse yolk sac. Cell 12:873-882

Wyckoff GJ, Wang W, Wu CI (2000) Rapid evolution of male reproductive genes in the descent of man. Nature 403:304-309

Yan YT, Stein SM, Ding J, Shen MM, Abate-Shen C (2000) A novel PF/PN motif inhibits nuclear localization and DNA binding activity of the ESX1 homeoprotein. Mol Cell Biol 20:661-671

Yanagihara M, Ishikawa S, Naito M, Nakajima J, Aburatani H, Hatakeyama M (2005) Paired-like homeoprotein ESXR1 acts as a sequence-specific transcriptional repressor of the human K-ras gene. Oncogene 24:5878-5887

Yang Z (1997) PAML: a program package for phylogenetic analysis by maximum likelihood. Comput Appl Biosci 13:555-556

Zeng K, Fu YX, Shi S, Wu CI (2006) Statistical tests for detecting positive selection by utilizing high-frequency variants. Genetics 174:1431-1439

Zhang J, Kumar S, Nei M (1997) Small-sample tests of episodic adaptive evolution: a case study of primate lysozymes. Molecular biology and evolution 14:1335-1338

Zhang J, Nei M (1996) Evolution of Antennapedia-class homeobox genes. Genetics 142:295-303

Zhang J, Rosenberg HF, Nei M (1998) Positive Darwinian selection after gene duplication in primate ribonuclease genes. Proc Natl Acad Sci U S A 95:3708-3713

CHAPTER 3

RELAXATION OF SELECTIVE CONSTRAINT AND LOSS OF FUNCTION IN THE EVOLUTION OF HUMAN BITTER TASTE RECEPTOR GENES

3.1 ABSTRACT

Bitter taste perception prevents mammals from ingesting poisonous substances because many toxins taste bitter and cause aversion. We hypothesize that human bitter taste receptor (TAS2R) genes might be relaxed from selective constraints because of the change in diet, use of fire, and reliance on other means of toxin avoidance that emerged in human evolution. Here we examine the intraspecific variations of all 25 genes of the human *TAS2R* repertoire. Our data show hallmarks of neutral evolution, including similar rates of synonymous (d_S) and nonsynonymous (d_N) nucleotide changes among rare polymorphisms, common polymorphisms, and substitutions, no variation in d_N/d_S among functional domains, segregation of pseudogene alleles within species, and fixation of loss-of-function mutations. These results, together with previous findings of large numbers of loss-of-function mutations in olfactory, pheromonal, and visual sensory genes in humans, suggest surprisingly reduced sensory capabilities of humans in comparison to many other mammals.

3.2 INTRODUCTION

Humans and most mammals can perceive and discriminate among five major taste modalities: sweet, sour, bitter, salty, and umami (the taste of sodium glutamate)

(Kinnamon and Cummings 1992; Lindemann 1996). Among these, bitter perception has a special role of preventing animals from ingesting poisonous substances, because many toxins taste bitter and cause aversion (Garcia and Hankins 1975; Glendinning 1994). The sense of the bitter taste begins by binding of bitter compounds to bitter taste receptors that are found on the surface of the taste receptor cells of the tongue and palate epithelium (Lindemann 1996; Chandrashekar et al. 2000). The receptors are encoded by a large family of seven-transmembrane G protein-coupled receptor genes named *TAS2R*s (or *T2R*s) and the roles of *TAS2Rs* in bitter taste have been demonstrated by both *in vitro* and *in vivo* functional assays (Adler et al. 2000; Chandrashekar et al. 2000; Matsunami et al. 2000; Bufe et al. 2002; Behrens et al. 2004). Unlike visual pigment genes or olfactory receptor genes for which only one gene is expressed in each visual or olfactory receptor cell, multiple *TAS2R* genes are found to be expressed in each bitter taste receptor cell in rodents, providing a plausible explanation for the uniform taste of many structurally distinct toxins (Chandrashekar et al. 2000). *TAS2R* genes do not contain introns in their protein-coding regions, which facilitated their detection in sequenced genomes. Twenty-five putatively functional *TAS2R* genes (with open reading frames [ORFs]) and 8 pseudogenes (with disrupted ORFs) have been identified from the human genome sequence and they are mapped to chromosomes 5, 7, and 12 (Shi et al. 2003). In comparison, the mouse genome contains 33 functional Tast2r genes and 3 pseudogenes (Shi et al. 2003). A phylogenetic analysis of these genes suggested considerable variation in the *TAS2R* repertoire among different mammalian lineages (Shi et al. 2003). Although only a minority of these *TAS2R* genes has been functionally characterized, their chromosomal location, sequence similarity, and phylogenetic relationships strongly suggest that they are involved in bitter perception.

Because TAS2Rs are directly involved in the interaction between mammals and their dietary sources, it is likely that the evolution of these proteins responds to and reflects dietary changes in organismal evolution. For example, there were significant changes in diet during human evolution (Harris 1992; Leonard 2002; Milton 2003). In particular, the amount of meat in hominid diet began to increase about 2 million years (MY) ago, while the amount of plant materials decreased (Harris 1992; Leonard 2002; Milton 2003). This dietary shift may have caused a reduction in the importance of bitter taste and *TAS2R* genes because animal tissues contain fewer bitter and toxic compounds than plant tissues (Glendinning 1994). Detoxification of poisonous foods by controlled use of fire starting ~0.8 MY ago (Goren-Inbar et al. 2004) may trigger a further functional relaxation in *TAS2R*s. We thus hypothesize that patterns of intra-specific polymorphism and recent evolution of human *TAS2R* genes should exhibit low selective constraints. Here we characterize the intra- and inter-specific variations of all 25 members of the human *TAS2R* repertoire and provide strong evidence supporting this hypothesis.

3.3 RESULTS

3.3.1 Equal levels of synonymous and nonsynonymous polymorphisms in human *TAS2R* genes

To examine the genetic variation of *TAS2R*s within humans, we sequenced all 25 functional genes in 22 humans of diverse geographic origins and one chimpanzee.

Because synonymous nucleotide changes do not alter protein sequences and are more or less neutral whereas nonsynonymous changes could be subject to natural selection, a comparison between them can reveal signals of selection (Li 1997; Nei and Kumar 2000). In most genes, the majority of nonsynonymous sites are under selective constraints, resulting in lower rates of polymorphisms and substitutions at nonsynonymous sites than at synonymous sites (Li 1997; Nei and Kumar 2000). In human *TAS2R*s, we identified 72 nonsynonymous and 33 synonymous polymorphic sites from 21,408 nucleotide sites, including 15,242 nonsynonymous and 6,166 synonymous sites, respectively (Tables 3.1 and 3.2, Figure online at http://hmg.oxfordjournals.org/cgi/data/ddh289/DC1/1). The number of polymorphisms per nonsynonymous site (4.72×10^{-3}, Watterson's $\theta=1.09\times10^{-3}$) is 88% of that per synonymous site (5.35×10^{-3}, $\theta= 1.23\times10^{-3}$), indicating that the overall selective constraints on the two types of sites are similar (P=0.31; Fisher's exact test) in *TAS2R* genes. Consistent with this observation, the nucleotide diversity per site (Li 1997; Nei and Kumar 2000) is virtually identical between nonsynonymous ($\pi_N=1.22\times10^{-3}$) and synonymous ($\pi_S=1.19\times10^{-3}$) sites (Table 3.1). Furthermore, while the *TAS2R* π_S is close to the average synonymous nucleotide diversity observed from a large number of human genes (1.1×10^{-3}) (Cargill et al. 1999), π_N is about 4 times the corresponding average (0.28×10^{-3}) (Cargill et al. 1999). These comparisons suggest that the similar magnitudes of π_N and π_S at *TAS2R*s are likely due to reduced selective constraints on nonsynonymous sites.

Alternatively, high π_N may result from balancing selection, which retains beneficial alleles in a population for a long time (Hughes and Nei 1988). Balancing selection has been suggested to account for the high π_N of the *TAS2R38* (also called *PTC*) gene (Wooding et al. 2004), which is largely responsible for the well known human polymorphism in tasting the synthetic compound phenylthiocarbamide (PTC) (Kim et al. 2003). A characteristic of balancing selection is the positiveness of $\pi - \theta$, which can be measured by Tajima's *D* statistic (Tajima 1989). For the present data, *D* is positive in 12 genes, 0 in one gene, and negative in 12 genes, with an overall value of -0.048 for all the genes analyzed together (Table 3.1). *D* is not significantly different from 0 for the 25 genes, individually or collectively. When the synonymous and nonsynonymous sites were separated, one gene (*TAS2R48*) had a significantly positive *D* at synonymous sites (P<0.05) and another (*TAS2R45*) had a significantly positive *D* at nonsynonymous sites (P<0.05). But the two significant cases may simply be due to multiple testing as 50 tests were conducted and 2.5 significant cases (at 5%) were expected by chance. These observations do not support the balancing selection hypothesis for the human *TAS2R* repertoire, although failure to detect balancing selection here does not preclude its operation at a few *TAS2R* genes. Similar results were obtained by Fu and Li's tests (Fu and Li 1993) (data not shown). Wooding et al. (Wooding et al. 2004) suggested the action of balancing selection on *TAS2R38* largely because the observation of a positive Tajima's *D* (1.55). This *D* value was not significantly higher than 0 under the assumption that the population size is constant, but it became significantly higher than 0 under specific models of population expansion (Wooding et al. 2004). They suggested that an instant population expansion from the effective size of 10,000 to 1,000,000 that occurred 100,000 years ago is most appropriate for humans (Rogers 1995; Wooding et al. 2004) (see also the manual of the

DFSC program of S. Wooding at http://www.xmission.com/~wooding/DFSC/README). We evaluated this model by computing *D* for 6 apparently neutral loci (see Table 3.3) of the human genome under this model. Surprisingly, 5 of the 6 loci (except the locus at Xq13.3) show significantly positive *D* values. Thus, we believe that use of the above population expansion model leads to false positive detection of balancing selection. Although this does not mean that use of the constant-population model is correct, it is certainly a more conservative and safer test for balancing selection, particularly when the details of human population expansion is still unclear.

Possible natural selection on human *TAS2R*s can be further scrutinized by comparing rare and common polymorphisms (Fay et al. 2001). We used the chimpanzee as the outgroup of humans to determine which human alleles are derived and which are ancestral, and then classified each polymorphism to either rare or common using 10% frequency for the derived allele as the cutoff (Table 3.2). We found that the ratio of the number of nonsynonymous polymorphisms to that of synonymous polymorphisms was similar between rare (33/15=2.20) and common (39/18=2.17) categories (*P*=0.57). This is consistent with the lack of purifying selection on *TAS2R*s, because purifying selection would prevent deleterious nonsynonymous mutations from becoming common and thus generate a lower nonsynonymous/synonymous ratio for common polymorphisms than for rare ones (Fay et al. 2001).

3.3.2 Pseudogenization of human *TAS2R*s

In addition to the many nonsynonymous polymorphisms, two nonsense polymorphisms were observed in human *TAS2R*s. The first was a C→T mutation at position 640 of *TAS2R7* that changed an Arg residue to a premature stop codon and resulted in a receptor that contains only five transmembrane domains (Figure online at http://hmg.oxfordjournals.org/cgi/data/ddh289/DC1/1). This apparently nonfunctional allele was observed once (in Andes Indian) in the 22 individuals surveyed. The relatively low frequency (2.3%) of the allele makes it difficult to distinguish whether it is neutral (but newly emergent) or deleterious. The second nonsense polymorphism (G→A at position 749) changed a Trp to a premature stop codon in *TAS2R46*, resulting in a truncated receptor with six transmembrane domains (Figure online at http://hmg.oxfordjournals.org/cgi/data/ddh289/DC1/1). This nonfunctional allele was observed 11 times in our samples. The moderate frequency (0.25) of this allele and its presence in various human populations (African Americans, Caucasians, Southeast Asians, Chinese, and Pacific Islanders) demonstrates that it is not under purifying selection. A comparison between the human and chimpanzee genome sequences indicates that chimpanzees have 6 *TAS2R* pseudogenes, while humans have two additional ones (*hps1* and *hps2* in (Shi et al. 2003)), both having been fixed, as revealed by our sequencing of 22 humans (Figures online at http://hmg.oxfordjournals.org/cgi/data/ddh289/DC1/2 and http://hmg.oxfordjournals.org/cgi/data/ddh289/DC1/3). We also confirmed that the chimpanzee orthologs of *hps1* and *hps2* have intact ORFs by sequencing one individual. Therefore, in the 6-7 million years (MY) since the human-chimpanzee split (Brunet et al. 2002), two functional *TAS2R* genes have turned into pseudogenes in the hominid lineage and another one or two are becoming pseudogenes in present-day humans. By contrast, no new *TAS2R* pseudogenes have been fixed in the chimpanzee lineage.

There are three residues that are absolutely conserved among all 63 mouse and rat Tas2rs (see below), suggesting that these residues are required for proper functioning of bitter taste receptors. However, two of them have changed in human TAS2Rs. Position 103 of human TAS2R13 is fixed with Phe, while this position is Leu in all mouse and rat Tas2rs. Similarly, human TAS2R14 is fixed with Met at position 205, while it is Leu in rodents. An *in vitro* study showed that human TAS2R14 responds to multiple bitter compounds (Behrens et al. 2004). It will be interesting to examine if human TAS2R13 is functional.

3.3.3 Equal rates of synonymous and nonsynonymous substitutions

When did the functional relaxation in human *TAS2R*s occur? This question may be addressed by comparing polymorphism and divergence data. A comparison between orthologous *TAS2R* genes from the 22 humans and one chimpanzee identified 104 nonsynonymous and 42 synonymous substitutions that have been fixed between species (Tables 3.1, 3.2). These numbers translate into identical rates of nonsynonymous (6.82×10^{-3}) and synonymous (6.82×10^{-3}) substitutions per site (P=0.52). When we measured the human-chimpanzee distance by comparing a randomly picked human allele with a randomly picked chimpanzee allele, as normally conducted, the synonymous and nonsynonymous distances both became 8.3×10^{-3} per site. These numbers are significantly ($P<0.05$) lower than the average human-chimpanzee distance (0.012 per site) observed from large genomic data (Chen et al. 2001; Ebersberger et al.

2002) and may reflect mutation rate variation within genome (Ellegren et al. 2003). The McDonald-Kreitman test (Mcdonald and Kreitman 1991) did not detect any difference between the intraspecific and interspecific patterns of nonsynonymous and synonymous variations for human *TAS2R*s (*P*=0.38; Table 3.2). From the single chimpanzee sequenced, 3 synonymous and 8 nonsynonymous polymorphisms were found. The nonsynonymous/synonymous ratio (8/3=2.67) is comparable to the ratio for human polymorphisms (72/33=2.18) and the ratio for fixed substitutions between species (104/42=2.48). We also conducted an HKA test (Hudson et al. 1987) by comparing the polymorphism and divergence data from human *TAS2R*s and those from 6 noncoding regions of the human genome that are at least 3000 nucleotides long and are not known to be under natural selection, but no difference was found (Table 3.3). These results suggest that the functional relaxation already started in the common ancestor of humans and chimpanzees and that there is no detectable difference in selection between the human polymorphism and divergence data.

An alternative explanation for the above between-species data is a more complex scenario involving purifying selection at some sites and positive selection at some other sites of *TAS2R*s. Previous studies showed that transmembrane (TM) domains of TAS2Rs are more conserved than extracellular (EC) and intracellular (IC) domains and that EC domains may be subject to positive selection between rapidly diversifying paralogous genes, consistent with the presumable tastant-TAS2R binding sites being located in the EC domains (Shi et al. 2003). To test the hypothesis of positive and purifying selection on human and chimpanzee *TAS2R*s, we estimated the d_N/d_S ratio in EC, TM, and IC domains, respectively. For comparison, we used *Tas2r* genes from the mouse and rat. To obtain these genes, we searched the rat genome sequence using all 33 mouse *Tas2r* genes as queries and identified 30 rat *Tas2r* genes. A phylogenetic tree of all putatively functional *TAS2R* genes from the human, chimpanzee, mouse, and rat was reconstructed (Figure 3.1, Figure online at http://hmg.oxfordjournals.org/cgi/data/ddh289/DC1/4). From this tree, 28 pairs of mouse and rat genes were apparently orthologous. We concatenated these 28 genes for the mouse and rat, respectively, and estimated the average d_N and d_S between them. Figure 3.2 shows that the d_N/d_S ratio is significantly lower than 1 for each of the three functional regions (EC, TM, and IC) in rodent *Tas2r* genes, demonstrating the operation of purifying selection between the orthologs. Among-domain variation in d_N/d_S, another characteristic of functional genes, is also evident, and TM domains show the lowest d_N/d_S. For both intraspecific and interspecific data of human *TAS2R*s, d_N/d_S is not significantly different from 1 for any of the three functional regions or the entire genes. Furthermore, no variation in d_N/d_S among functional regions is seen. Compared with rodent *Tas2r*s, human *TAS2R*s have significantly elevated d_N/d_S in the TM domains. These observations are consistent with the hypothesis of functional relaxation in humans (and chimpanzees), but do not support the alternative hypothesis of a combination of positive and purifying selection, because the latter predicts an elevation in d_N/d_S in EC domains while maintaining low d_N/d_S in functionally conserved TM domains.

Similarly, one may hypothesize that some *TAS2R*s of humans are under positive selection while some others are under purifying selection, giving an average d_N/d_S of ~1 for the repertoire. Table 3.1 lists the d_N/d_S ratio for each of the 25 human *TAS2R* genes and some ratios appear much higher than others, although none of them are significantly different from 1. We used computer simulation to test whether this among-gene variation was simply due to chance. In the simulation, we assumed that every gene has the expected d_N and d_S identical to the corresponding averages of the 25 human *TAS2R* genes and then generated an expected distribution of d_N/d_S from 5000 simulations (Figure 3.3). When this distribution was compared with the observed distribution, no significant difference was found (P=0.65, χ^2 test; Fig. 3.3), suggesting that the apparent among-gene variation in d_N/d_S shown in Table 3.1 is explainable by chance alone.

3.4 DISCUSSION

In this work, we characterized the intra- and inter-specific variations of the entire human bitter taste receptor gene repertoire. Our intra-specific data show equal levels of synonymous and nonsynonymous polymorphisms, equal nonsynonymous/synonymous ratios for rare and common polymorphisms, equal nonsynonymous/synonymous ratios among functional domains, segregation of nonfunctional alleles in populations, and fixation of pseudogenes in the species. All these observations support the lack of selective constraint on human *TAS2R* genes. Our inter-specific comparison between the human and chimpanzee also suggests that *TAS2R* genes have been under neutral evolution without much constraint. If a complete functional relaxation occurred in the common ancestor of humans and chimpanzees, it is perplexing why fixations of mutations that disrupt *TAS2R* ORFs occurred only twice in humans and did not occur at all in chimpanzees. Using computer simulation (see Materials and Methods), we estimated that the average half-life of human *TAS2R* genes is 6.77 MY in the absence of natural selection, meaning that after 6.77 MY of neutral evolution, a *TAS2R* gene has a 50% chance of becoming a fixed pseudogene. From the observation that only two out of 27 *TAS2R* genes have become fixed pseudogenes during hominid evolution, we obtained the maximum likelihood estimate of the starting time (*T*) of the complete functional relaxation to be 0.75 MY ago, though any *T* within 0.1 to 2.6 MY ago cannot be rejected at 5% significance level. It is likely that an incomplete functional relaxation started early in the ancestry of humans and chimpanzees but a second wave of more complete relaxation occurred recently in the hominid lineage alone. This would explain the lack of pseudogene formation in chimpanzees and the paucity of human pseudogenizations. Because each *TAS2R* recognizes multiple related toxic compounds (Bufe et al. 2002; Behrens et al. 2004) and each taste receptor cell expresses multiple *TAS2R* genes (Chandrashekar et al. 2000), it is possible that an incomplete functional relaxation occurs when the number or amount of toxins that a species encounters reduces.

As mentioned, a dietary change that started 2 MY ago (Harris 1992; Leonard 2002; Milton 2003) resulted in an increase of animal tissues and decrease of plant tissues in hominid diet, which reduced the number of toxic foods that hominids came across. Controlled use of fire was evident about 0.8 MY ago (Goren-Inbar et al. 2004); the reliance on TAS2Rs to detect toxins further diminished because cooking significantly detoxifies poisonous food (Harris 1992). It is interesting that the likelihood estimate of the starting time (0.75 MY ago) of the complete functional relaxation in human *TAS2R* genes coincides with the beginning of the fire use in hominid evolution, although our estimate has a large variance. Our data suggest that chimpanzee *TAS2R*s are likely under relaxed selective constraint as well, although to a lesser degree, as evident from the lack of pseudogenization. It has been noted that chimpanzees occasionally eat meat (2-13% of diet), whereas other great apes (gorillas and orangutans) almost never do so (Milton 2003). Furthermore, among the plant foods, chimpanzees eat mostly ripe fruits while gorillas and orangutans eat more leaves, unripe fruits, bark, and pith (Milton 2003). Ripe fruits contain considerably fewer toxins than do leaves and unripe fruits (Glendinning 1994). These factors, when combined, may have reduced the selective pressures on chimpanzee *TAS2R*s. A broader survey of *TAS2R* genes in primates may provide a better understanding of the ecology and selective agents behind the evolution of *TAS2R* genes and the bitter taste.

Our finding that the TAS2R bitter taste receptor gene repertoire of humans is under relaxed selective constraint has several implications. First, humans have lost and continue to lose *TAS2R* genes, which would result in a decrease in the number of bitter compounds that we can taste. Second, the segregation of nonfunctional *TAS2R* alleles in current human populations indicates among-individual variation in bitter sensitivity. Third, functional relaxation may also allow the appearance of new *TAS2R* alleles that can bind previously unrecognizable tastants. While the emergence of these new alleles may increase the diversity in bitter recognition among humans, it likely has little effect on fitness because of the neutral nature of the new alleles. It should be noted that loss of selective constraint does not result in loss of function instantly. Probably because of the relatively short time since the loss of selective constraints on human *TAS2R* genes, many human *TAS2R* genes may still be functional and we can still taste many bitter compounds. But loss of function will result after sufficient time of evolution under no selective constraint.

Our finding is intriguing when compared with the evolutionary patterns of other human sensory genes. Olfactory receptor genes have been inactivated in the human lineage at a higher rate than in chimpanzees and other primates. In humans, over 50% of olfactory receptor genes are pseudogenes, in contrast to 30-35% in other apes and less than 20% in rodents (Gilad et al. 2003; Gilad et al. 2004). In fact, humans have fewer than 400 functional olfactory receptor genes (Niimura and Nei 2003) and they appear to be under weak or no selective constraints (Gimelbrant et al. 2004), while mice have over 1000 functional genes (Zhang et al. 2004). Humans, apes, and Old World monkeys have lost important components of the vomeronasal pheromone signal transduction pathway and are insensitive to vomeronasal pheromones (Liman and Innan 2003; Zhang and Webb 2003). Humans also have an unusually high frequency of red/green color blindness (e.g., 8% in male Caucasians) that is not found in wild apes or Old World monkeys (Surridge et al. 2003). Deafness also occurs at a relatively high frequency (0.08%) in humans; nonfunctional GJB2 alleles, which are responsible for genetic deafness in many populations, have a total frequency of ~1.8% in United States (Nance and Kearsey 2004). Although genes involved in these sensory systems may have deteriorated at different times in the evolutionary lineage of humans, it is compelling that sensitivities to a number of sensory signals are weaker in humans than in many of our mammalian relatives. It is possible that in the evolution of apes, and particularly humans, sensory capabilities became a less important component of an individual's fitness.

3.5 MATERIALS AND METHODS

3.5.1 Sequencing human and chimpanzee *TAS2R* genes

Genomic DNAs of one chimpanzee (*Pan troglodytes*) and 22 unrelated humans (*Homo sapiens*) of diverse geographic origins (3 Pygmy Africans, 6 African Americans, 5 Caucasians, 3 Southeast Asians, 2 Chinese, 2 Pacific Islanders, and 1 Andes Indian) were purchased from Coriell Cell Repositories. Gene-specific primers for amplifying the 25 *TAS2R* genes were designed according to the human genome sequence. The protein-coding region of each *TAS2R* gene has 900-1,000 nucleotides, most of which were amplified in our experiments. After removing the primer-encoded regions, the total number of nucleotides examined here was 21,408, or on average 856 per gene. Polymerase chain reactions (PCRs) were performed with high fidelity DNA polymerase under conditions recommended by the manufacturer (Invitrogen). PCR products were separated on 1.5% agarose gel and purified using the Gel Extraction Kit (Qiagen), before being sequenced from both directions using the dideoxy chain termination method with an automated DNA sequencer. Sequencher (GeneCodes) was used to assemble the sequences and to identify DNA polymorphisms. Two human pseudogenes (*hps1* and *hps2*) were also sequenced in the 22 humans and one chimpanzee. The primer sequences are available upon request.

3.5.2 Evolutionary analyses

Numbers of synonymous and nonsynonymous sites and numbers of synonymous and nonsynonymous nucleotide changes were counted following (Zhang et al. 1998).

The number of synonymous changes per synonymous site (d_S) and the number of nonsynonymous changes per nonsynonymous sites (d_N) were then computed (Nei and Kumar 2000). Watterson's θ, nucleotide diversity π, Tajima's D test (Tajima 1989), and HKA test (Hudson et al. 1987) were computed or conducted by DnaSP (Rozas et al. 2003). Rare and common polymorphisms were defined using the cutoff of 10% frequency for the derived allele. Use of different cutoffs (5% and 15%) did not change our result. The sequence data of six noncoding regions used in the HKA test were from (Zietkiewicz et al. 1998; Harris and Hey 1999; Kaessmann et al. 1999; Fullerton et al. 2000; Zhao et al. 2000; Yu et al. 2001). Mouse *Tas2r* gene sequences were obtained from (Shi et al. 2003). Rat *Tas2r* genes were identified by BLAST searches of the rat genome sequence using the mouse genes as queries. A neighbor-joining tree (Saitou and Nei 1987) of the putatively functional *TAS2R* genes of the human, chimpanzee, mouse, and rat was reconstructed using the protein Poisson distance (Nei and Kumaer 2000). The bootstrap test (with 2000 replications) was used to examine the reliability of the observed branching patterns (Felsenstein 1985). MEGA2 (Kumar et al. 2001) was used for the phylogenetic analysis. Twenty-eight pairs of orthologous *Tas2r* genes from the mouse and rat were identified and used for computing d_S and d_N. Functional domains in TAS2Rs were defined following (Adler et al. 2000). Computer simulation was used to evaluate the expected variation in d_N/d_S among *TAS2R* genes. Because the total numbers of fixed synonymous and nonsynonymous differences in the 25 orthologous genes of humans and chimpanzees were 42 and 104, respectively (Table 3.1), the average numbers per gene were 1.68 and 4.16, respectively. Since nucleotide substitution is a Poisson process, we generated a Poisson random number with the mean of 1.68 as the number of synonymous substitution for a gene and an independent Poisson random number with the mean of 4.16 as the number of nonsynonymous substitution for the gene. The d_N/d_S ratio for the gene was then computed following (Zhang et al. 1998), using the average numbers of synonymous (246.64) and nonsynonymous (609.68) sites per gene for the *TAS2R* genes. When the number of synonymous substitution was 0, d_N/d_S was designated as NA. Such simulation was repeated 5,000 times and a distribution of d_N/d_S was generated. This distribution was compared with the observed distribution from the 25 *TAS2R*s by a χ^2 test. We used the program PSEUDOGENE (Zhang and Webb 2003) to estimate the half-life ($t_{1/2}$) of each of the human *TAS2R* genes and obtained an average of 6.77±0.05 MY. In the computation, we used a point nucleotide substitution rate of 6.4×10^{-10} per site per year, which was estimated from the synonymous substitution rates in *TAS2R* genes under the assumption of 6.5 MY as the time since the human-chimpanzee split (Brunet et al. 2002). We also used a substitution rate of 0.81×10^{-10} per site per year for ORF-disruptive indels, which was estimated from human-chimpanzee genomic comparisons (Britten 2002; Podlaha and Zhang 2003; Zhang and Webb 2003). The starting time of the complete functional relaxation (T), as well as its confidence interval, was estimated using a likelihood approach (Zhang and Webb 2003).

3.6 ACKNOWLEDGMENTS

We thank Soochin Cho, David Webb, and two anonymous reviewers for valuable comments. This work was supported by a startup fund of the University of Michigan and a research grant from the National Institutes of Health (GM67030) to J.Z.

Figure 3.1 Evolutionary relationships of 113 putatively functional *TAS2R* genes from the human, chimpanzee, mouse, and rat. The tree is reconstructed by the neighbor-joining method with protein Poisson distances. Bootstrap percentages (≥50) from 2,000 replications are shown at interior nodes. The mouse and rat genes with uncertain orthology are marked with triangles and are not used in computing the d_N/d_S ratios presented in Figure 3.2. The protein sequence alignment used for the tree reconstruction is provided in Figure online (http://hmg.oxfordjournals.org/cgi/data/ddh289/DC1/4)

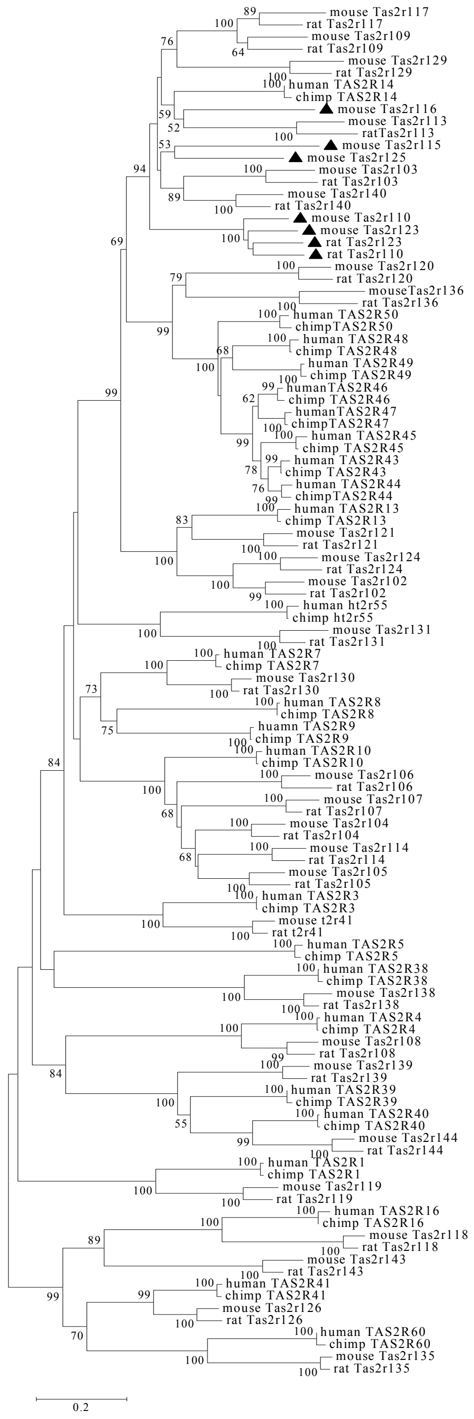

Figure 3.2 Comparison of d_N/d_S among different functional domains of TAS2Rs. Black bars show the d_N/d_S ratios computed from the concatenated sequences of 28 pairs of orthologous *Tas2r* genes of the mouse and rat. Shaded bars show the d_N/d_S ratios of the fixed differences between human and chimpanzee for the concatenated sequences of 25 pairs of orthologous *TAS2R* genes. White bars show the d_N/d_S ratios computed from the human polymorphisms at the 25 *TAS2R* genes. All comparisons are conducted using Fisher's exact test following (Zhang et al. 1997). Significant levels: *, 5%; **, 0.5%; ***, 0.05%. The test result of the null hypothesis of d_N/d_S=1 for each bar is indicated above the bar. Comparisons between two bars are indicated with brackets. Non-significant results are not indicated. EC, four extracellular domains; TM, seven transmembrane domains; IC, four intracellular domains; Total, entire proteins.

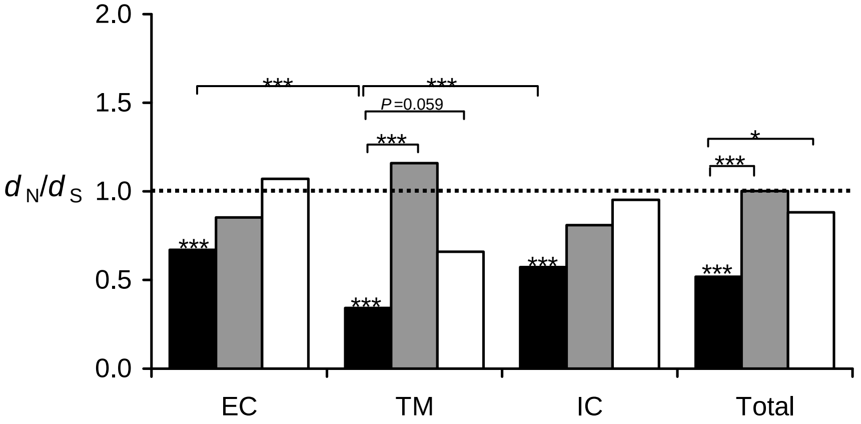

Figure 3.3 Expected and observed distributions of d_N/d_S among 25 human *TAS2R* genes. The expected distribution (white bars) under equal d_N/d_S ratios among genes was generated by computer simulation (see Materials and Methods), whereas the observed distribution (black bars) was from the d_N/d_S column in Table 3.1. NA, not applicable due to zero synonymous substitution. There is no significant difference between the two distributions (P>0.5; χ^2 test).

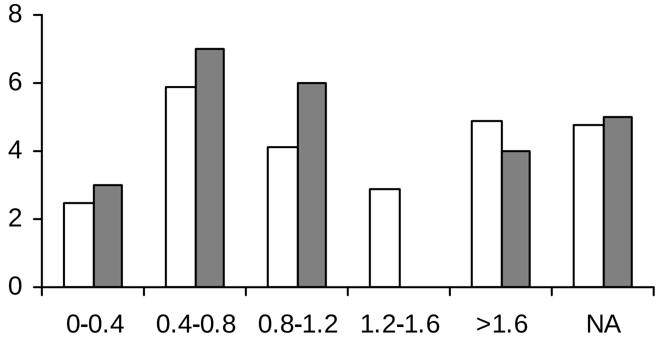

Table 3.1 Intra- and inter- variations of human *TAS2R* genes.

			Sysnonymous changes					Nonsynonymous changes					Total					
Gene names	Chr.[1]	*L*[2]	*S*[3]	π (%)[4]	θ (%)[5]	*D*[6]	*d*[7]	*S*	π (%)	θ (%)	*D*	*d*	*S*	π (%)	θ (%)	*D*	*d*	d_N/d_S[8]
TAS2R1	5	825	1	0.04	0.10	-0.85	2	2	0.05	0.08	-0.56	4	3	0.05	0.08	-0.87	6	0.82
TAS2R3	7	864	2	0.22	0.18	0.37	2	0	0.00	0.00	0.00	1	2	0.06	0.05	0.37	3	0.21
TAS2R4	7	810	0	0.00	0.00	0.00	1	2	0.11	0.08	0.59	1	2	0.07	0.06	0.59	2	0.43
TAS2R5	7	801	1	0.04	0.10	-0.85	3	3	0.11	0.12	-0.15	7	4	0.09	0.11	-0.48	10	0.96
TAS2R7	12	876	0	0.00	0.00	0.00	2	0	0.00	0.00	0.00	4	0	0.00	0.00	0.00	6	0.82
TAS2R8	12	831	2	0.22	0.20	0.24	0	1	0.01	0.04	-1.12	2	3	0.07	0.08	-0.39	2	NA
TAS2R9	12	867	0	0.00	0.00	0.00	3	1	0.08	0.04	1.54	4	1	0.06	0.03	1.54	7	0.54
TAS2R10	12	849	2	0.12	0.20	-0.69	0	1	0.04	0.04	0.27	5	3	0.07	0.08	-0.40	5	NA
TAS2R13	12	837	0	0.00	0.00	0.00	2	2	0.09	0.08	0.36	11	2	0.07	0.05	0.36	13	2.14
TAS2R14	12	879	2	0.33	0.18	1.47	3	1	0.03	0.04	-0.53	4	3	0.11	0.08	0.57	7	0.53
TAS2R16	7	807	2	0.11	0.20	-0.83	2	3	0.12	0.12	-0.04	1	5	0.12	0.14	-0.48	3	0.20
TAS2R38	7	945	0	0.00	0.00	0.00	3	4	0.21	0.14	1.16	2	4	0.15	0.10	1.16	5	0.28
TAS2R39	7	957	1	0.02	0.08	-1.12	1	3	0.03	0.10	-1.57	2	4	0.02	0.10	-1.76	3	0.79
TAS2R40	7	918	0	0.00	0.00	0.00	1	1	0.03	0.04	-0.14	2	1	0.02	0.03	-0.14	3	0.80
TAS2R41	7	870	3	0.14	0.26	-1.00	1	1	0.04	0.04	0.27	5	4	0.07	0.11	-0.71	6	2.14
TAS2R43	12	870	2	0.00	0.19	-1.30	1	7	0.21	0.26	-0.47	2	9	0.17	0.24	-0.84	3	0.78
TAS2R44	12	888	3	0.23	0.27	-0.28	5	7	0.27	0.26	0.18	8	10	0.26	0.26	0.02	13	0.66
TAS2R45	12	828	1	0.02	0.10	-1.12	2	6	0.45	0.23	2.39*	5	7	0.32	0.19	1.82	7	1.01
TAS2R46	12	804	1	0.04	0.10	-0.85	3	2	0.12	0.80	0.05	6	3	0.10	0.11	-0.40	9	0.78
TAS2R47	12	867	2	0.18	0.18	-0.03	0	2	0.08	0.07	0.12	0	4	0.11	0.11	0.05	0	NA
TAS2R48	12	753	2	0.45	0.20	2.19*	0	6	0.10	0.26	-1.62	6	8	0.20	0.24	-0.47	6	NA
TAS2R49	12	855	3	0.38	0.28	0.75	0	9	0.50	0.34	1.37	2	12	0.47	0.32	1.35	2	NA
TAS2R50	12	831	2	0.29	0.19	0.97	1	3	0.09	0.12	-0.53	5	5	0.15	0.14	0.15	6	2.01
hT2R55	12	885	1	0.10	0.09	1.60	3	4	0.24	0.15	1.57	7	5	0.20	0.13	1.91	10	0.95
TAS2R60	7	891	0	0.00	0.00	0.00	1	1	0.01	0.04	-0.85	8	1	0.01	0.03	-0.85	9	3.34
Sum		21408	33	0.12	0.12	-0.05	42	72	0.12	0.11	0.09	104	105	0.12	0.11	-0.05	146	1.00

[1] Chromosomal location.

[2] Number of sequenced nucleotides.

[3] Number of polymorphic sites.

[4] Nucleotide diversity per site.

[5] Watterson's θ per site.

[6] Tajima's *D*. **, P<0.05.*

[7] Number of fixed nucleotide differences between human and chimpanzee.

[8] Number of fixed nonsynonymous differences per nonsynonymous site between human and chimpanzee, divided by the number of fixed synonymous differences per synonymous site. NA, not applicable because of zero synonymous differences.

Table 3.2 Rates of synonymous and nonsynonymous nucleotide changes in human *TAS2R*s.

	Nonsynonymous	Synonymous	N/S ratio
Number of sites sequenced	15242	6166	2.47
Rare polymorphisms	33	15	2.20
Common polymorphisms	39	18	2.17
Fixed changes	104	42	2.48

None of the N/S ratios are significantly different from each other (Fisher's test).

Table 3.3 Comparison between TAS2R genes and neutrally evolving human sequences in intra- and inter-specific variation.

Genomic regions (references)	Sequence length (nt.)	π (%)[1]	θ (%)[2]	d (%)[3]	θ/d	HKA Prob.[4]
25 *TAS2R* genes (this study)	21408	0.121	0.115	0.831	0.138	
Noncoding region at 1q24 (42)	8991	0.058	0.095	0.623	0.152	0.669
β-globin initiation region at 11p15 (43)	6076	0.129	0.107	1.284	0.083	0.508
Noncoding region at 22q11 (44)	9091	0.088	0.139	1.353	0.103	0.312
Dystrophin intron-dys44 at Xp21 (45)	7475	0.135	0.102	0.604	0.169	0.779
PDHA1 introns at Xp22 (46)	3530	0.225	0.211	0.992	0.213	0.648
Noncoding region at Xq13.3 (47)	10200	0.045	0.083	0.922	0.090	0.369

[1] Nucleotide diversity per site; for X chromosome data, it is corrected by multiplication by 4/3.

[2] Watterson's estimate of polymorphism per site; for X chromosome, it is corrected by multiplication by 4/3.

[3] Number of nucleotide differences per site between human and chimpanzee sequences.

[4] Probability from the HKA test (30), with comparison to the *TAS2R* data.

3.7 LITERATURE CITED

Adler E, Hoon MA, Mueller KL, Chandrashekar J, Ryba NJP, Zuker CS (2000) A novel family of mammalian taste receptors. Cell 100:693-702

Behrens M, Brockhoff A, Kuhn C, Bufe B, Winnig M, Meyerhof W (2004) The human taste receptor hTAS(2)R(14) responds to a variety of different bitter compounds. Biochemical and Biophysical Research Communications 319:479-485

Britten RJ (2002) Divergence between samples of chimpanzee and human DNA sequences is 5%, counting indels. Proceedings of the National Academy of Sciences of the United States of America 99:13633-13635

Brunet M, Guy F, Pilbeam D, Mackaye HT, Likius A, Ahounta D, Beauvilain A, et al. (2002) A new hominid from the Upper Miocene of Chad, central Africa. Nature 418:145-151

Bufe B, Hofmann T, Krautwurst D, Raguse JD, Meyerhof W (2002) The human TAS2R16 receptor mediates bitter taste in response to beta-glucopyranosides. Nature Genetics 32:397-401

Cargill M, Altshuler D, Ireland J, Sklar P, Ardlie K, Patil N, Lane CR, Lim EP, Kalyanaraman N, Nemesh J, Ziaugra L, Friedland L, Rolfe A, Warrington J, Lipshutz R, Daley GQ, Lander ES (1999) Characterization of single-nucleotide polymorphisms in coding regions of human genes. Nature Genetics 22:231-238

Chandrashekar J, Mueller KL, Hoon MA, Adler E, Feng LX, Guo W, Zuker CS, Ryba NJP (2000) T2Rs function as bitter taste receptors. Cell 100:703-711

Chen FC, Vallender EJ, Wang H, Tzeng CS, Li WH (2001) Genomic divergence between human and chimpanzee estimated from large-scale alignments of genomic sequences. Journal of Heredity 92:481-489

Ebersberger I, Metzler D, Schwarz C, Paabo S (2002) Genomewide comparison of DNA sequences between humans and chimpanzees. American Journal of Human Genetics 70:1490-1497

Ellegren H, Smith NGC, Webster MT (2003) Mutation rate variation in the mammalian genome. Current Opinion in Genetics & Development 13:562-568

Fay JC, Wyckoff GJ, Wu CI (2001) Positive and negative selection on the human genome. Genetics 158:1227-1234

Felsenstein J (1985) Confidence-Limits on Phylogenies - an Approach Using the Bootstrap. Evolution 39:783-791

Fu YX, Li WH (1993) Statistical Tests of Neutrality of Mutations. Genetics 133:693-709

Fullerton SM, Bond J, Schneider JA, Hamilton B, Harding RM, Boyce AJ, Clegg JB (2000) Polymorphism and divergence in the beta-globin replication origin initiation region. Molecular Biology and Evolution 17:179-188

Garcia J, Hankins WG (1975) The evolution of bitter and the acquisition of toxiphobia. In Denton DA and Coghlan JP (eds), Olfaction and Taste V, Proceedings of the 5th International Symposium in Melbourne, Australia. Academic Press, New York, pp. 39-45.

Gilad Y, Man O, Paabo S, Lancet D (2003) Human specific loss of olfactory receptor genes. Proceedings of the National Academy of Sciences of the United States of America 100:3324-3327

Gilad Y, Wiebel V, Przeworski M, Lancet D, Paabo S (2004) Loss of olfactory receptor genes coincides with the acquisition of full trichromatic vision in primates. Plos Biology 2:120-125

Gimelbrant AA, Skaletsky H, Chess A (2004) Selective pressures on the olfactory receptor repertoire since the human-chimpanzee divergence. Proceedings of the National Academy of Sciences of the United States of America 101:9019-9022

Glendinning JI (1994) Is the Bitter Rejection Response Always Adaptive. Physiology & Behavior 56:1217-1227

Goren-Inbar N, Alperson N, Kislev ME, Simchoni O, Melamed Y, Ben-Nun A, Werker E (2004) Evidence of hominin control of fire at Gesher Benot Ya'aqov, Israel. Science 304:725-727

Harris DR (1992) Human diet and subsistence. In Jones, S., Martin R and Pilbeam D (eds), The Cambridge Encyclopedia of Human Evolution. Cambridge University Press, Cambridge, pp. 69-74.

Harris EE, Hey J (1999) X chromosome evidence for ancient human histories. Proceedings of the National Academy of Sciences of the United States of America 96:3320-3324

Hudson RR, Kreitman M, Aguade M (1987) A Test of Neutral Molecular Evolution Based on Nucleotide Data. Genetics 116:153-159

Hughes AL, Nei M (1988) Pattern of Nucleotide Substitution at Major Histocompatibility Complex Class-I Loci Reveals Overdominant Selection. Nature 335:167-170

Kaessmann H, Heissig F, von Haeseler A, Paabo S (1999) DNA sequence variation in a non-coding region of low recombination on the human X chromosome. Nature Genetics 22:78-81

Kim UK, Jorgenson E, Coon H, Leppert M, Risch N, Drayna D (2003) Positional cloning of the human quantitative trait locus underlying taste sensitivity to phenylthiocarbamide. Science 299:1221-1225

Kinnamon SC, Cummings TA (1992) Chemosensory Transduction Mechanisms in Taste. Annual Review of Physiology 54:715-731

Kumar S, Tamura K, Jakobsen IB, Nei M (2001) MEGA2: molecular evolutionary genetics analysis software. Bioinformatics 17:1244-1245

Leonard WR (2002) Food for thought - Dietary change was a driving force in human evolution. Scientific American 287:106-115

Liman ER, Innan H (2003) Relaxed selective pressure on an essential component of pheromone transduction in primate evolution. Proceedings of the National Academy of Sciences of the United States of America 100:3328-3332

Lindemann B (1996) Taste reception. Physiological Reviews 76:719-766

Matsunami H, Montmayeur JP, Buck LB (2000) A family of candidate taste receptors in human and mouse. Nature 404:601-+

Mcdonald JH, Kreitman M (1991) Adaptive Protein Evolution at the Adh Locus in Drosophila. Nature 351:652-654

Milton K (2003) The critical role played by animal source foods in human (Homo) evolution. Journal of Nutrition 133:3886S-3892S

Nance WE, Kearsey MJ (2004) Relevance of connexin deafness (DFNB1) to human evolution. American Journal of Human Genetics 74:1081-1087

Niimura Y, Nei M (2003) Evolution of olfactory receptor genes in the human genome. Proceedings of the National Academy of Sciences of the United States of America 100:12235-12240

Podlaha O, Zhang JZ (2003) Positive selection on protein-length in the evolution of a primate sperm ion channel. Proceedings of the National Academy of Sciences of the United States of America 100:12241-12246

Rogers AR (1995) Genetic-Evidence for a Pleistocene Population Explosion. Evolution 49:608-615

Rozas J, Sanchez-DelBarrio JC, Messeguer X, Rozas R (2003) DnaSP, DNA polymorphism analyses by the coalescent and other methods. Bioinformatics 19:2496-2497

Saitou N, Nei M (1987) The Neighbor-Joining Method - a New Method for Reconstructing Phylogenetic Trees. Molecular Biology and Evolution 4:406-425

Shi P, Zhang JZ, Yang H, Zhang YP (2003) Adaptive diversification of bitter taste receptor genes in mammalian evolution. Molecular Biology and Evolution 20:805-814

Surridge AK, Osorio D, Mundy NI (2003) Evolution and selection of trichromatic vision in primates. Trends in Ecology & Evolution 18:198-205

Tajima F (1989) Statistical-Method for Testing the Neutral Mutation Hypothesis by DNA Polymorphism. Genetics 123:585-595

Wooding S, Kim UK, Bamshad MJ, Larsen J, Jorde LB, Drayna D (2004) Natural selection and molecular evolution in PTC, a bitter-taste receptor gene. American Journal of Human Genetics 74:637-646

Yu N, Fu YX, Sambuughin N, Ramsay M, Jenkins T, Leskinen E, Patthy L, Jorde LB, Kuromori T, Li WH (2001) Global patterns of human DNA sequence variation in a 10-kb region on chromosome 1. Molecular Biology and Evolution 18:214-222

Zhang JZ, Kumar S, Nei M (1997) Small-sample tests of episodic adaptive evolution: A case study of primate lysozymes. Molecular Biology and Evolution 14:1335-1338

Zhang JZ, Rosenberg HF, Nei M (1998) Positive Darwinian selection after gene duplication in primate ribonuclease genes. Proceedings of the National Academy of Sciences of the United States of America 95:3708-3713

Zhang JZ, Webb DM (2003) Evolutionary deterioration of the vomeronasal pheromone transduction pathway in catarrhine primates. Proceedings of the National Academy of Sciences of the United States of America 100:8337-8341

Zhang XM, Rodriguez I, Mombaerts P, Firestein S (2004) Odorant and vomeronasal receptor genes in two mouse genome assemblies. Genomics 83:802-811

Zhao ZM, Jin L, Fu YX, Ramsay M, Jenkins T, Leskinen E, Pamilo P, Trexler M, Patthy L, Jorde LB, Ramos-Onsins S, Yu N, Li WH (2000) Worldwide DNA sequence variation in a 10-kilobase noncoding region on human chromosome 22. Proceedings of the National Academy of Sciences of the United States of America 97:11354-11358

Zietkiewicz E, Yotova V, Jarnik M, Korah-Laskowska M, Kidd KK, Modiano D, Scozzari R, Stoneking M, Tishkoff S, Batzer M, Labuda D (1998) Genetic structure of the ancestral population of modern humans. Journal of Molecular Evolution 47:146-155

CHAPTER 4

ADAPTIVE PSEUDOGENIZATION OF *CASPASE12* IN HUMAN EVOLUTION

4.1 ABSTRACT

Pseudogenization is a widespread phenomenon in genome evolution, and it has been proposed to serve as an engine of evolutionary change, especially during human origins (the "less-is-more" hypothesis). Here we provide population genetic evidence that positive selection drove the nearly complete fixation of a null allele of human *CASPASE12*, a gene implicated in susceptibility to severe sepsis. We estimate that the selective advantage of the null allele is ~0.9% and the pseudogenization started shortly before the out-of-Africa migration of modern humans. This adaptive gene loss might have occurred because of changes in our environment or genetic background that altered the threat from or response to sepsis. Our finding opens the door for understanding the roles of gene losses in human origins, and the demonstration that gene loss itself can be adaptive supports and extends the "less-is-more" hypothesis.

4.2 INTRODUCTION

Although humans are highly similar to chimpanzees at the genomic sequence and protein sequence levels (Chen and Li 2001; Britten 2002; Ebersberger et al. 2002; Wildman et al. 2003; Watanabe et al. 2004; The Chimpanzee Sequencing and Analysis Consortium 2005), the two species differ dramatically in many aspects of their biology such as bipedalism, brain size, language/speech capability, and susceptibility to the human/simian immunodeficiency virus (HIV/SIV). With rapid progress in human genetics, comparative genomics, and molecular evolution, the genetic basis of these differences has begun to be unraveled. For example, the conserved transcriptional factor FOXP2 is required for speech development in humans (Lai et al. 2001) and it experienced two adaptive amino acid replacements in hominin evolution, suggesting that these two substitutions were at least partially responsible for the emergence of human speech and language (Enard et al. 2002; Zhang et al. 2002). Compared to such amino acid replacements, gene gains and losses are more dramatic genetic changes (Olson 1999; Olson and Varki 2003; Zhang 2003; Fortna et al. 2004; Li and Saunders 2005). In particular, gene loss, or pseudogenization, leads to immediate loss of gene function, which probably affects organisms to a greater extent than most amino acid replacements do. A number of genes are known to have been lost in the human lineage since its divergence from the chimpanzee lineage (Chou et al. 1998; Szabo et al. 1999; Winter et al. 2001; Gilad et al. 2003; Hamann et al. 2003; Meyer-Olson et al. 2003; Stedman et al. 2004; Wang et al. 2004; Fischer et al. 2005; Go et al. 2005; Perry et al. 2005). Recently, Olson (Olson 1999) and Olson and Varki (Olson and Varki 2003) proposed the "less-is-more" hypothesis, suggesting that gene loss may serve as an engine of evolutionary change. This hypothesis is particularly intriguing for human evolution, as several human gene losses have been proposed to provide opportunities for adaptations and be responsible for human-specific phenotypes. For example, the pseudogenization of the sarcomeric myosin gene *MYH16* at the time of the emergence of the genus *Homo* is thought to be responsible for the marked size reduction in hominin masticatory muscles, which may have allowed the brain-size expansion (Stedman et al. 2004) (but see (Perry et al. 2005). In another example, the human-specific inactivation of the gene encoding the enzyme CMP-N-acetylneuraminic acid hydroxylase (CMAH) led to the deficiency of the mammalian common sialic acid Neu5Gc (N-glycolylneuraminic acid) on the human cell surface (Chou et al. 1998). This inactivation was due to an Alu-mediated sequence replacement (Hayakawa et al. 2001) that occurred ~2.7 million years ago (Chou et al. 2002) and may have had several important consequences to human biology and evolution (Varki 2001).

There has been no demonstration of positive selection driving the loss of a human gene, although the loss may have subsequently allowed future adaptations. Such passive pseudogenization incidences are not themselves adaptations. To explore the possibility of adaptive pseudogenization, we focus on CASPASE12 evolution in human population. CASPASE12 belongs to the caspase family, which are *c*ysteinyl *asp*artate protein*ases* that play important roles in the processing of inflammatory cytokines and the initiation and execution of apoptosis (Alnemri et al. 1996; Lamkanfi et al. 2002). In humans, 11 functional caspase genes are known, *CASPASE1-10* and *CASPASE14*. Human *CASPASE12* (*CASP12*) was identified as a pseudogene following the cloning of mouse *Caspase12* (Fischer et al. 2002). Compared with other mammalian orthologs, human *CASP12* contains a premature stop codon due to a C to T nonsense mutation at nucleotide position 629 of exon 4 (Fischer et al. 2002; Saleh et al. 2004). This mutation leads to the production of truncated nonfunctional CASP12 in humans (Saleh et al. 2004). The null T allele is fixed in a sample of 347 non-Africans and has a frequency of 89% in 776 individuals of African descent (Saleh et al. 2004). Interestingly, the T allele is associated with a reduced incidence and mortality of severe sepsis (Saleh et al. 2004), suggesting that the loss of functional CASP12 is beneficial to present-day humans. In this work, we provide evidence that the nearly complete fixation of a null allele at *CASPASE12* (Fischer et al. 2002; Saleh et al. 2004; The Chimpanzee Sequencing and Analysis Consortium 2005) has been driven by positive selection, probably because the allele confers lowered susceptibility to severe sepsis.

4.3 RESULTS

4.3.1 Adaptive loss of *CASP12* in human evolution

To test whether the nearly complete fixation of the null allele at *CASP12* has been driven by positive selection, we looked for signals of recent (incomplete) selective sweeps by examining the intraspecific variation of putatively neutral regions surrounding the C/T polymorphism. The positive selection hypothesis predicts that the level of polymorphism in these regions is lower in the null T allele than in the C allele, especially in the proximity of the C/T polymorphism, due to the hitchhiking effect (Maynard Smith and Haigh 1974). Furthermore, the frequency distribution of the neutral polymorphisms in the T allele should deviate from the neutral expectation, generating negative values of Tajima's *D* (Tajima 1989) and Fay and Wu's *H* (Fay and Wu 2000).

From a sample of 63 humans of African descent, we identified 4 C/C homozygotes and 43 T/T homozygotes. We sequenced the 4 C/C homozygotes and 4 randomly chosen T/T homozygotes in 9 noncoding regions of varying distances from the C/T polymorphism (Figure 4.1). The sequenced regions vary in size from ~600 to 2,400 nucleotides. In total, 53 and 29 single nucleotide polymorphisms (SNPs) were identified from 8,925 nucleotide sites in C/C and T/T individuals, respectively (Figure 4.2; Table 4.1). Although the T allele is much more prevalent than the C allele in the population, the T allele has a significantly lower number of SNPs per nucleotide than the C allele in the linked regions (P<0.01, Fisher's exact test). Nucleotide diversity per site (π) is also lower in the T alleles (π_T=0.00131±0.00019) than in the C alleles (π_C=0.00218±0.00031) (P=0.02, two-tail Z test). More strikingly, although the variation of π_C across the 9 regions is more or less random, that of π_T exhibits a V shape, with the bottom of the valley located in region 4, which has its 3' end only 607 nucleotides from the C/T polymorphism (Figure 4.1). When one moves ~10,000 nucleotides from this polymorphism, π_T rises to a level comparable to π_C. To exclude the possibility that the low π_T observed around the C/T polymorphism was due to the use of a small sample, we sequenced 7 additional T/T individuals of African descent in regions 4, 5, and 6. The π_T values obtained from the combined data of 11 individuals were either lower than or similar to those from the 4 individuals (Table 4.1), suggesting that the observation of low π_T is not due to a small sample. In region 4, where the greatest reduction in polymorphism is observed, only 1 SNP is found across the 2413 nucleotide positions among the 22 T alleles sequenced. By contrast, 19 SNPs were found in the same region among 8 C alleles examined. Region 4 was also sequenced in 6 non-Africans (all non-Africans are T/T homozygotes (Saleh et al. 2004)), but no SNP was detected and all non-African T alleles are identical to the predominant T allele from Africans. This indicates a common origin of African and non-African T alleles.

In a formal test of the selective sweep hypothesis, we used coalescent simulations to examine whether the polymorphisms observed in region 4 can be explained by neutral models of evolution. Such tests require a sample that is representative of the population under investigation. We thus sequenced 20 additional African T/T homozygotes so that our sample comprises 62/70=89% of T alleles and 8/70=11% C alleles, expected in populations of African descent (Saleh et al. 2004). In the 70 chromosomes sequenced, the two most common haplotypes observed (with a total frequency of 61/70) are both from T alleles and these two haplotypes have only one nucleotide difference. Let k_1 be the number of chromosomes with the most common haplotype in a sample and k_2 be the number of chromosomes with the most frequent haplotype among those that are one nucleotide different from the most common haplotype in the sample. We first simulated the evolution of a population with a constant size. In 0.066% of the 50,000 replications, we observed $k_1+k_2 \geq 61$. We also simulated various demographic changes to mimic the evolution of human populations, and $k_1+k_2 \geq 61$ was observed in fewer than 1% of simulation replications in all models considered (Table 4.2). These demographic models included ancient or recent population expansions, severe bottleneck, repeated bottlenecks with subsequent expansion, and population subdivision and admixture (Evans et al. 2005) (see Materials and Methods). Previous studies suggested that the models used here are much more stringent than that associated with the real demographic history of humans (Zietkiewicz et al. 1998; Harpending and Rogers 2000). Hence, our tests are conservative.

We also computed statistics *D* and *H* for regions 4 and 5 in the T allele, as these two regions have significantly lower π_T than π_C (Table 4.1). Both statistics were significantly negative in region 5 (D=-2.08, P<0.01; H=-4.71, P<0.025), consistent with the expectations from a selective sweep. *D* (-0.23, P=0.47) and *H* (-0.90, P=0.09) were not significantly negative in region 4, probably because the number of SNPs is too small for the statistic tests to be powerful. It should be noted that the above tests are less rigorous than the coalescent simulations because the tests are conducted on subsets of the genealogy (Evans et al. 2005). Linkage disequilibrium (LD) can also be used to test recent selective sweeps if long-range haplotypes can be reliably inferred (Sabeti et al. 2002). In the present case, however, long-range haplotypes are difficult to infer with certainty due to the small number of C/C homozygotes available. But the genotypes shown in Figure 4.2 provide a visual indication of longer LD in T alleles than in C alleles and a decay of LD when one moves away from the C/T polymorphism, consistent with the recent origin of T alleles. Taken together, our observations, especially the proximity of the π_T valley to the C/T polymorphism and the coalescent simulations, strongly suggest that the spread of the T allele among Africans and non-Africans has been driven by positive selection and that the selective advantage was directly conferred by the C→T nonsense mutation.

4.3.2 Dating the pseudogenization event and selective sweep in *CASP12*

When did the pseudogenization of human *CASP12* start? We took two approaches to estimate the age of the T allele. In the first method, we used the information of noncoding region 4, which is longest among the 9 sequenced regions and is also closest to the C/T polymorphism. The founding haplotype of T alleles is inferred, and the proportion (P) of present-day T alleles identical to the founding haplotype is estimated. It can be shown that $P=(1-r)^G$, where G is the age of the T allele in generation and r is the total rate of mutation and recombination per sequence per generation (Stephens et al.

1998). In the present case, it is easy to infer the founding haplotype (for region 4) because of the low polymorphism and the availability of an outgroup (chimpanzee) sequence. *P* is estimated to be 0.811 based on the observation of 60 copies of the founding haplotype in a total of 74 T alleles sequenced (including both Africans and non-Africans). The mutation rate is estimated to be $23/(12\times10^{6})\times25 = 4.792\times10^{-5}$ per sequence per generation. Here 23 is the average number of nucleotide differences between human and chimpanzee in region 4, 12×10^{6} is twice the divergence time in year between the two species (Brunet et al. 2002), and 25 is the average human generation time in years. The recombination rate is estimated to be $0.7\times10^{-8}\times3720=2.269\times10^{-5}$ per sequence per generation, where 0.7×10^{-8} is the pedigree-based recombination rate per generation per nucleotide at the *CASP12* locus (Kong et al. 2002) and 3720 is the number of nucleotides between the 5' end of region 4 and the C/T polymorphism. We thus estimated that *G*=2,970 generations (Figure 4.3A), which corresponds to 74,250 years. The 95% confidence interval for *P* is between 0.647 to 1. If we consider the sampling error of *P*, the 95% confidence interval for the estimated time is from 0 to 154 thousand years. The standard error of the estimated mutation rate is $1/\sqrt{23}$=21% of the estimate, while the error of the recombination rate is difficult to evaluate.

In the second method, we used a deterministic selection model (Hartl and Clark 1997) to estimate the number of generations required for the T allele to rise to its present-day frequency among individuals of African descent. It has been estimated that the incidence of severe sepsis is *I*=0.59% and the mortality rate is *M*=26.5% among African Americans (Alexander et al. 2004). The genotype frequencies among individuals of African descent are $f_{C/C}$=1.675%, $f_{C/T}$=18.6%, and $f_{T/T}$=79.77%, respectively (Saleh et al.

2004). Here we used the genotype frequency data from ref. (Saleh et al. 2004) because their sample is considerably larger than ours. The proportions of the three genotypes among severe sepsis patients have been estimated to be P(C/C | sepsis)=10.5%, P(C/T | sepsis)=29.0%, and P(T/T | sepsis)=60.5% (Saleh et al. 2004). Using Bayes theorem, we calculated the survival rate (S) for a given genotype X by S_X=1-MP(sepsis | X) =1-IMP(X | sepsis)/f_X, and obtained $S_{C/C}$=0.9902, $S_{C/T}$=0.9976, and $S_{T/T}$=0.9988. Here we assumed that the pre-reproductive-age incidence of sepsis in much of the human history is comparable to the total incidence of sepsis estimated today (Alexander et al. 2004). The relative fitness of C/C to the fitness of T/T is therefore $W_{C/C}$ =$S_{C/C}$/$S_{T/T}$=0.991. Similarly, $W_{C/T}$ =$S_{C/T}$/$S_{T/T}$=0.999 and $W_{T/T}$ =1. The selective disadvantage of C/C compared with T/T is s =1- $W_{C/C}$ =0.009 and the degree of dominance of the C allele relative to the T allele is h=(1-$W_{C/T}$)/(1-$W_{C/C}$)=0.11. The number of generations required for a given change in allele frequency was calculated using the differential equation $dp/dt=p(1-p)s[ph+(1-p)(1-h)]$ with the current T frequency p =0.891 (Saleh et al. 2004) and the initial T frequency p_0 =1/(2N), where N is the effective population size of humans (Hartl and Clark 1997). The calculated number of generations is t =2,111 (Figure 4.3B), under the assumption of an effective population size of 10^4 individuals (Takahata et al. 1995; Harpending et al. 1998). In this computation, we ignored the effect of random genetic drift because 2Ns =180>>1 and the behavior of the alleles is dominated by selection (Kimura 1983). Because of the sampling error, the 95% confidence interval of p is [0.875, 0.907], which gave the 95% confidence interval of the time required for the T allele to reach today's frequency to be 51 to 55 thousand years. Note that the actual error of the time estimate may be considerably larger because the estimation errors of h and s

are difficult to assess. Here we assumed that positive selection acted as soon as the null allele appeared. It is possible that the null allele was initially neutral, but later became beneficial due to a change in the genetic or environmental background. If this is the case, the appearance of the T allele would be earlier than dated by this method.

Strictly speaking, the first approach we used was to date the appearance of the T allele, whereas the second approach was to date the onset of the selective sweep. These two events were not necessarily simultaneous, although the appearance of the T allele was a prerequisite for the selective sweep. Despite the potentially large errors, the two estimates were close, suggesting that the T allele might have been beneficial since its appearance. Because the T alleles of Africans and non-Africans share the same origin, the C→T nonsense mutation must predate the out-of-Africa migration of modern humans, which is believed to have occurred 40-60 thousand years ago (Cavalli-Sforza and Feldman 2003). Our dating suggests that the pseudogenization of *CASP12* began not long before this migration. As a comparison, it is interesting to compute the mean time required for a neutral allele to rise to the current frequency of p=0.891. This can be estimated by $-4Np(\ln p)/(1-p)$ =37,736 generations, or 943,000 years (Kimura and Ohta 1973). In the above, N is the effective population size of humans and is assumed to be 10^4. Thus, it would have taken a considerably longer time for the null allele to reach today's frequency if it were neutral.

4.4 DISCUSSION

Our population genetic study provided strong evidence that the nearly complete fixation of a null allele at human *CASP12* has been driven by positive selection, possibly because it confers resistance to severe sepsis. *CASP12* is a functional gene in all mammals surveyed except humans (Saleh et al. 2004), suggesting that it is indispensable in a typical mammal. The functional human CASP12 acts as a dominant-negative regulator of essential cellular responses including the NF-κB and IL-1 pathways; it attenuates the inflammatory and innate immune response to endotoxins (Saleh et al. 2004). Because an appropriate level of immune response that is neither excessive nor insufficient is important to an organism, one can imagine that the immune suppression function of CASP12 becomes harmful when the immune system cannot fully respond to a challenge. It is likely that during human evolution alterations in our genetic and/or environmental background resulted in a malfunction of the immune response to endotoxins, which rendered the previously necessary function of CASP12 deleterious in humans and the null allele advantageous over the functional one. Identification of such genetic and/or environmental alterations will be valuable for understating human-specific immune functions. It is interesting to note that mouse Casp12 is implicated in amyloid-induced neuronal apoptosis, whereas the functional form of human CASP12 does not have this function. The reasons and consequences of this difference, particularly in relation to the human-specific pathology of Alzheimer's disease, are intriguing (The Chimpanzee Sequencing and Analysis Consortium 2005).

The "less-is-more" hypothesis emphasized that gene loss can sometimes play an active role in evolution (Olson 1999), with the premise that gene loss may provide opportunities for future adaptations. Our finding that gene loss itself can be adaptive supports and extends the "less-is-more" hypothesis. In the context of pathogenic threats, it is interesting to mention two examples where human null alleles are selected for in certain geographic areas (Stephens et al. 1998; Hamblin et al. 2002). In the first example, a null allele generated by a 32-nucleotide deletion in the *CCR5* chemokine receptor gene was subject to positive selection in Caucasians in the recent human history (Stephens et al. 1998) (but see (Sabeti et al. 2005). CCR5 is used by pathogens, such as HIV, as a coreceptor to enter host cells; the null allele protects humans from attacks of these pathogens. The exact pathogens that were responsible for the spread of the CCR5 null allele, however, are still under debate (Galvani and Novembre 2005). In the second example, a null allele at the Duffy blood group locus was shown to be beneficial in some Africans, probably because it confers resistance to malaria (Hamblin et al. 2002). Nevertheless, in both of these examples, the null alleles appear to be less fit than the functional alleles when the pathogens are rare or absent. Thus, the positive selection for the null alleles is limited to small geographic areas and it is unlikely that they will lead to the eventual loss of the two human genes. By contrast, *CASP12* has been lost in non-Africans and is nearly lost in Africans.

How often does adaptive gene loss occur in general? While this problem has not been investigated systematically, two non-human cases have been reported recently. The first occurred in a gene responsible for pheromone synthesis in insects and the pseudogenization led to the origin of a partially reproductively isolated race of *Drosophila melanogaster* (Takahashi et al. 2001; Greenberg et al. 2003). The second case involves a gene whose functional product prevents selfing in plants and the pseudogenization event allowed the evolution of self-pollination in *Arabidopsis thaliana* (Shimizu et al. 2004). Given the high frequency of pseudogenization in eukaryotic genomes, one may speculate that adaptive gene loss is not uncommon. Interestingly, two of the three adaptive pseudogenizations so far documented happened to genes that are involved in chemoreception or immunity, consistent with the previous finding that genes of these functions tend to evolve rapidly with high rates of turnover (Hughes 1999; Grus et al. 2005). Although detection of adaptive gene loss is restricted due to a rapid decay of population genetic signals of selective sweeps (Przeworski 2003), it is possible that adaptive gene loss is more frequent than previously thought, especially from the above two functional categories. This said, the study of the roles that gene losses play in evolution has just begun; more empirical evidence is needed to demonstrate the importance of the “less-is-more” hypothesis during evolution in general and human evolution in particular.

4.5 MATERIALS AND METHODS

4.5.1 DNA amplification and sequencing of *CASP12* alleles

All human genomic DNA samples were purchased from Coriell Cell Repositories. The genotypes of 63 individuals of African descent at the C/T polymorphism (position 629 of exon 4) were determined by sequencing a portion of exon 4. These individuals included 48 African Americans, 6 African pygmies, and 9 Africans (south of the Sahara). Four C/C homozygotes (3 African Americans and 1 African pygmy), 43 T/T homozygotes, and 16 C/T heterozygotes were identified. The T allele has a frequency of 81±0.035% in our sample, slightly lower than that (89%) reported in a previous study, which was based on a much larger sample (Saleh et al. 2004). All 4 C/C individuals and 4 randomly picked T/T individuals (3 African Americans and 1 African pygmy) were sequenced in 9 noncoding regions as shown in Figure 4.1. To ensure that the low polymorphism found among T/T individuals in regions 4, 5, and 6 was not due to the small sample size, we sequenced 7 additional T/T individuals (all African Americans) in the three regions. The genotypes of 6 non-Africans (2 Caucasians, 1 Chinese, 2 Pacific Islanders, and 1 Andes) at the C/T polymorphism were also determined by the same approach and all were found to be T/T homozygotes. (Note that the fixation of the T allele in non-Africans was previously demonstrated in a sample of 347 individuals (Saleh et al. 2004).) Region 4 was sequenced in these 6 non-Africans and no SNPs were found. For conducting coalescent simulations by the ms program (Hudson 2002), we sequenced 20 additional T/T individuals of the African descent for region 4, so that our sample of Africans comprised 4 C/C and 31 T/T individuals, with the frequency of T alleles being 89%, which is expected for Africans (Saleh et al. 2004). Our sample can be treated as a random sample under the reasonable assumption of random mating with respect to the C/T polymorphism.

The experimental procedure was as follows. Fragment-specific primers were designed according to the human genome sequence. Polymerase chain reactions (PCRs) were performed with MasterTaq (Eppendorf) under conditions recommended by the manufacturer. PCR products were separated on 1.5% agarose gel and purified using the Gel Extraction Kit (Qiagen). Amplified DNA fragments were sequenced from both directions in an automated DNA sequencer using the dideoxy chain termination method. Sequencher (GeneCodes) was used to assemble the sequences and to identify DNA polymorphisms. All singletons were confirmed by an independent PCR and sequencing experiment. After removing the primer regions, each sequenced fragment is 500-800 nucleotides long. All the SNPs identified in this study are listed in Table 4.3.

4.5.2 Population genetic analysis

Nucleotide diversity per site π (Tajima 1989), Tajima's *D* (Tajima 1989), and Fay and Wu's *H* (Fay and Wu 2000) were computed by DnaSP (Rozas and Rozas 1999). Gaps in the sequence alignments were excluded from the analysis. The chimpanzee genome sequence available in GenBank was used as an outgroup in computing *H*. Tajima's test (Tajima 1989) and Fay and Wu's test (Fay and Wu 2000) were conducted by DnaSP using coalescent simulations with 50,000 replications under the assumption of no recombination, which gave more conservative results than when recombination is considered. To test the hypothesis of selective sweeps more rigorously, we modeled various demographic scenarios of human populations by coalescent simulations (50,000 replications per model). The parameters used in the coalescent simulations are described in Supplementary Methods. Two methods were used to estimate the age of the T allele, as described in detail in Results/Discussion.

4.5.3 Demographic history simulation

Our sample for region 4 included 4 C/C and 31 T/T individuals of African descent. Thus, the sample frequency of the T allele is 89%, same as the expected value for humans of African descent (Saleh et al. 2004). In the 70 chromosomes sequenced, 19 SNPs were found. The two most common haplotypes observed (with a total frequency of 61/70) are from T alleles and these two haplotypes have only one nucleotide difference. Let k_1 be the number of copies of the most common haplotype in a sample and k_2 be the number of copies of the most frequent haplotype among those that are one nucleotide different from the most common haplotype in the sample. In coalescent simulations, we calculated the proportion of cases (out of 50,000 replications) in which $k_1+k_2 \geq 61$. We used the ms program (Hudson 2002) to generate independent samples under a variety of neutral models with different demographic histories. The number of alleles and the number of segregating sites were set to be 70 and 19, respectively. The pedigree-based recombination rate of R=0.7×10^{-8} per generation per nucleotide at the *CASP12* locus (Kong et al. 2002) was used. We examined 9 demographic models following Evans and colleagues (Evans et al. 2005). We assumed an effective population size of N=10^4 (Takahata et al. 1995; Harpending et al. 1998), as the genetic variants of non-Africans are usually subsets of those of Africans. In the following command lines, 2413 is the length of region 4 in nucleotide, and 0.675 is the population recombination rate for region 4 when N=10^4 is used ($\rho=4NR=4\times10^4\times0.7\times10^{-8}\times2413=0.675$).

The 9 models tested and the command lines used in the ms program are:

1) Constant population with an effective size of 10^4,

```
./ms 70 50000 -s 19 -r 0.675 2413
```

2) An ancient population expansion from 10^4 at 5,000 generations ago exponentially to 10^7 today,

```
./ms 70 50000 -s 19 -r 675 2413 -G 55262.04223 -eG 0.000125 0
```

3) A recent population expansion from 10^4 at 1,000 generations ago exponentially to 10^7 today,

```
./ms 70 50000 -s 19 -r 675 2413 -G 276310.2112 -eG 0.000025
```

4) A severe bottle neck starting 5,000 generations ago that reduced the population from 10^4 instantly to 10^3 and lasted until 2,500 generations ago at which point the population

started to expand exponentially to 10^7 today,

```
./ms 70 50000 -s 19 -r 675 2413 -G 147365.446 -eG 0.0000625 0 -eN 0.000125 0.001
```

5) Repeated bottlenecks for five successive rounds starting 7000 generations ago, each from 10^4 instantly to 10^3 for 500 generations followed by exponential recovery back to 10^4 over another 500 generations, except at the end of the fifth bottleneck 2500 generations ago which was followed by exponential growth to 10^7 today,

```
./ms 70 50000 -s 19 -r 675 2413 -G 147365.446 -eG 0.0000625 0 -eN 0.000075 0.001 -eG 0.000075
184206.8074 -eG 0.0000875 0 -eN 0.0001 0.001 -eG 0.0001 184206.8074 -eG 0.0001125 0 -eN 0.000125 0.001 -eG
0.000125 184206.8074 -eG 0.0001375 0 -eN 0.00015 0.001 -eG 0.00015 184206.8074 -eG 0.0001625 0 -eN 0.000175
0.001
```

6) Population structure where the initial 70 chromosomes were split equally into 2 different subpopulations under constant population size with 1 migration per generation,

```
./ms 70 50000 -s 19 -r 0.675 2413 -es 0.0 1 0.5 -eM 0.0 1.0
```

7) Population structure where the initial 70 chromosomes were split equally into 3 different subpopulations with 1 migration per generation,

```
./ms 70 50000 -s 19 -r 0.675 2413 -es 0.0 1 0.3333 -es 0.0 1 0.5 -eM 0.0 1.0
```

8) Population structure where the initial 70 chromosomes were split equally into 4 different subpopulations with 1 migration per generation,

```
./ms 70 50000 -s 19 -r 0.675 2413 -es 0.0 1 0.25 -es 0.0 1 0.333 -es 0.0 1 0.5 -eM 0.0 1.0
```

9) Population structure where the initial 70 chromosomes were split equally into 5 different subpopulations with 1 migration per generation,

```
./ms 70 50000 -s 19 -r 0.675 2413 -es 0.0 1 0.2 -es 0.0 1 0.25 -es 0.0 1 0.333 -es 0.0 1 0.5 -eM 0.0 1.0
```

4.6 ACKNOWLEDGMENTS

We thank Soochin Cho, Ondrej Podlaha, Peng Shi, and three referees for valuable comments on an earlier version of the manuscript. This work was supported by research grants from University of Michigan and National Institutes of Health (R01GM067030) to J.Z.

Figure 4.1 Intraspecific DNA sequence variation in noncoding regions linked with the human *CASPASE12* gene. *CASPASE12* is shown in blue, with the exons depicted by solid blue bars on the chromosome. The premature stop codon generated by the C→T nonsense mutation is shown by an asterisk in exon 4. The 9 noncoding regions sequenced are indicated below the chromosome. Exons, introns, the 9 noncoding regions, and spaces between regions are drawn to scale as indicated. Red circles (connected by the red dotted line) show nucleotide diversity per site among African T alleles (π_T) and the red boxes shows $\pi_T \pm$ one standard error of π_T. Green squares (connected by the green dotted line) show nucleotide diversity per site among African C alleles (π_C) and the green boxes shows $\pi_C \pm$ one standard error of π_C. The broken green line shows the mean π_C across the 9 noncoding regions sequenced. Black triangles (connected by the black solid line) show the ratio between π_T and π_C for each region. π_C is estimated from 8 alleles. π_T is estimated from 22 alleles for regions 4, 5, and 6, and from 8 alleles for the other regions. When only 8 alleles are used, π_T is 0.00018±0.00007, 0.00129±0.00071, and 0.00145±0.00057 for regions 4, 5, and 6, respectively. π_T is significantly lower than π_C in regions 4 and 5 (Table 4.1).

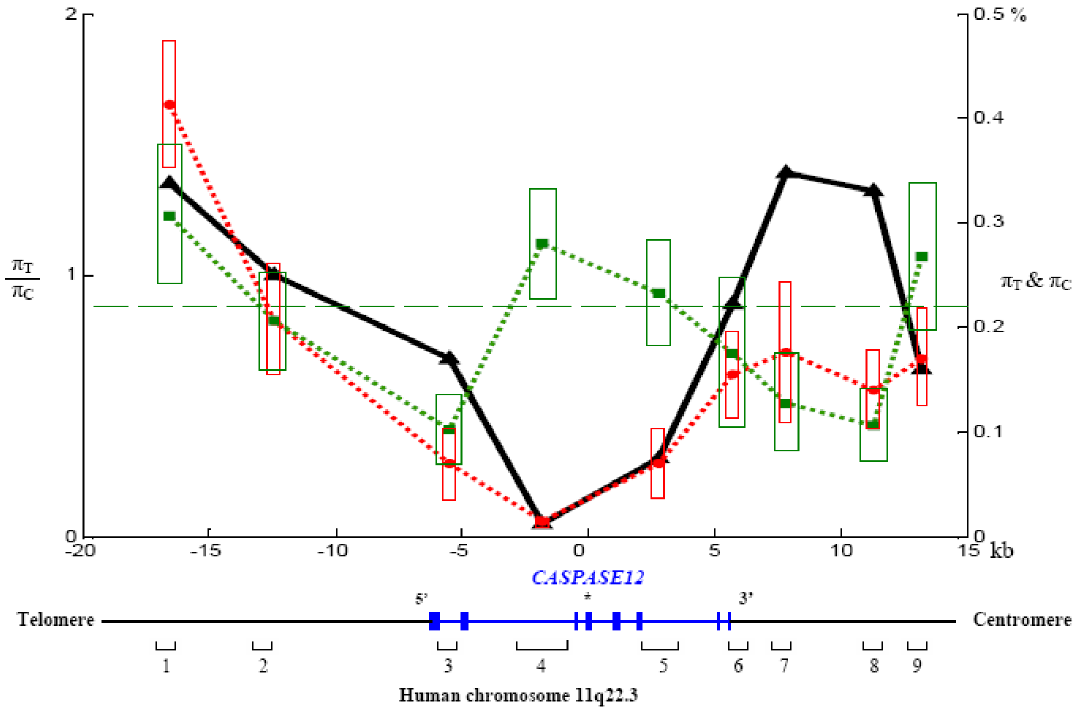

Figure 4.2 Genotypes of the 4 C/C homozygotes and 4 T/T homozygotes that were sequenced in all 9 noncoding regions. Each row represents one human individual and each column represents one SNP site. The top 4 individuals are homozygous for the functional *CASP12* allele and the bottom 4 individuals are homozygous for the null allele. Blue, yellow, and green squares indicate homozygotes for the ancestral allele, homozygotes for the derived allele, and heterozygotes, respectively, at each SNP site. The nucleotide position of each SNP site is given at the bottom of the figure with the ancestral/derived nucleotides indicated. The nucleotide positions are relative to the start codon ATG. On the top of the figure is the chromosome, with the exons of *CASP12* depicted by solid blue bars on the chromosome. The premature stop codon generated by the C→T nonsense mutation is shown by an asterisk in exon 4. The 9 noncoding regions sequenced are indicated below the chromosome.

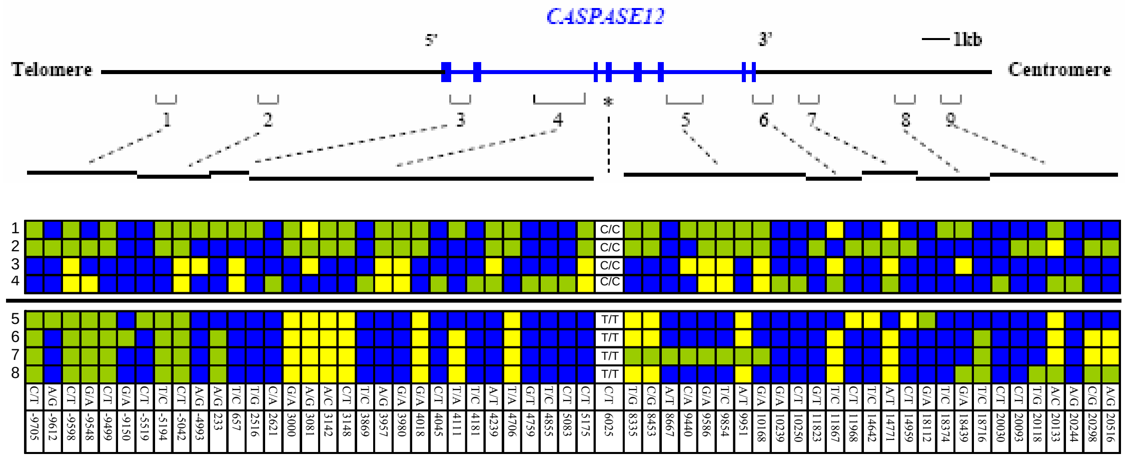

Figure 4.3 Estimating the age of the null allele and the onset of the selective sweep. (**A**) Decline of the frequency (*P*) of the founding haplotype of the null allele over generations (*G*). We used the formula $P=(1-r)^G$, with the sum of the mutation and recombination rate *r* being 7.061×10^{-5} per generation. The dashed line shows the estimated *P* at present and its corresponding *G*. (**B**) The increase of the frequency (*p*) of the null allele over generations (*t*) by positive selection, based on the differential equation $dp/dt=p(1-p)s[ph+(1-p)(1-h)]$. Here we used p_0=0.00005, *h*=0.11, *s*=0.009. The dashed line shows the estimated *p* at present and its corresponding *t*.

A.

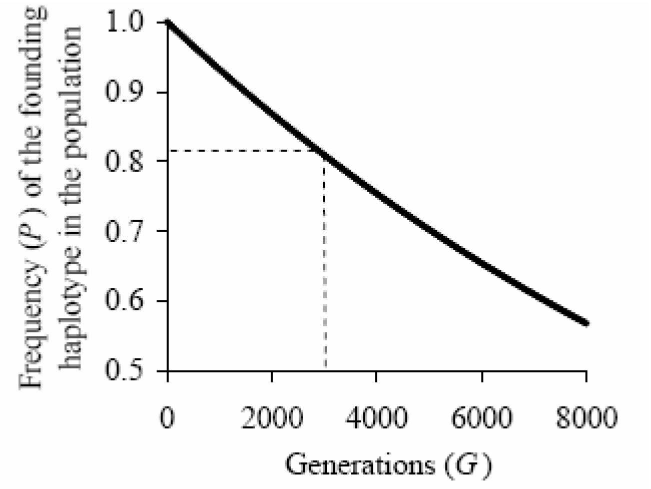

B.

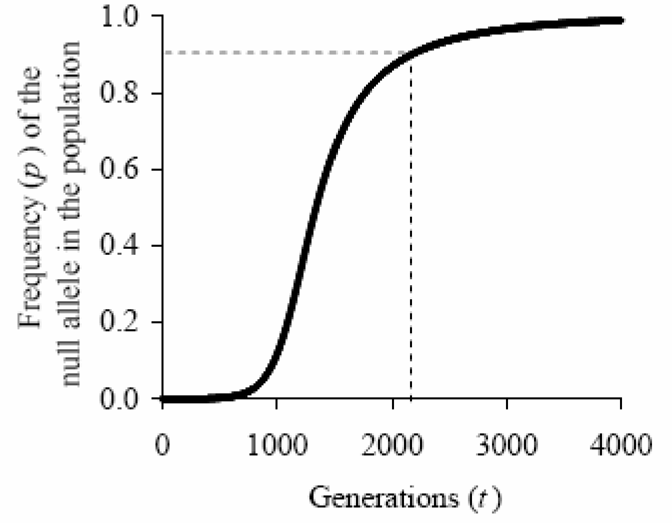

Table 4.1 Intraspecific variations in 9 noncoding regions linked to human CASPASE12.

Region[1]	Length (nucleotide)	Allele[2]	# of SNPs	π	Standard error of π	Probability[3]
1	674	C (8)	5	0.00307	0.00067	
		T (8)	5	0.00413	0.00050	0.205
2	675	C (8)	3	0.00206	0.00049	
		T (8)	3	0.00206	0.00035	1.000
3	773	C (8)	2	0.00102	0.00033	
		T (8)	1	0.00069	0.00016	0.368
4	2413	C (8)	19	0.00280	0.00053	
		T (8)	1	0.00018	0.00007	<0.001
		T (22)	1	0.00015	0.00004	<0.001
5	1553	C (8)	9	0.00233	0.00051	
		T (8)	8	0.00129	0.00071	0.234
		T (22)	10	0.00069	0.00033	0.007
6	592	C (8)	3	0.00175	0.00071	
		T (8)	2	0.00145	0.00057	0.741
		T (22)	4	0.00155	0.00041	0.807
7	730	C (8)	3	0.00127	0.00046	
		T (8)	3	0.00176	0.00069	0.555
8	738	C (8)	2	0.00106	0.00034	
		T (8)	3	0.00126	0.00038	0.695
9	777	C (8)	7	0.00267	0.00071	
		T (8)	3	0.00179	0.00046	0.298

[1] The chromosomal locations of the 9 regions are shown in Figure 4.1.

[2] C is the (ancestral) functional allele and T is the (derived) null allele. The number of chromosomes sequenced is given in parentheses. Eight T chromosomes were initially sequenced for all the regions. Subsequently, we sequenced another 14 T chromosomes for regions 4, 5, and 6.

[3] The probability that the nucleotide diversity is identical between T and C alleles for the region concerned (two-tail Z test).

Table 4.2 Results from coalescent simulations.

Demographic models[1]	Probability (%)[2]
Constant population size	0.066
Ancient population expansion	0.006
Recent population expansion	0.068
Several bottlenecks	0.232
Repeated bottlenecks with subsequent expansion	0.126
Population structure with 2 subpopulations	0.066
Population structure with 3 subpopulations	0.116
Population structure with 4 subpopulations	0.358
Population structure with 5 subpopulations	0.824

[1] The parameters used are detailed in Materials and Methods.

[2] Proportion of cases with $k_1+k_2 \geq 61$ in 50,000 simulation replications. See main text for details.

Table 4.3 SNPs identified in the noncoding regions linked with CASP12.

Nucleotide positions[1]	SNPs[2]	Allele frequency (%)[3]	Sample size[4]
-9705	C/T	37.5	8
-9612	A/G	12.5	8
-9598	C/T	62.5	8
-9548	G/A	43.7	8
-9499	C/T	37.5	8
-9150	G/A	6.3	8
-5519	C/T	6.3	8
-5194	T/C	37.5	8
-5042	C/T	62.5	8
-4993	A/G	18.8	8
233	A/G	25.0	8
657	T/C	31.3	8
2516	T/G	1.4	35
2621	C/A	1.4	35
2674	A/G	1.4	35
3000	G/A	91.4	35
3081	A/G	95.7	35
3142	A/C	91.4	35
3148	C/T	91.4	35
3869	T/C	1.4	35
3957	A/G	8.6	35
3980	G/A	8.6	35
4018	G/A	91.4	35
4045	C/T	1.4	35
4111	T/A	70.0	35
4181	T/C	1.4	35
4239	A/T	7.1	35
4706	T/A	91.4	35
4759	G/T	1.4	35
4855	T/C	1.4	35
5083	C/T	1.4	35
5175	C/T	8.6	35
8335	T/G	76.7	15
8453	C/G	76.7	15
8642	G/A	6.7	15
8667	A/T	3.3	15
8893	C/T	6.7	15
9440	C/A	13.3	15
9586	G/A	23.3	15
9854	T/C	23.3	15
9951	A/T	76.7	15
10168	G/A	23.3	15
10239	G/A	3.3	15
10250	C/T	3.3	15
11823	G/T	3.3	15
11867	T/C	73.3	15
11968	C/T	20.0	15
14642	T/C	18.8	8
14771	A/T	75.0	8
14959	C/T	18.8	8
18112	G/A	6.3	8
18374	T/C	6.3	8
18439	G/A	25.0	8
18716	T/C	18.6	8
20030	C/T	6.3	8
20093	C/T	6.3	8
20118	T/G	12.5	8
20133	A/C	68.8	8
20244	A/G	6.3	8
20298	C/G	37.5	8
20516	A/G	37.5	8

[1] The nucleotide positions are relative to the start codon ATG of the *CASP12* gene.

[2] The ancestral/derived nucleotides are given for each SNP.

[3] Frequency of the derived allele estimated from individuals of African descent.

[4] Number of sequenced human individuals with African descent.

4.7 LITERATURE CITED

Alexander S, Lilly E, Angus D, Barnato A, Linde-Zwirbe W (2004) Racial variation in the incidence, ICU utilization, and mortality of severe sepsis. Critical Care Medicine 32

Alnemri ES, Livingston DJ, Nicholson DW, Salvesen G, Thornberry NA, Wong WW, Yuan J (1996) Human ICE/CED-3 protease nomenclature. Cell 87:171

Britten RJ (2002) Divergence between samples of chimpanzee and human DNA sequences is 5%, counting indels. Proc Natl Acad Sci U S A 99:13633-13635

Brunet M, Guy F, Pilbeam D, Mackaye HT, Likius A, Ahounta D, Beauvilain A, et al. (2002) A new hominid from the Upper Miocene of Chad, Central Africa. Nature 418:145-151

Cavalli-Sforza LL, Feldman MW (2003) The application of molecular genetic approaches to the study of human evolution. Nat Genet 33 Suppl:266-275

Chen FC, Li WH (2001) Genomic divergences between humans and other hominoids and the effective population size of the common ancestor of humans and chimpanzees. Am J Hum Genet 68:444-456

Chou HH, Hayakawa T, Diaz S, Krings M, Indriati E, Leakey M, Paabo S, Satta Y, Takahata N, Varki A (2002) Inactivation of CMP-N-acetylneuraminic acid hydroxylase occurred prior to brain expansion during human evolution. Proc Natl Acad Sci U S A 99:11736-11741

Chou HH, Takematsu H, Diaz S, Iber J, Nickerson E, Wright KL, Muchmore EA, Nelson DL, Warren ST, Varki A (1998) A mutation in human CMP-sialic acid hydroxylase occurred after the Homo-Pan divergence. Proc Natl Acad Sci U S A 95:11751-11756

Ebersberger I, Metzler D, Schwarz C, Paabo S (2002) Genomewide comparison of DNA sequences between humans and chimpanzees. Am J Hum Genet 70:1490-1497

Enard W, Przeworski M, Fisher SE, Lai CS, Wiebe V, Kitano T, Monaco AP, Paabo S (2002) Molecular evolution of FOXP2, a gene involved in speech and language. Nature 418:869-872

Evans PD, Gilbert SL, Mekel-Bobrov N, Vallender EJ, Anderson JR, Vaez-Azizi LM, Tishkoff SA, Hudson RR, Lahn BT (2005) Microcephalin, a gene regulating brain size, continues to evolve adaptively in humans. Science 309:1717-1720

Fay JC, Wu CI (2000) Hitchhiking under positive Darwinian selection. Genetics 155:1405-1413

Fischer A, Gilad Y, Man O, Paabo S (2005) Evolution of bitter taste receptors in humans and apes. Mol Biol Evol 22:432-436

Fischer H, Koenig U, Eckhart L, Tschachler E (2002) Human caspase 12 has acquired deleterious mutations. Biochem Biophys Res Commun 293:722-726

Fortna A, Kim Y, MacLaren E, Marshall K, Hahn G, Meltesen L, Brenton M, Hink R, Burgers S, Hernandez-Boussard T, Karimpour-Fard A, Glueck D, McGavran L, Berry R, Pollack J, Sikela JM (2004) Lineage-specific gene duplication and loss in human and great ape evolution. PLoS Biol 2:E207

Galvani AP, Novembre J (2005) The evolutionary history of the CCR5-Delta32 HIV-resistance mutation. Microbes Infect 7:302-309

Gilad Y, Man O, Paabo S, Lancet D (2003) Human specific loss of olfactory receptor genes. Proc Natl Acad Sci U S A 100:3324-3327

Go Y, Satta Y, Takenaka O, Takahata N (2005) Lineage-specific loss of function of bitter taste receptor genes in humans and nonhuman primates. Genetics 170:313-326

Greenberg AJ, Moran JR, Coyne JA, Wu CI (2003) Ecological adaptation during incipient speciation revealed by precise gene replacement. Science 302:1754-1757

Grus WE, Shi P, Zhang YP, Zhang J (2005) Dramatic variation of the vomeronasal pheromone receptor gene repertoire among five orders of placental and marsupial mammals. Proc Natl Acad Sci U S A 102:5767-5772

Hamann J, Kwakkenbos MJ, de Jong EC, Heus H, Olsen AS, van Lier RA (2003) Inactivation of the EGF-TM7 receptor EMR4 after the Pan-Homo divergence. Eur J Immunol 33:1365-1371

Hamblin MT, Thompson EE, Di Rienzo A (2002) Complex signatures of natural selection at the Duffy blood group locus. Am J Hum Genet 70:369-383

Harpending H, Rogers A (2000) Genetic perspectives on human origins and differentiation. Annu Rev Genomics Hum Genet 1:361-385

Harpending HC, Batzer MA, Gurven M, Jorde LB, Rogers AR, Sherry ST (1998) Genetic traces of ancient demography. Proc Natl Acad Sci U S A 95:1961-1967

Hartl D, Clark A (1997) Principles of Populations Genetics. Sinauer, Sunderland, Massachusetts

Hayakawa T, Satta Y, Gagneux P, Varki A, Takahata N (2001) Alu-mediated inactivation of the human CMP- N-acetylneuraminic acid hydroxylase gene. Proc Natl Acad Sci U S A 98:11399-11404

Hudson RR (2002) Generating samples under a Wright-Fisher neutral model of genetic variation. Bioinformatics 18:337-338

Hughes A (1999) Adaptive Evolution of Genes and Genomes. Oxford University Press, New York

Kimura M (1983) The Neutral Theory of Molecular Evolution. Cambridge University Press, Cambridge

Kimura M, Ohta T (1973) Age of a Neutral Mutant Persisting in a Finite Population. Genetics 75:199-212

Kong A, Gudbjartsson DF, Sainz J, Jonsdottir GM, Gudjonsson SA, Richardsson B, Sigurdardottir S, Barnard J, Hallbeck B, Masson G, Shlien A, Palsson ST, Frigge ML, Thorgeirsson TE, Gulcher JR, Stefansson K (2002) A high-resolution recombination map of the human genome. Nat Genet 31:241-247

Lai CS, Fisher SE, Hurst JA, Vargha-Khadem F, Monaco AP (2001) A forkhead-domain gene is mutated in a severe speech and language disorder. Nature 413:519-523

Lamkanfi M, Declercq W, Kalai M, Saelens X, Vandenabeele P (2002) Alice in caspase land. A phylogenetic analysis of caspases from worm to man. Cell Death Differ 9:358-361

Li WH, Saunders MA (2005) The chimpanzee and us. Nature 437:50-51

Maynard Smith J, Haigh J (1974) The hitch-hiking effect of a favourable gene. Genet Res 23:23-35

Meyer-Olson D, Brady KW, Blackard JT, Allen TM, Islam S, Shoukry NH, Hartman K, Walker CM, Kalams SA (2003) Analysis of the TCR beta variable gene repertoire in chimpanzees: identification of functional homologs to human pseudogenes. J Immunol 170:4161-4169

Olson MV (1999) When less is more: gene loss as an engine of evolutionary change. Am J Hum Genet 64:18-23

Olson MV, Varki A (2003) Sequencing the chimpanzee genome: insights into human evolution and disease. Nat Rev Genet 4:20-28

Perry GH, Verrelli BC, Stone AC (2005) Comparative analyses reveal a complex history of molecular evolution for human MYH16. Mol Biol Evol 22:379-382

Przeworski M (2003) Estimating the time since the fixation of a beneficial allele. Genetics 164:1667-1676

Rozas J, Rozas R (1999) DnaSP version 3: an integrated program for molecular population genetics and molecular evolution analysis. Bioinformatics 15:174-175

Sabeti PC, Reich DE, Higgins JM, Levine HZ, Richter DJ, Schaffner SF, Gabriel SB, Platko JV, Patterson NJ, McDonald GJ, Ackerman HC, Campbell SJ, Altshuler D, Cooper R, Kwiatkowski D, Ward R, Lander ES (2002) Detecting recent positive selection in the human genome from haplotype structure. Nature 419:832-837

Sabeti PC, Walsh E, Schaffner SF, Varilly P, Fry B, Hutcheson HB, Cullen M, Mikkelsen TS, Roy J, Patterson N, Cooper R, Reich D, Altshuler D, O'Brien S, Lander ES (2005) The case for selection at CCR5-Delta32. PLoS Biol 3:e378

Saleh M, Vaillancourt JP, Graham RK, Huyck M, Srinivasula SM, Alnemri ES, Steinberg MH, Nolan V, Baldwin CT, Hotchkiss RS, Buchman TG, Zehnbauer BA, Hayden MR, Farrer LA, Roy S, Nicholson DW (2004) Differential modulation of endotoxin responsiveness by human caspase-12 polymorphisms. Nature 429:75-79

Shimizu KK, Cork JM, Caicedo AL, Mays CA, Moore RC, Olsen KM, Ruzsa S, Coop G, Bustamante CD, Awadalla P, Purugganan MD (2004) Darwinian selection on a selfing locus. Science 306:2081-2084

Stedman HH, Kozyak BW, Nelson A, Thesier DM, Su LT, Low DW, Bridges CR, Shrager JB, Minugh-Purvis N, Mitchell MA (2004) Myosin gene mutation correlates with anatomical changes in the human lineage. Nature 428:415-418

Stephens JC, Reich DE, Goldstein DB, Shin HD, Smith MW, Carrington M, Winkler C, et al. (1998) Dating the origin of the CCR5-Delta32 AIDS-resistance allele by the coalescence of haplotypes. Am J Hum Genet 62:1507-1515

Szabo Z, Levi-Minzi SA, Christiano AM, Struminger C, Stoneking M, Batzer MA, Boyd CD (1999) Sequential loss of two neighboring exons of the tropoelastin gene during primate evolution. J Mol Evol 49:664-671

Tajima F (1989) Statistical method for testing the neutral mutation hypothesis by DNA polymorphism. Genetics 123:585-595

Takahashi A, Tsaur SC, Coyne JA, Wu CI (2001) The nucleotide changes governing cuticular hydrocarbon variation and their evolution in Drosophila melanogaster. Proc Natl Acad Sci U S A 98:3920-3925

Takahata N, Satta Y, Klein J (1995) Divergence time and population size in the lineage leading to modern humans. Theor Popul Biol 48:198-221

The Chimpanzee Sequencing and Analysis Consortium (2005) Initial sequence of the chimpanzee genome and comparison with the human genome. Nature 437:69-87

Varki A (2001) Loss of N-glycolylneuraminic acid in humans: Mechanisms, consequences, and implications for hominid evolution. Am J Phys Anthropol Suppl 33:54-69

Wang X, Thomas SD, Zhang J (2004) Relaxation of selective constraint and loss of function in the evolution of human bitter taste receptor genes. Hum Mol Genet 13:2671-2678

Watanabe H, Fujiyama A, Hattori M, Taylor TD, Toyoda A, Kuroki Y, Noguchi H, et al. (2004) DNA sequence and comparative analysis of chimpanzee chromosome 22. Nature 429:382-388

Wildman DE, Uddin M, Liu G, Grossman LI, Goodman M (2003) Implications of natural selection in shaping 99.4% nonsynonymous DNA identity between humans and chimpanzees: enlarging genus Homo. Proc Natl Acad Sci U S A 100:7181-7188

Winter H, Langbein L, Krawczak M, Cooper DN, Jave-Suarez LF, Rogers MA, Praetzel S, Heidt PJ, Schweizer J (2001) Human type I hair keratin pseudogene phihHaA has functional orthologs in the chimpanzee and gorilla: evidence for recent inactivation of the human gene after the Pan-Homo divergence. Hum Genet 108:37-42

Zhang J (2003) Evolution by gene duplication: an update. Trends Ecol Evolut 18:292-298

Zhang J, Webb DM, Podlaha O (2002) Accelerated protein evolution and origins of human-specific features: Foxp2 as an example. Genetics 162:1825-1835

Zietkiewicz E, Richer C, Sinnett D, Labuda D (1998) Monophyletic origin of Alu elements in primates. J Mol Evol 47:172-182